CORROSION FATIGUE OF 2024-T4 ALUMINIUM ALLOY IN CONTACT WITH SUPERPHOSPHATE FERTILIZER

A thesis presented for the
degree of Doctor of Philosophy in Mechanical Engineering,
in the University of Canterbury,
Christchurch, New Zealand.

by
N.A. MILLER
1968

A C K N O W L E D G E M E N T S.

I gratefully acknowledge the financial assistance received from the State Services Commission, who by granting me a D.S.I.R. Study Award enabled me to undertake this research. I also acknowledge the assistance and support I have received from the Director and Staff of Chemistry Division, D.S.I.R.

My grateful thanks also go to Professor R.J. Rastrick, Head of Department of Mechanical Engineering, who acted as my Supervisor, and to members of his staff for their help and encouragement. In particular the assistance of Mr. E. Retallick and the workshop staff, in preparing the many fatigue specimens used in this research and for the manufacture of some items of equipment, is gratefully acknowledged.

During the period of this research I have had many helpful and stimulating discussions with my colleagues of the Metals Section, Chemistry Division, D.S.I.R. and with my fellow post-graduate students in the Department of Mechanical Engineering. Their interest and encouragement is much appreciated.

Most of the photographs that appear in the thesis are the work of the Photography Section, Chemistry Division, D.S.I.R. and I wish to record my thanks to Mr. A.L. Tilbury for this work.

My thanks also go to Mrs. N. Newman for the typing of the thesis.

Finally, I wish to express my thanks and appreciation to my wife without whose understanding and encouragement this research could not have been carried out.

ABSTRACT.

The aim of this research was to establish the effects of superphosphate fertilizer on the fatigue life of 2024 - T4 aluminium alloy. Rotating beam, direct stress and reverse bend fatigue tests were carried out on both notched and un-notched specimens. The results showed that moist superphosphate caused a dramatic loss in fatigue life even at stresses as low as 4 tons/sq.in.. It was found that the type of fracture obtained in air was the same for all stress systems studied, but that the cycle frequency and the presence of a stress concentrator such as a notch modified the type of fracture produced in air tests. The presence of the corrodent profoundly modified the shape of the fracture and valley fractures were produced with all the stress systems studied.

Research studies included the effect of superphosphate on fatigue crack initiation and propagation and it was found that although the corrodent had a marked effect on the crack propagation rates, it had little, if any, effect on the crack initiation. From these studies a tentative theory of corrosion accelerated fatigue has been postulated. This theory has been used to explain the results obtained in the present research.

TABLE OF CONTENTS.

LIST OF FIGURES.

LIST OF TABLES.

THE FATIGUE BEHAVIOUR OF 2024-T4 ALUMINIUM ALLOY IN CONTACT WITH SUPERPHOSPHATE FERTILIZER

CHAPTER ONE.

1. INTRODUCTION.

In the highly mechanised New Zealand agricultural industry, wide use is made of light aircraft for the spreading of agricultural chemicals, mainly fertilizers, on pasture lands and crops. Some idea as to the size and importance of this aerial top dressing industry to New Zealand can be gained from the figures for current fertilizer production. The current production of superphosphate fertilizers is approximately 2,000,000 tons, worth about $30 million, of which about 1,000,000 tons is spread by aerial top dressing techniques. In addition to the superphosphate fertilizers some 1,000,000 tons of crushed limestone is applied to pasture lands and of this amount some 60,000 tons (6% of total) is accounted for by aerial top dressing techniques. There is considerable capital investment in equipment to apply these fertilizers and there are over 300 agricultural aircraft together with loading equipment and service facilities in use in New Zealand. In addition to the aerial top dressing fleet there is a large capital investment in bulk top dressing trucks and privately owned top dressing units.

One of the problems the aerial top dressing industry has to face is the risk of fatigue failures of aircraft components. Top dressing aircraft operate under severe conditions and the take-off, in-flight and landing loads imposed on structural members are high with greatly increased risk of fatigue failures. Fatigue failures of such components as landing gear and propellors are not uncommon and the risk of a major structural failure is always present. Any component failure means the prospect of an accident with possible injuries to the pilot, or loss of life, as well as extensive damage to the aircraft. Thus it is of considerable economic importance to avoid component failures if possible. An unknown factor is the effect of superphosphate on the fatigue properties of the materials commonly used in the construction of light aircraft. It is possible that the combined effects of corrosion and fatigue loading could cause rapid fatigue failures with enhanced risk of a catastrophic failure.

Attempts are at present being made by the civil aviation authorities both in New Zealand and Australia to estimate the safe life of agricultural aircraft. In both countries, work is under way measuring the in-flight loads sustained by various types of aircraft engaged in aerial top dressing[1,2]* in an effort to establish the load spectrum. However, to make realistic estimates of the safe lives of these aircraft,

* Numbers in parenthesis refer to references to be given at the end of the thesis.

information as to the effects of agricultural chemicals, especially superphosphate fertilizers, on the fatigue life of the alloys used in their construction is necessary. In addition to aiding the estimation of safe life, any information which can improve the safety margin in aerial top dressing is of value, both in possible saving of lives and in prevention of damage to aircraft.

During the loading and spreading operations, especially with those involving solids such as superphosphate, the aircraft becomes liberally coated with fine dust. This dust lodges on external structural members such as tail planes and landing gear, and also penetrates the interior of the aircraft lodging on the main spar and other internal structural members. The presence of any moisture means increased risk of corrosion attack on the exposed alloy members and this is especially so if the protective coating has been damaged during service or inspection. One question which requires to be resolved is at what stage is the dust deposited on the aircraft, during the loading operations or during the spreading operations. From studies at the Auckland University School of Engineering[3] it has been demonstrated that very little dust is picked up during actual spreading operations and that the dust is deposited on the aircraft during the actual loading operations. One way of reducing this dust pick up is to use granulated superphosphate rather than the powder form, and several manufacturers are now supplying granulated superphosphate for aerial top dressing work.

Information is available on the influence of a number of agricultural chemicals on the corrosion of several different materials used in the construction of aircraft,[4] but this data has been gathered from static laboratory corrosion tests without any applied stress. There is to date no information available regarding the effects of these chemicals on the fatigue properties of the alloys commonly used in aircraft. The only reference to corrosion fatigue of aircraft components being caused by superphosphate is an Australian paper,[5] but no specific information is given. The present investigation, which is under the sponsorship of Chemistry Division, D.S.I.R., is aimed at examining the effects of superphosphate fertilizers on the fatigue properties of 2024-T4 aluminium alloy. This alloy was selected as it is the most commonly used alloy in the light aircraft engaged in aerial top dressing and especially as it is used in the construction of aircraft built in New Zealand, such as the Fletcher FU24. Superphosphate fertilizers were selected as the corrodents because of their known corrosive properties toward aluminium alloys and because they are the most widely used fertilizers in New Zealand.

Several grades of superphosphate fertilizer are used in New Zealand but the three major types are standard superphosphate (25% of total production), aerial superphosphate (21% of total) and potassic mixtures (24% of total). The remaining 30% of current production is made up of a number of special mixtures containing trace elements such as copper, cobalt, molybdenum

and sulphur. It is often reported, erroneously, that superphosphate contains free sulphuric acid, but these fertilizers while being free from sulphuric acid normally contain 2 - 3% of phosphoric acid (H_3PO_4). The presence of phosphoric acid is necessary for chemical stability of some of the phosphatic compounds in the superphosphate fertilizers. The aerial superphosphate has a very low free acid content and is thus somewhat more stable under humid conditions than other grades, this is necessary to ensure that the fertilizer runs freely from the hopper during spreading operations. Aerial superphosphate and a 33% potassic superphosphate were used as corrodents in the current investigation as these grades represent the bulk of the fertilizers spread by aerial top dressing techniques.

CHAPTER TWO.

2. THE MECHANISM OF METAL FATIGUE.

2.1 Introduction.

With the vast output of literature on the subject of metal fatigue, estimated now to be at the rate of over 700 papers per year,[6] it could perhaps be said with reasonable confidence that metal fatigue should no longer be a problem in engineering. However, the amount of literature available is, it seems, in inverse proportion to our understanding of the basic mechanisms of the formation and propagation of cracks in metals and alloys undergoing cyclic stress. The volume of literature available to the researcher also helps to cause confusion as it is virtually impossible to be aware of all that has been and is being published. Another factor which has to be considered is that as far as the actual mechanism of fatigue is concerned virtually only those papers published in the late 1960's appear to be of any real value and many prominent researchers have modified or altered views which they have advanced only a few years earlier.

The importance of the problem of metal fatigue in engineering is emphasised by the flood of literature on this topic and this is especially true for the transportation industry in general and the aeronautical industry in particular. It is in the field of aeronautical engineering that perhaps the bulk of the work has been carried out, and there is a considerable body of information available on the fatigue

properties of the high strength aluminium alloys. There is also a danger here in that many workers dealing with the aluminium alloys, often in thin sheet, try to base a universal theory of fatigue on their results. It is felt that this approach is open to criticism, as the face centred cubic (fcc) aluminium alloys are not necessarily representative of the behaviour of say, body centred cubic (bcc) alloys, and work on thin sheet similarly is not necessarily representative of bulk material such as extruded and rolled sections.

There are two methods of approach to the problem of fatigue, one based on continuum mechanics and the other on the basic microstructural mechanism of crack initiation and propagation. These two approaches serve to emphasise the different interests of two groups of researchers in the field of fatigue. The continuum mechanics approach is more the engineering approach for here is the effort to reduce the problem of crack propagation to a mathematical model from which predictions of crack growth rates can be made which will enable the designer to select such stress levels that catastrophic failure of a part can be avoided. This approach could be termed the "safe-life" approach. The continuum approach ignores the question of crack initiation assuming there is a crack present and is really only interested in its rate of growth.

The metallurgist,on the other hand, is concerned with the basic atomic mechanism of fatigue crack initiation and propagation and in examining, and he hopes, explaining the features of a fatigue crack. Such topics as the effect of precipitate particles, grain size and orientation, grain boundaries and environment form part of the microstructural approach. The metallurgist is thus concerned with why a crack forms and propagates, while the engineer is interested in how long it will take the crack to grow to dangerous proportions. Ideally, the perfect theory will combine both approaches but at present this combination, while desired by both groups, is not yet possible. It must be emphasised that both methods of approach to the problem of metal fatigue have their value and each can help the other to a better understanding of the problem.

The growth of a fatigue crack can be divided into three phases; nucleation, propagation and final failure. The nucleation period can be further sub-divided into a period of cyclic slip resulting in the formation of persistent slip bands, the development of these bands into micro-cracks which in turn develop into a macro-crack. Two problems to be decided are at what point a micro-crack is formed and when does a micro-crack become a macro-crack. One thing is certain and it is that a crack forms early in the total fatigue life of the structure or test piece under consideration. The percentage of the fatigue life spent in nucleation and

crack propagation depends very much on the geometry of the particular part. If the structure is one utilising thin plates with built in stress concentrations then the formation of a dominant macro-crack takes place relatively early in the fatigue life and hence the major part of the total fatigue life is taken up by crack propagation. It is in this type of situation, such as is found in aircraft, that the continuum mechanics approach proves very valuable. With a large and bulky part with no distinct stress concentrator, such as arises in the testing of a fatigue specimen, then a large percentage of the total life is spent in the nucleation stage, although technically it is considered that a micro-crack forms very early in the life. This type of situation is the usual one studied by the metallurgist and his major problem is deciding at what stage a macro-crack can be said to have formed.

2.2 The Continuum Mechanics Approach.

An excellent review of continuum models is given by Erdogan[7] in a publication dealing with crack propagation theories in general. In this publication he covers the various models that have been put forward and also sets out his own approach. In his introduction to the section dealing with fatigue crack propagation Erdogan states that

> "Partly due to the fact that crack propagation represents a large portion of the fatigue life mostly in thin plates and shells, partly because of the importance of fatigue in such elements as

they appear in the airplane design and ship building and partly because of the analytical simplicity of the problem resulting from a two dimensional idealization, the existing quantitative continuum models of fatigue crack propagation have almost exclusively dealt with a plate with a straight through crack subjected to uni-axial repeated extensional loads. If ℓ is the half length or length of the crack and n is the number of load cycles, in all these models, it is assumed that $\frac{d\ell}{dn}$ is a continuous function of such variables as the external load, the dimensions and the material properties. The primary objective is then to determine this function."

One of the earlier models which has enjoyed some success in predicting crack propagation rates is that put forward by Head[8]. Head considered an infinite plate, a central crack of length 2ℓ and one dimensional repeated loads of range value σ, and used a mechanical model assuming rigid-plastic work-hardening elements ahead of the crack tip and elastic elements over the remainder of the plate. He arrived at the following relationship;

$$\frac{d\ell}{dn} = \frac{\ell^{3/2}}{p^{\frac{1}{2}}} \quad f(\sigma) \qquad \ldots\ldots\ldots\ldots\ldots\ldots\ldots\ldots\ldots\ldots 1$$

where p is the size of the plastic zone at the crack tip and σ is the applied load. $f(\sigma)$ was found to be of the form,

$$f(\sigma) = C_1 \frac{\sigma^3}{(\sigma_{ys} - \sigma)} \quad \ldots\ldots\ldots\ldots\ldots 2$$

and combining 1 and 2;

$$\frac{d\ell}{dn} = C_1 \frac{\sigma^3 \ell^{3/2}}{(\sigma_{ys} - \sigma) p^{\frac{1}{2}}} \quad \ldots\ldots\ldots\ldots\ldots 3$$

where σ_{ys} is the yield stress and C_1 is a material constant which has to be determined experimentally. The plastic zone size p, is assumed to be constant.

Frost and Dugdale[9] showed that p, the plastic zone size, is not constant but is dependent on crack length and is proportional to $\sigma^2 \ell$. From their analysis they arrived at the conclusion that $\frac{d\ell}{dn}$ is linearly dependent on crack length. From experimental data they observed that $\frac{d\ell}{dn}$ is proportional to σ^3 and thus

$$\frac{d\ell}{dn} = C_2 \sigma^3 \ell \quad \ldots\ldots\ldots\ldots\ldots 4$$

Where C_2 is a characteristic parameter of the material.

Liu[10] arrived at the conclusion that

$$\frac{d\ell}{dn} = F(\sigma, \sigma_m) \ell \quad \ldots\ldots\ldots\ldots\ldots 5$$

Where F is a function of the mean stress (σ_m) and the range of the external loads (σ). From a further analysis[11] considering a hysteresis energy dissapation model he pointed out that the effect of the mean stress in crack propagation is not significant and the function F is proportional to σ^2,

thus;

$$\frac{d\ell}{dn} = C_3 \sigma^2 \ell \qquad \ldots\ldots\ldots\ldots\ldots\ldots 6$$

where C_3 is a material constant.

McEvily and co-workers[12 - 13] approached the problem from the point of view of stress concentration. They argued that the local stress immediately ahead of the crack tip is raised to the fracture level as a result of work hardening under cyclic load thus causing rupture. It was then stated that the crack propagation rate must be a function of the maximum stress around the crack tip.

$$\frac{d\ell}{dn} = f(\sigma_{max}) \qquad \ldots\ldots\ldots\ldots\ldots\ldots 7$$

Assuming the crack to be a flat elliptical hole σ_{max} may be expressed as

$$\sigma_{max} = K_s \sigma = (1 + 2\sqrt{\frac{\ell}{\rho}})\sigma \qquad \ldots\ldots\ldots\ldots 8$$

Where K_s is the static stress concentration factor and ρ is the radius of curvature at the tip region of the crack. Thus;

$$\frac{d\ell}{dn} = A(\sigma\sqrt{\ell})^4 \qquad \ldots\ldots\ldots\ldots\ldots\ldots 9$$

Other workers have followed along the lines suggested by McEvily and Illg basing their arguments on the stress intensity factor K, ($K = \sigma\sqrt{\ell}$). The central point of this argument is that the stress intensity factor is a parameter which represents both the geometry and the external loads and is the true measurement of the stress state around the

crack tip . Hence it should be the most important factor affecting the crack growth rate.

In a critical analysis of various continuum models, Paris and Erdogan[14] arrived at the tentative conclusion that,

$$\frac{d\ell}{dn} = C_4 K^4 , \quad K = \sigma\sqrt{\ell} \qquad \ldots\ldots\ldots\ldots\ldots\ldots\ldots\ldots 10$$

where C_4 is a material constant which is a function of material parameters derived experimentally. This model has been found to be quite satisfactory for the high strength aluminium alloys but has not proved to be as satisfactory for copper base alloys.[7]

The more recent work, as for example that reported in the American Society for Testing and Materials publication, "Fatigue Crack Propagation",[15] continues along the lines of using the stress intensity factor as a correlation parameter. Two recent papers appear to confirm that Equation 10 is a reasonable approximation for crack growth rates. Weertman[16] in a theoretical approach arrives at,

$$\frac{d\ell}{dn} = C_5 (\sigma\sqrt{\ell})^4 \qquad \ldots\ldots\ldots\ldots\ldots\ldots\ldots\ldots 11$$

where C_5 is a material constant. It is of the identical form to 10 above as $K = \sigma\sqrt{\ell}$. In an experimental approach Pearson[17] measured actual growth rates and arrived at,

$$\frac{d\ell}{dn} = 3.43 \times 10^7 (K/E)^{3.6} \qquad \ldots\ldots\ldots\ldots\ldots\ldots\ldots\ldots 12$$

This is of course of the form,

$$\frac{d\ell}{dn} = \text{Constant} \times K^{3.6} \qquad \ldots\ldots\ldots\ldots\ldots\ldots\ 13$$

In his review of continuum models[7] Erdogan puts forward his own model based on considerations of dislocation density at the crack tip and the force necessary to cause dislocation movement and hence crack growth. Here is an attempt to combine both the continuum and the microstructural approaches. From his arguments he arrives at the following formula;

$$\frac{d\ell}{dn} = A\, p_{max}^{a_1}\, p_r^{a_2} \qquad \ldots\ldots\ldots\ldots\ldots\ldots\ 14$$

where A, a_1, a_2, are positive constants to be determined experimentally, p_{max} is the maximum plastic zone size at the crack tip and p_r is the plastic zone size for the range of strains in the material.

Miller et al[18] concluded that the crack growth rate was proportional to the square of the plastic-strain amplitude (ϵ_p) and from experimental data derive the following formula,

$$\frac{d\ell}{dn} = B\,(\epsilon_p)^2 \qquad \ldots\ldots\ldots\ldots\ldots\ 15$$

The factor B was found to increase and decrease with corresponding changes in stacking fault energy. Their formula appears to bear some resemblance to that put forward

by Erdogan but in his case a_1 and a_2 are both less than unity and thus the crack growth rate depends on some power of the plastic zone size which lies between 1 and 2.

The existing continuum models are based almost exclusively on propagation rates of fatigue cracks in thin plates under symmetric plane extensional loads and are thus not necessarily applicable to rod or other bulky sections. They also in the main, ignore the effects of microstructural variables and environment, although it is difficult to see how these variables can be brought into the continuum approach. The theories are often based on experimental data derived from tests using a simulated fatigue crack, often a fine saw cut, and it can be suggested that the early rates of crack propagation measured are not necessarily representative of actual growth rates that would occur in practice. The theory proposed by Erdogan is an attempt to approach from the basic microstructural angle in that he bases his argument on dislocation movement under applied stress, but as he himself points out, even his theory fails to take into account such variables as grain size and environment.

Most of the continuum models set out in the literature are based on sine-wave cyclic loading but in practice random loading is more likely to be encountered. Many researchers in the field of fatigue are now using random loading testing and it is to be hoped that a continuum model to cover the case of random loading can be developed. However, it can be

said that the continuum models available do give the designer a working tool when designing to avoid fatigue, provided their limitations are kept in mind.

2.3 Microstructural Mechanisms of Fatigue.

The initiation and growth of a fatigue crack takes place in three phases - 1) crack nucleation

2) microcrack propagation

3) macrocrack propagation with final failure following the macrocrack stage. Unfortunately, while there is general agreement that a fatigue crack forms and propagates in these three phases, there is considerable discussion as to just how and by what mechanism the process proceeds. All workers agree that slip under cyclic loading plays a major role in all three phases. There have been a number of review articles written recently covering various aspects of fatigue crack initiation and growth but all the authors agree that there is still doubt as to the actual mechanisms by which a fatigue crack is formed and grows. Some of the problems which arise are due to different researchers using different stressing systems (e.g., torsion, reverse bend or tension), different materials and alloy systems, and different types of specimen (e.g., strip compared to bulk specimens). A further problem is that many researchers have used high strain amplitudes in order to shorten specimen life and thus speed up the testing programme. It is felt that such high strain tests do not necessarily reproduce the fatigue

damage that would occur in practice, that is, in a low strain long life situation. There is indeed considerable grounds for speculation concerning some of the phenomena observed in fatigue tests as these have often been observed on the surfaces of highly polished, large grained specimens, conditions which are not found very often in normal engineering applications.

As in the continuum models, the bulk of the work on crack initiation and propagation has been carried out using the fcc aluminium alloys. The alloys of interest are the high strength, age hardening ones and can be said to form a rather special group of materials. In these alloys, for tests run in air, several stages of fatigue crack propagation can be distinguished. Initially the fatigue crack starts on a plane inclined at 45^{o} to the maximum tensile stress, then after a very short number of cycles, it changes direction to run at 90^{o} to the maximum tensile stress, finally, over the latter stages, changing direction again back on to a plane at 45^{o} to the tensile stress. In this latter stage very rapid crack propagation occurs. In the case of bending stress or direct stress fatigue testing the specimen axis coincides with the direction of the maximum tensile stress and thus the inclination of the fracture surface relative to the specimen axis is the same as that relative to the maximum tensile stress. This is not the case in torsion fatigue testing and a somewhat different crack morphology results. Figure 2/1 taken from a paper by Forsyth[19] illustrates the general mode of failure in bending or direct

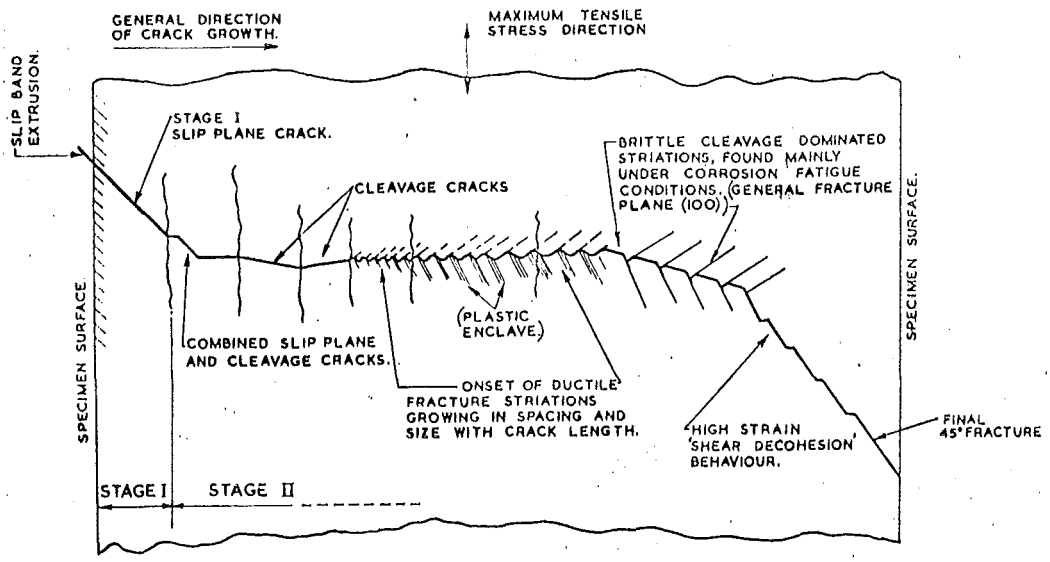

Figure 2/1: A schematic illustration of the various modes of fatigue fracture observed in strong aluminium alloys. This is a composite arrangement of possible modes, and does not necessarily represent a general sequence. (From Forsyth - Reference 19).

stress fatigue testing.

The development of fractography, that is the study of fracture surfaces using an optical microscope, has led to the observation of several striking features on fatigue crack surfaces. These features, or striations, appear to be related to the loading history of the specimen as their spacing is apparently related to the level of cyclic load imposed. Each striation is formed by the movement of the crack front under one load cycle and thus the number of striations present and their spacing can be taken as an indication of the number of load cycles imposed and the level of stress in each load cycle. Two basic types of striation have been observed, one running more or less at right angles to the applied tensile stress across the fracture surface, and the other a river type which is parallel to the tensile stress. The river pattern striation appears to be somewhat similar to those found on cleavage fracture surfaces.

2.3.1 Initiation of Fatigue Cracks.

The first major step towards understanding the initiation of fatigue cracks was due to Wood and co-workers.[20 - 22] They carried out torsion fatigue tests on copper and observed the formation of pores or voids which developed into microcracks. Wood divided the idealized fatigue curve (S - N curve) into three ranges (Figure 2/2); the high strain amplitude or H range, the low strain amplitude or F

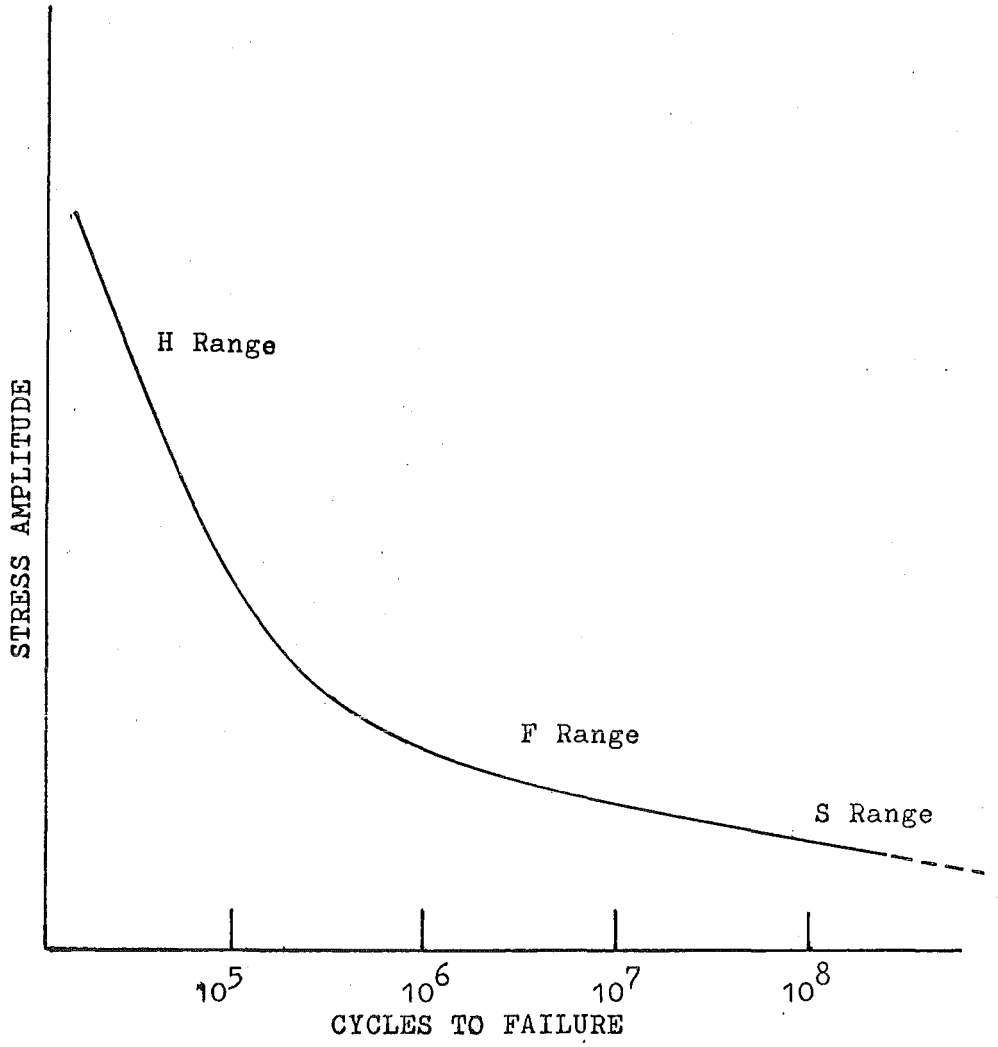

Figure 2/2: Idealised fatigue curve postulated by Wood[22] showing the three suggested ranges.

range, and the very low strain or S range. The H range covered specimen lives up to about 10^5 cycles, the F range 10^5 - 10^8 cycles and the S range lives greater than 10^8 cycles. Wood et al[22] showed that different phenomena occur in each of the three ranges. In the H range, the pores were observed to form in the boundaries of sub-grains which formed during the fatigue test. The pores coalesced into cavities along the sub-grain boundaries and finally linked into embryo cracks which still followed the sub boundaries. These embryo cracks developed in turn into microcracks (confined within a single grain) and these in turn developed into macrocracks, after which final fracture soon followed. The pores were observed to form after about 1/200th of the specimen life.

In the F range a different mode of initiation was observed. After about 1/1000th of the expected life persistent slip bands appeared in the specimen surface and these became the sites for the formation of small isolated pores. These pores multiplied, coalescing into cavities that were elongated along the slip bands and finally disintegrating the slip bands along their whole length to form fissures penetrating the interior of the specimen. Wood termed these fissures fatigue zones and noted that they formed along the planes of maximum shear stress. The fatigue zones were observed to multiply until some developed into microcracks, then into macrocracks and thus caused ultimate failure.

In the S range it was observed that up to about 10^7 cycles some slip movements were concentrated in slip bands long enough to form fatigue zones but the fatigue zones formed were few and apparently harmless. After about 10^7 cycles distortion zones developed and these persisted in increasing number without producing anything more than short isolated islands of disintegration. Wood concluded that continued cycling actually destroyed any fatigue zones thus giving the prolonged life in the S or psuedo-safe range. Wood observed that intrusions and extrusions were seen on the specimen surface but dismissed these as being a side effect of fatigue damage rather than a cause of fatigue crack initiation. In this latter point he appears to differ from some later workers.

Forsyth and co-workers[19,23 - 26] presented a somewhat different picture to that of Wood. In their work on high strength aluminium alloys they noted the formation of broad slip bands, which persisted after etching of the specimen surface. These persistent slip bands were up to 500 $\mathring{A}$ wide and along the bands precipitation re-solution occurred, also a sub-grain structure formed in these zones. They further observed that microcracks formed in the zones. Two types of crack formation are described in their work, Stage I cracking occurring at 45° to the specimen axis, that is along the maximum shear planes, and Stage II cracking at 90° to the specimen axis. The initial crack is formed by Stage I cracking and in this point Forsyth agrees with Wood. The Stage I

cracking occupies only a small fraction of the total fracture surface area but can account for a large portion of the actual fatigue life especially at low strain amplitudes.

In a more recent study[26] of Stage I or shear mode cracking in aluminium alloys using reverse bend and torsion testing, Stubbington and Forsyth showed that such cracking occurred on the $\{111\}$* crystal planes. Persistent slip bands and associated fatigue cracks ran from the specimen surface towards the neutral axis along planes at approximately 45^{o} to the test piece surface.

A recent report by Wilkov and Shield[27] puts forward evidence which appears to support the mechanism proposed by Wood in the F range. They studied both single and polycrystalline specimens of fcc metals and observed that fatigue damage always began as a sequence of small cavities oriented on the slip traces. These cavities increased in number and size, ultimately joining to form either a continuous microcrack or a shallow surface intrusion. Two distinct modes of formation and coalescence of the cavities were noticed and the fatigue damage observed was a combination of the two modes. In the first mode, cavity and intrusion formation was restricted to a single slip line. The cavities form along the slip line and join together to form a

* Using the standard crystallographic nomenclature.

continuous intrusion. In the second mode the cavities form in two slip directions and coalesce to form a shallow surface depression parallel to the principal slip trace.

Wilkov and Shield, unlike Wood, noted that although sub-grains were formed, the deep intrusions did not form in the sub-boundaries although the surface cavities appeared to nucleate initially in the regions near grain boundaries. They further observed that [27, p.20]

> "A threshold stress does not appear to exist, in that cavities are always formed after a sufficient number of cycles at even the lowest stress levels. However, a given stress level, determined by the test condition, is required to cause their propagation into an intrusion."

Any change in test condition which increased the ability of a dislocation to cross slip, such as an increase in stacking fault energy, temperature, stress or change in orientation, increased the width of the second mode of fatigue damage.

Two recent reviews, one by Ham[28] and the other by Schijve[29] do not include the work of Wilkov and Shield. Ham notes that there is general agreement that slip, especially cross slip, plays the major part in the initiation of a fatigue crack and that this slip can cause intrusions or notches 1000 Å deep in a very few cycles. These intrusions serve as stress raisers to ensure that slip continues in the locality. He adopts the view that such phenomena as

cavities, pores, persistent slip bands and extrusions occur after the formation of the initial intrusion. He does not however offer any explanation as to how these deep intrusions are formed. Schijve notes that the nucleation of a microcrack under cyclic torsion is different from that under cyclic tension due to the absence of crack opening and further notes that crack nucleation early in the fatigue life is a feature of both high and low amplitude fatigue loading.

In summary it can be said that the bulk of the evidence points to the formation of persistent slip bands, in which microcracks form, as being the most likely explanation of the mechanism of fatigue crack initiation. It is also evident that cross slip plays a large part in the formation of cavities from which the microcracks develop. However, as yet the picture is far from clear and much more research is required before the initiation of a fatigue crack is fully understood.

2.3.2 Fatigue Crack Propagation.

Possibly because it is easier to study, but more probably because of its greater practical interest, the mechanism of fatigue crack propagation has received considerably more attention over recent years than the initiation mechanism. Most workers are in general agreement on the Stage I and Stage II modes of cracking suggested by Forsyth[19] but there are three main schools of thought as to the actual mechanism of crack propagation in the two modes.

Forsyth suggests a shear mode in Stage I[26] and a cleavage mode in Stage II[25]; while Backofen and others[18, 30 - 33] suggest propagation along sub-grain boundaries and Laird[34] suggests a plastic blunting mechanism. All three suggested mechanisms are open to question and none of them have been generally accepted.

Factors which appear to affect crack propagation, especially the rate of crack propagation, include the level of applied stress, cycle frequency, microstructure of the material, the properties of the material such as stacking fault energy and strain hardening index, and the presence of any stress concentrator such as a notch or a defect.

At high strain amplitudes, fatigue fracture is predominantly by Stage II cracking at propagation rates of the order of microns per cycle. At low amplitudes, Stage I cracking predominates at rates measurable in Angstroms per cycle and it can occupy up to 90 percent of the specimen life but only a small fraction of the fracture surface. In reading the literature care must be taken in checking the use of terminology. An example of this occurs in the paper by Schijve[29] where he apparently completely contradicts the above statement concerning crack propagation in that he refers to rapid crack propagation in the shear mode (at 45° to the specimen axis) and slow crack propagation in the tensile mode (at 90° to the axis). However, further study

shows that Schijve is referring not to Forsyth's Stage I and Stage II cracking, but to the overall features of the fracture surfaces as observed in aluminium alloys in air. In these alloys the fracture starts at 45^{o} to the specimen axis (Stage I cracking), changes to 90^{o} to the specimen axis (Stage II cracking) and then back to 45^{o} to the specimen axis. The latter stage is near the end of the specimen life and rapid crack propagation does indeed occur.

The work of Forsyth and others has fairly definitely established the Stage I and Stage II modes of cracking. The Stage I cracking occurs along the shear planes and is normally at 45^{o} to the specimen axis. This stage follows after the formation of the intrusions described in the section on initiation and is probably a continuation of the slip process. Stubbington and Forsyth[26] have shown that the shear mode cracking occurs on $\{111\}$ crystal planes in high strength aluminium alloys and they produce evidence which suggests that reversed slip is the mechanism for the formation of the cracks. In the Stage II or tensile mode Forsyth et al[25] claim that cleavage plays a major part in the crack propagation and suggest that it is occurring on $\{100\}$ crystal planes. This latter suggestion is somewhat difficult to accept as there is little or no direct evidence to suggest that cleavage can in fact occur in fcc materials. Schijve suggests that the apparent cleavage observed by Forsyth is in fact a ductile fracture but with little

plastic deformation. Most workers appear to disagree with Forsyth on this concept of cleavage occurring in fcc materials.

Backofen and others[18, 30 - 33] claim that crack propagation occurs by cracking along the sub-grain boundaries which are produced in the material during fatigue loading. Miller et al[18] have shown that stacking fault energy appears to be a controlling parameter in crack propagation and from this they deduce that the crack is in fact propagating along the sub-grain boundaries because an increase in stacking fault energy (which favours sub-grain formation) leads to an increase in crack propagation rates. This work appears to be supported by that of Wilkov and Shield in that they found that an increase in stacking fault energy led to increased fatigue damage but Wilkov and Shield while observing sub-grain formation did not observe crack propagation along the sub-grain boundaries.

McEvily and Boettner[13] on the other hand, while agreeing that materials of lower stacking fault energy have an increased resistance to transgranular crack growth and that this correlation may be due to the effect of stacking fault energy on cross slip, point out that the increased resistance to this growth is somewhat offset by a greater tendency for crack growth along grain boundaries and twin boundaries as the stacking fault energy is lowered. They also agree with Forsyth that crack propagation is a two stage process with the first stage being a continuation of the cyclic shearing

responsible for crack initiation. The second stage is distinguished by a different mode of growth which depends strongly on the normal stresses at the crack tip.

Work by Chin and Backofen,[30] Holden,[31] Williams and Smith,[32] and Grosskreutz and Waldow[33] shows the formation of sub-grain structures in the material under test and that the fatigue crack apparently propagates along the sub-grain boundaries. The work of Grosskreutz and Waldow was done on thin foils and the fatigue damage observed during testing, using an electron microscope. While they observed a sub-grain structure with associated cracking it is questionable whether their work can be taken to be representative of the behaviour of bulk specimens.

The third mechanism proposed for fatigue crack propagation is that advanced by Laird[34] and this is the plastic blunting mechanism. Laird agrees with the two stage process of crack propagation with the first stage propagating at 45^{o} to the stress axis and the second stage at 90^{o} to the axis. From observations of Stage II cracking he postulates the plastic blunting mechanism and by inference concludes that a similar mechanism operates in Stage I cracking. In the plastic blunting mechanism Laird postulates that during the tension cycle deformation due to slip occurs at the crack tip and that this deformation takes place along the shear planes. The deformation continues until a rounded or blunt crack tip is formed and the degree of plastic strain in the

region of the crack tip is such as to prevent further crack growth. During the compression cycle, material at the crack tip folds back into the crack, forming two small notches on either side of the crack tip. These notches act as a source of dislocations during the following tension cycle. Laird shows metallographic evidence to illustrate how his proposed mechanism leads to the observed striations. A basic criticism of his work is that he worked with high strain amplitudes and very short specimen lives (of the order of 2000 cycles). At such high strain amplitudes the type of fatigue damage is not necessarily the type of damage that occurs under low strain amplitudes with long specimen lives. A further criticism is that some of his evidence comes from tests on plastic materials and it is very doubtful if such evidence can be used to support a theory of crack propagation in a crystalline material such as a metal.

In summary it can be said that while a great deal of research has been and is being carried out in the field of fatigue crack propagation, we are as yet far from understanding the mechanism by which such cracks propagate. Three mechanisms have been suggested and all leave questions unanswered, but it is possible that the crack propagation is in fact a combination of several different mechanisms, different aspects of which have been observed by the various workers. Many of the theories have been advanced in an effort to explain the appearance of striations on the fracture surfaces and their

apparent relationship to the load history of the specimen.

The environment has been found to have a major effect on the formation of fatigue cracks and their rates of propagation and this factor is covered in Chapter Three.

CHAPTER THREE.

3. THE EFFECT OF ENVIRONMENT ON METAL FATIGUE.

3.1 Introduction.

The first published paper to describe the effects of environment on metal fatigue was written by Haigh in 1917.[35] Haigh observed the effect of sea water on the fatigue strengths of wire towing ropes and noted how the fatigue life was considerably reduced. His paper resulted in a number of other researchers, both in America and England, studying this new phenomenon of corrosion fatigue, that is the conjoint action of corrosion and fatigue. Most researchers used wet corrosive media and a 3% NaCl solution was the most commonly used corrodent. The reason for using this corrodent was probably due to the interest in naval problems and also to the interest in seaplanes during the 1920's and 1930's. A great deal of the research was directed at examining the corrosion fatigue properties of the then aircraft alloys and there was considerable interest in the properties of thin steel wires such as were used for wing rigging.

The most important contribution to the understanding of corrosion fatigue was due to McAdam in America. His work is still the most comprehensive and is the only work which covers a wide range of materials, corrodents, stress conditions and test frequency. Other notable contributions in the early investigations were due to Gough and Sopwith in England.

Interest in corrosion fatigue lapsed somewhat in the late 1930's and 1940's, except for the work of Evans and others at Cambridge University. Evans investigated the mechanism of corrosion fatigue and his electro-chemical theory is still the most generally accepted theory of corrosion fatigue.

The last 20 years has seen renewed interest in the effects of environment on metal fatigue, but research has moved away from wet corrosive media to investigating the effects of gaseous environments, a number of researchers having shown that such environments also markedly affect the fatigue properties of metals and alloys. The present interest in space exploration has focused attention on the fatigue behaviour of metals and alloys, especially the light alloys, under conditions of near vacuum. Most of the recent literature therefore is concerned with the effects of gaseous environments and cover mostly the light alloys. There is a tendency to treat wet corrosive media and gaseous environments as representing two entirely different phenomena.

A number of review articles have been published covering corrosion fatigue and the subject matter covered reflects the change in emphasis. The earliest review is written by Gough[36] in 1932 and he covers the work of McAdam very well indeed. The next major review is by Gilbert[37] in 1956, and he covers all the work up to that date including that reviewed by Gough. A less comprehensive review was published by Gould,[38] also

in 1956. All these reviews concentrate mainly on wet corrosive media as this was the main field of study up to that time. Evans discusses corrosion fatigue in his book on corrosion[39] and gives details of the various techniques used to apply the corrodent to the specimen. The effect of gaseous environments is reviewed by Wadsworth[40] in 1958, Hudson[41] in 1965, and Achter[42] in 1967. These last three review articles indicate the renewed interest in the effects of environment on metal fatigue in the last 20 years and indicate the increased volume of literature in this field.

3.2 Wet Corrosive Media.

The most outstanding contributor in the field of wet corrosive media and their effect on metal fatigue was the American, McAdam,[43 - 47] who over a period of some 15 years carried out research covering a wide variety of materials and used a number of different corrodents. His work is still the only really comprehensive study of the problem of corrosive fatigue. McAdam's work is very well reviewed by both Gough[36] and Gilbert[37]. McAdam found that for all the materials tested the S - N curve in the corrodent was lower than the corresponding curve in air. He also noted the rapid onset of corrosion fatigue in aluminium and its alloys and that the effect of pre-corroding in these alloys was almost as serious as the actual corrosion fatigue tests, in producing a reduced fatigue life. From his work McAdam postulated the concept of a corrosion fatigue limit to explain the typical shape of the

S - N curves which resembled those obtained for steel in air, but this concept did not receive general assent. From studies using different frequencies of stress cycle he showed that time of test and the number of cycles of test must be treated as independent variables and suggested that a given number of cycles will produce greater damage at a low frequency than at a higher frequency due to corrosive effects, while a given time will produce greater damage when the frequency is high than when it is low because of the greater extent of fatigue damage. The mechanism of corrosion fatigue suggested by McAdam was a two stage process, the first stage being the formation of pits and crevices by corrosion attack and the second stage a purely fatigue stage initiated by the corrosion pits. Thus the corrodent was considered to play no part in the crack propagation stage. To test the validity of this theory McAdam carried out two stage tests, in which specimens were subjected to a period of corrosion fatigue followed by a fatigue test to destruction in air. McAdam claimed that his results proved the validity of his theory.

It is interesting to note that McAdam's work showed less scatter in the corrosion fatigue results than for results of tests in air and this feature has been observed by most researchers. Another feature is that the reduction in fatigue life for an aluminium - 4% copper alloy, was apparently due solely to corrosive attack alone in that pre-corrosion gave the same reduction in fatigue life. In general McAdam found

that the method of stressing did not appear to have a large effect on corrosion fatigue results and that variation in mean stress produced similar changes to those observed in air fatigue tests, that is increased mean stress reduced the fatigue life. In all his test work McAdam used a drip feed of the corrodent on to the specimen surface. Some experimental work on the effects of protective coatings was also carried out by McAdam and he found that by shielding with red lead or cotton strips the fatigue life of the specimen could be improved both in corrosion fatigue and in air. McAdam's work covered the corrosion fatigue of nickel, monel metal, other nickel-copper alloys, aluminium, aluminium-manganese alloys, an aluminium-4% copper alloy (duralumin), copper alloys and various steels. As corrodents he used 3% NcCl solution, distilled water, and various river waters.

During the same period that McAdam was active in America, Gough and Sopwith were active in England. Their work[48 - 53] was almost as comprehensive as that of McAdam's, but they concentrated mainly on steels, copper alloys and aluminium-4% copper alloy, but investigated the effects of protective coatings more thoroughly and finally moved into the field of gaseous environments. In the wet corrosive media experiments Gough and Sopwith used a spray of 3% NaCl solution as the corrodent. Some of their research was on bicrystal and single crystals of aluminium and in the bicrystalline specimens they observed cracking at slip bands where preferential corrosion

occurred.[50] They also noted the occurrence of pitting and that although these pits joined up to form large cavities these apparently had nothing to do with the fatigue failure.

From results of their later work[51] Gough and Sopwith rejected McAdam's idea of a corrosion fatigue limit. In a study of the effects of protective coatings[52] they covered a wide range of coatings on a 0.5% carbon steel in a 3% NaCl solution. They found that zinc, cadmium and aluminium coatings gave very good protection and that an enamel coating gave longer life than the bare material, but it was not as good as the metallic coatings in protecting from corrosion fatigue. As with McAdam they found that the application of a mean stress considerably reduced the corrosion fatigue life of the material. In their later work Gough and Sopwith turned to a study of the effects of gaseous environments on metal fatigue.

Following on from Gough and Sopwith, Evans and co-workers at Cambridge University carried out a series of experiments aimed at establishing the mechanism of corrosion fatigue.[54 - 57] For their work they used a Haigh-Robertson wire fatigue machine and tested steel wires 0.1 inch in diameter at 6000 r.p.m. One and two stage tests were used and 3% NaCl solution was used as the corrodent. They developed a method for continuously measuring the electrical potential between the oxide film on the wire and the corrosive solution and found that a drop in potential during the test indicated

that the oxide film had been ruptured. Once the film was broken rapid failure of the specimen followed. The wire was totally immersed during the corrosion fatigue test, rotating in a bath of the corrodent. Like Gough and Sopwith, Evans found that zinc coatings could improve the corrosion fatigue life of steel.

The mechanism of corrosion fatigue put forward by Evans and Simnad[56] was an electro-chemical one. They postulated that during stressing certain regions of the metal surface became anodic to other regions thus setting up electro-chemical cells on the metal surface. Once the oxide film on the metal surface is ruptured, electro-chemical attack is possible where the metal is exposed and thus rounded cavities similar to those of normal corrosive attack form on the metal surface. Due to the action of the applied stress assisting the corrosive attack, these cavities develop into narrow pits or crevices extending down into the metal. The rate of propagation of these pits tend to decrease as they grow, thus allowing time for the growth of further pits before fracture occurs as a result of a normal fatigue crack initiating at the bottom of one crevice and propagating to give final failure. Thus Evans and Simnad agree with McAdam's concept of corrosion fatigue being a two stage process with the first stage being purely a corrosive attack on the metal surface which produces deep pits. In the second stage which is purely a fatigue stage, a fatigue crack develops from one of these pits thus causing final

failure. Evidence supporting the electro-chemical mechanism is that cathodic protection either by protective coatings or by application of a cathodic e.m.f., can inhibit or prevent the onset of corrosion fatigue.

With the development of the dislocation theory and the demonstration that metals deform by slip due to dislocation movement, some doubts were raised as to the validity of Evans' electro-chemical mechanism for corrosion fatigue. Accordingly, Whitwham and Evans[57] investigated the effects of dry fatigue followed by corrosion fatigue. They used similar wires to the previous investigations and found that dry fatigue followed by corrosion fatigue had no effect on the corrosion fatigue life. From this work they claimed that the electro-chemical concept of corrosion fatigue was in fact the valid one.

Some later workers appear to still doubt the validity of the electro-chemical mechanism, notably the Russians Vedenkin and Sinyavskiy.[58] In the Russian work they used the technique of measuring electrical potentials developed by Evans but showed that the potential drop in fact coincided with the formation of a crack, showing the deterioration of the metal potential with cyclic loading to be the result rather than the cause of crack formation. They also showed that the cathodic protection mechanism was not so much the suppression of local currents between stressed and unstressed portions of the metal, but more the formation of an alkaline environment around the cathode with a concentration sufficient

to promote passivation of the cathode surface.

Two recent studies of corrosion fatigue in wet corrosive media cast further doubts as to the validity of the electro-chemical mechanism. Kitagawa[59] using two stage wet-dry tests showed that the corrodent has a significant effect on the crack propagation rate and that after a certain stage the total life remained constant whether the test was continued in corrodent or air. Until this stage was reached however, removal of the specimen from the corrodent caused a slowing down of crack propagation. In his paper there is no mention as to whether he dried the specimens after removing them from the 3% NaCl spray and it is possible that some corrodent remained trapped in existing cracks. However, his work would suggest that Evans and McAdam were wrong in suggesting that the corrodent was involved only in the initiation of corrosion fatigue cracks. Cornet and Behrsing[60] in a study using high purity aluminium single crystals produced evidence of the presence of persistent slip bands in both air and corrosion fatigue. These workers claim that their investigation has demonstrated that the processes of fatigue and corrosion fatigue are quite similar. However, in view of the somewhat contradictory findings in the fatigue properties of single as compared with poly-crystalline specimens in studies of air fatigue,especially in regard to crack propagation rates, it is felt that their claim must be treated with some caution.

Other notable workers in the field of wet corrosion fatigue include Stubbington and Forsyth[61 - 62] who would appear also to disagree with the electro-chemical mechanism of corrosion fatigue. These workers report the presence of river pattern striations on corrosion fatigue fracture surfaces and this would support the idea that slip is playing some part in the process. Forsyth draws some of his evidence for the cleavage mechanism of Stage II cracking in air fatigue tests from his work on corrosion fatigue.

Recent studies by Lorkovic,[63 - 64] Panseri,[65] and Endo and Miyao[66] add some information to the field of corrosion fatigue. Panseri et al studied the effects of varying frequency and obtained results similar to those reported by McAdam some 30 years earlier. They also studied the effect of composition in aluminium-magnesium alloys and found that variation in composition had no apparent effect on the corrosion fatigue life. Endo and Miyao studied the effects of combined torsion and bending at various cycle frequencies and found similar effects to those reported by McAdam.

There have been very few investigations on the effect of temperature on corrosion fatigue and those reported give completely contradictory results. Gould[67] showed that by increasing the temperature from 15°C. to 45°C. the endurance of steel wires was halved while Cornet and Golan[68] showed

that higher test temperatures gave improved corrosion fatigue life. Cornet and Behrsing[69] found no temperature effects on single aluminium crystals in distilled water or 4% NaCl solution. It would appear that the results reported earlier are due to experimental features rather than an effect on the actual mechanism of corrosion fatigue.

A large group of researchers have studied the effects of protective coatings on corrosion fatigue.[70 - 83] The coatings studied include plated, sprayed and clad metallic coatings, enamels, paints, anodizing, rubbers, oils and other organic chemicals. In all cases an improvement in corrosion fatigue life was noted especially where water vapour and oxygen were excluded from the specimen surface. There is some evidence to suggest that cathodic currents can also prevent corrosion fatigue.[56,58, 78 - 80] Radd et al[84, 85] have shown that the pH value of a 3% NaCl solution saturated with NaOH affects the corrosion fatigue of steel and that below a pH value of 11.1 corrosion fatigue is apparently stifled. It has been suggested by various authors[86, 87] that the effect of electro-deposited coatings on corrosion fatigue is a complex combination of mechanical and chemical effects.

From a study of the published literature dealing with the effects of wet corrosive media on metal fatigue it can be said that certain features are clearly established, but that there is still some doubt as to the actual mechanism by which

corrosion fatigue occurs. The generally accepted theory is that of an electro-chemical mechanism put forward by Evans and Simnad, but more recent authors tend to suggest that the mechanism of corrosion fatigue and air fatigue are in fact the same. The factors involved in corrosion fatigue testing are - the type of stress applied; the time of the test; the frequency of stress cycle; the nature of the corrodent; the surface condition of the specimen including the nature of the protective coating if any; and the method of applying the corrodent. The methods of applying the corrodent can apparently markedly affect the test results as contradictory results have been reported for totally immersed specimens compared to specimens tested in a spray of corrodent. Most workers use either a drip or flow feed or corrodent on to the specimen surface, or spray the corrodent into a suitable chamber containing the specimen.

A notable characteristic of corrosion fatigue failures is the multiplicity of cracks as distinct from ordinary fatigue. As a consequence the fracture frequently shows a characteristic serrated appearance, and many subsidiary cracks can usually be found near the main one. Corrosion fatigue cracks are usually transcrystalline although some cases of intercrystalline cracking have been reported.

Several workers have reported the presence of striations on corrosion fatigue fractures, notably Stubbington and Forsyth. Work by Thompson and Mulhearn[88] in Australia, however, showed that striations on fatigue fracture surfaces were progressively removed by corrosion even with such mild corrosive conditions as a warm and humid atmosphere. In the light of this work it is felt that there must be caution in interpreting any surface features on corrosion fatigue fractures.

3.3 Gaseous Environments.

It is now generally recognised that gaseous environments can also affect the fatigue properties of metals and alloys. The researches in this field come into two categories; those dealing with fatigue under conditions of vacuum or partial vacuum, and those dealing with dry and damp gases including air. The problem of gaseous environments has received more attention than wet corrosive media over the last 20 years and various theories have been put forward to explain their effects.

The first to show the influence of gaseous environments on metal fatigue were Gough and Sopwith[89 - 90] who tested copper, brass, lead and armco iron in laboratory air, partial vacuum, dry purified air, damp purified air, dry and wet nitrogen, using reversed direct stresses. They noted a decrease in fatigue life in damp gases but an improvement in fatigue life in both dry gases and partial vacuum. From their observations they concluded that oxygen in the presence

of water vapour is responsible for the loss in fatigue properties in the damp gases. Their work led to the rather surprising observation that fatigue tests in damp air are in fact a type of corrosion fatigue test.

Wadsworth and co-workers[40, 91 - 93] continued the study of the effects of vacuum and gases on the fatigue lives of copper, aluminium, gold and a 0.5% carbon steel. They found that for both annealed pure metals and alloys, cracks formed very early in the test (usually after about 2% of the expected life) and that the fatigue life was effectively determined by the rate of crack propagation. This infers that the main effect of gaseous environments was on crack propagation rather than on crack initiation. For all metals other than gold, the presence of air increased the rate of crack propagation and hence reduced the fatigue life. A greater effect was noticed at lower strains where the specimens had longer lives. In cases where other gases were used, only those gases which combined easily with the metal had any effect. Thus water vapour was as effective as air on aluminium but was without effect on copper. Where oxygen affected a metal it was necessary for the oxygen to be present as a gas during the fatigue test. From the results of their work and other researchers, Wadsworth and his co-workers suggested that the effect on fatigue life is due to chemical attack at the tip of the crack. The change in fatigue life produced by the gas depends on the gas-metal combination and is also sensitive

to the presence of impurities in the metal.

In their experimental work, Wadsworth et al observed the presence of persistent slip bands both in gas and vacuum and noted that the fatigue cracks formed in the slip bands.

Snowden[94 - 96] in a series of researches on lead showed that surface deformation is greater in vacuum than in air although vacuum gave the longer fatigue life. He also found that the fatigue life was sensitive to the gas pressure and that three distinct ranges were observed. In the high pressure range the fatigue life remained constant and cracking was intercrystalline, in the intermediate range the fatigue life increased rapidly with decreasing pressure and in the low pressure range the life remained unaffected by further reductions in pressure. In all three ranges failure occurred by extensive slip deformation. Snowden suggested that aluminium should behave in a similar manner at high temperatures. As with Wadsworth's research, Snowden's results showed a greater effect on fatigue life at lower strain amplitudes.

Several other workers have noted the dependence of fatigue life on gas pressure recorded by Snowden. Achter et al[97] and Hordon[98, 99] in studies involving nickel, stainless steel, copper and aluminium in air, vacuum and inert gases, noted that these metals also showed the three pressure ranges reported by Snowden for lead. They also reported that the

critical gas pressure required for fatigue life improvement was temperature dependent, a higher temperature requiring a higher critical gas pressure. Hordon attributed the effect of gas pressure to the related kinetics of residual oxygen and water vapour absorption at crack surfaces and fatigue crack growth. Both workers noted the major effect of the gases was on crack propagation rates.

Broom and Nicholson[100] from studies on age-hardened aluminium alloys showed that by drying the air and also by coating the specimen surface with butyl rubber which has a low permeability to water vapour, the fatigue life could be improved. These workers also noticed that failure occurred by slip and suggested that the diffusion of hydrogen ions into the metal was the cause of the reduction in fatigue life. The idea that the presence of hydrogen ions had some influence on the process of fatigue in aluminium alloys and steel gained some support from the work of Holshouser and Bennet[101] who showed the evolution of hydrogen from metal surfaces during fatigue. However, no hydrogen gas evolution was observed during fatigue tests on copper, brass, cadmium, nickel, stainless steel, tin, titanium or zinc. This would indicate that the presence of hydrogen ions affecting metal fatigue is not a universal phenomenon.

A combination test to determine the effects of atmospheric corrosion on the fatigue life of aluminium alloys was devised by Leybold et al.[102] Fatigue tests were conducted outdoors by applying 4,000 cycles of load in a ten minute period each working day, while the specimens were subjected to atmospheric conditions over a period of several months. For comparative purposes similar specimens were tested indoors. Atmospheric corrosion was found to shorten the average lives of the specimens by a factor of about 3 for 7075 - T6 and 2024 - T3 in the bare condition,and by a factor of about 1.5 for clad 7075 - T6 and had no significant effect on the average life of 2024 - T3 clad specimens. Specimens of 7075 - T6 alloy exposed for six weeks at zero stress showed a greater loss in fatigue life than did similar specimens in the atmospheric fatigue test. This result is similar to that of McAdam who also found that for aluminium alloys, pre-corrosion shortened the fatigue life almost as much as did corrosion fatigue.

Several researchers have recently investigated the effects of relative humidity and water vapour on the fatigue crack growth in aluminium alloys including the 2024 - T3 alloy. Dunsby and Wiebe[103] showed that low relative humidity gave the best fatigue life and high humidity the poorest. This result possibly explains some of the scatter found in air fatigue tests and the difference between various reported fatigue properties for aluminium alloys especially. Other

workers [104 - 106] have shown that the main effect of water vapour is to increase the crack propagation rates and thus cause reduction in fatigue. Bradshaw and Wheeler[104] and Hartman[105] reported that the crack shows a change in direction during tests in the presence of water vapour, changing from 90° to the tensile stress to 45° to the tensile stress. As a similar change has been reported by other workers for fatigue tests in laboratory air, it is not certain just what the significance of this change is.

In summary it can be said that the major effect of gaseous environments is on crack propagation rates rather than on crack initiation. The crack growth rates of some metals are accelerated more by the presence of oxygen than by water vapour, while for others the reverse is true. Increases of cyclic frequency and of stress decreases the magnitude of the effect of the environment. Temperature and gas pressure both appear to play some part in the mechanism. There have been two explanations proposed to explain the effects of gaseous environments; one is that a process of corrosive attack at the crack tip accelerates the crack propagation rate and the other suggests that oxide layers formed on the crack surfaces in the presence of oxygen gas prevents the rewelding of crack surfaces. The experimental evidence confirms that in gaseous and vacuum environments the normal fatigue mechanisms of cyclic slip, microcrack formation and macrocrack formation occur.

Thus there is no distinction between vacuum tests and air tests as far as the mechanism of fatigue is concerned and the only problem to be explained is why the air crack propagates faster than the vacuum crack. The theory of corrosive attack at the crack tip is the most likely explanation. If air fatigue can be thought of as a mild corrosion fatigue test then this raises some question as to the validity of the electro-chemical mechanism of wet corrosion fatigue crack formation. It seems likely that corrosion fatigue occurs by slip and that the main effect of the corrodent is to assist crack propagation rates.

CHAPTER FOUR.

4. ROTATING BEAM FATIGUE TESTS.

4.1 Test Materials and Equipment.

The material used for all the fatigue test programmes was 2024 - T4 aluminium alloy, supplied in the form of ¾ in. diameter extruded rod. All the rod, which had been specially supplied by the manufacturers, was from the same heat and had been extruded and heat treated together. The alloy was tested in the "as received" condition, that is, solution treated and naturally aged. No attempt was made to re-heat treat the alloy because

a) it was felt that the material as supplied would be very similar to that used in the aviation industry, and

b) of the difficulty in controlling the heat treatment conditions and achieving uniformity of treatment when using a small laboratory furnace for batch treatment.

The chemical composition, mechanical properties and heat treatment of the alloy are given in Table 4/I.

TABLE 4/I - Composition and Properties of 2024 - T4 Alloy.

Element.	Manufacturer's Data %	Actual Analysis %	Mechanical Properties.
Iron	0.26	0.25	U.T.S. 33.5 Tons/ sq.in.
Copper	4.45	4.35	
Silicon	0.09	0.09	0.1% P.S. 25.2 Tons/ sq.in.
Manganese	0.74	0.85	
Magnesium	1.46	1.70	% Elong. 20%
Titanium	0.02	-	
Aluminium	Rem	Rem	E 4.8×10^3 Tons/ sq.in.

Heat Treatment: 65 minutes at 495°C. ± 3°C. and naturally aged.

The test specimen used for the rotating beam tests is shown in Figure 4/1 but the following description of specimen preparation applies to all the fatigue test specimens used in this research. All test specimens were machined from the extruded rod and were left approximately 0.015 in. oversize. The machined specimens were then hand polished to the final diameter using a lathe to rotate the specimen and a rotating brass drum to hold the polishing paper in contact with the specimen. A photograph of the polishing rig is shown in Figure 4/2. The speeds of lathe and drum were so arranged that the peripheral speeds of specimen and drum over the arc of contact were equal. This arrangement resulted in the final polishing scratches being parallel to the specimen axis.

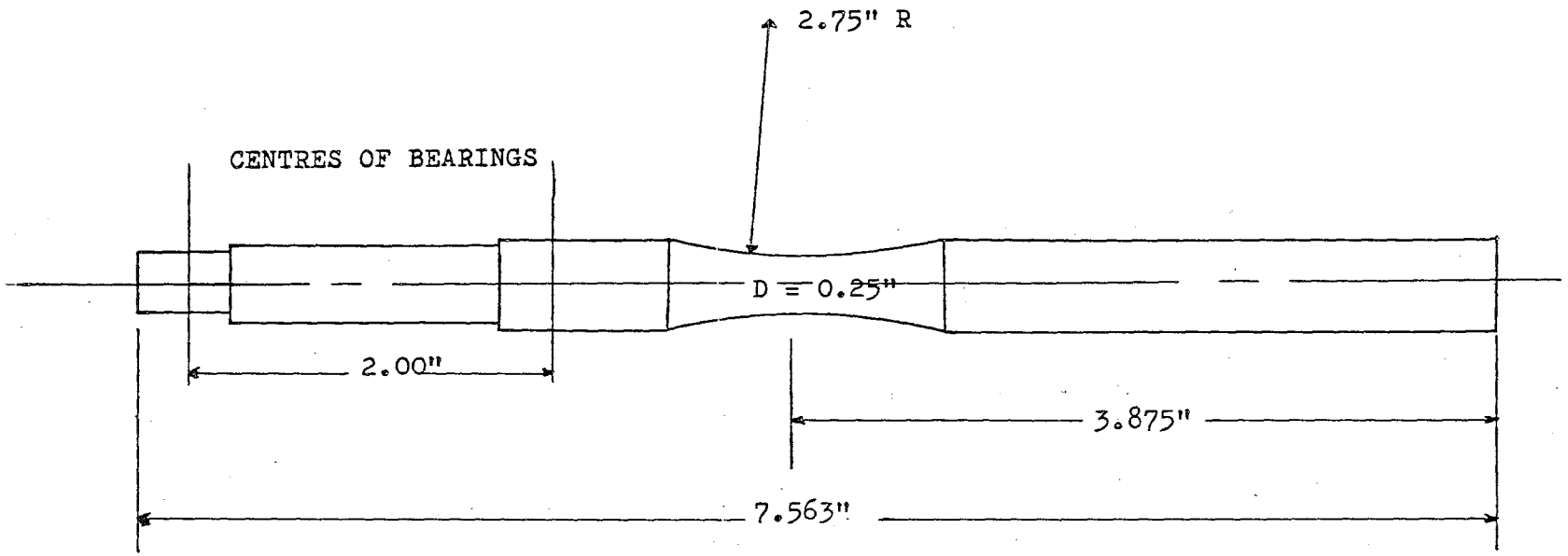

Figure 4/1: Rotating beam fatigue test specimen.

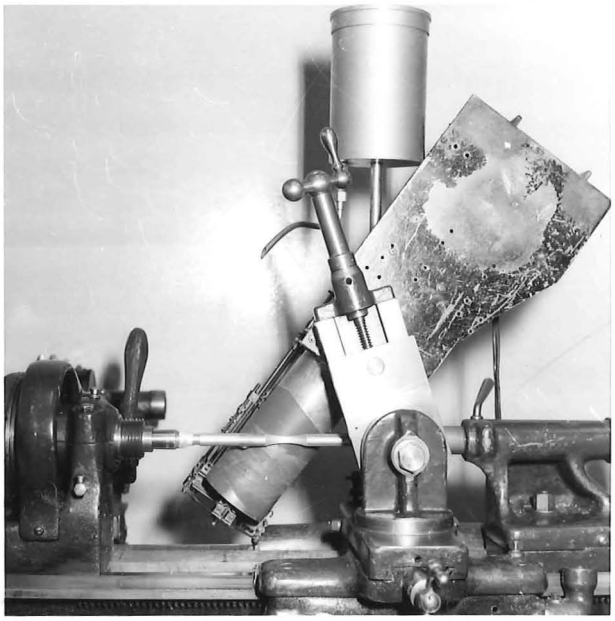

Figure 4/2: Polishing machine used for final polishing of fatigue test specimens after machining.

Two stages of polishing were employed; 120 grade paper being used for the initial rough polish which brought the diameter down to within 0.002 in. of the finished diameter, and 600 grade paper for the final polish. Both grades of paper were lubricated with kerosene. After polishing, the specimens were washed in acetone and the actual finished diameter measured, using a Leitz tool-maker's microscope. A check for eccentricity was made while measuring the finished diameter and any specimen found to be eccentric was discarded, normally however, eccentricity was negligible.

When measuring the diameters of the specimens, each specimen was held between centres and the diameter measurement obtained using the micrometer on the microscope table. A magnification of 9.5 was used for all measurements. By holding the specimens between centres a simple check for eccentricity was to slowly rotate the specimen and check the line up of the edge of the specimen surface with the cross wires of the microscope. Where eccentricity was detected several measurements of the specimen diameter were taken at points around the circumference. As a standard procedure the specimen diameter was measured at two diametrically opposite points. Specimens were rejected if the eccentricity exceeded 0.001 in. The accuracy claimed for the instrument is 0.0001 in. and it was found that this accuracy could be consistently obtained provided the same procedure was followed for each measurement.

However, when the known scatter of fatigue test results was considered it was felt that the measurement of the specimen diameters to three significant decimal places was sufficiently accurate.

Two or three specimens out of each batch prepared were examined under a metallurgical microscope to check on surface finish which was found to be quite consistent over all specimens examined. The standard surface finish consisted of 600 grade polishing scratches parallel to the specimen axis over the centre portion of the specimen. The groove depth from 600 grade paper polishing is of the order of 15 microns, i.e., 0.0006 in.

The test specimens were polished in batches of sufficient number to complete the immediate test programme. An effort was made to leave the specimens for a week after polishing and to start the fatigue test within two weeks of finishing polishing. This was however not always found to be practicable especially when some tests occupied a longer time than estimated. No effort was made to protect the specimens from oxidation after polishing.

The superphosphate used as the corrodent in the test programme was standard aerial superphosphate as used in aerial top dressing. This type of superphosphate is basically a diluted superphosphate containing 10% ground serpentine rock. The components are the same as for normal superphosphate

except that the free H_3PO_4 acid is reduced and some of the $Ca(H_2PO_4)_2$ is possibly converted to $(Ca,Mg)(H_2PO_4)_2$ and $(Ca,Mg)HPO_4$. The physical condition under high humidity conditions is superior to superphosphate and it is thus preferred for aerial topdressing. A 12lb. sample of the superphosphate was obtained from the manufacturers and the whole batch ground so as to pass through a size 72 British Standard Screen. The ground superphosphate was then thoroughly mixed and stored under constant atmospheric conditions in the temperature controlled fatigue laboratory. Some concern was felt that the superphosphate might age on standing and thus vary in chemical composition, however, when this point was discussed with the Chief Chemist (Mr.Gallaher) of the New Zealand Fertiliser Manufacturers' Research Association it was confirmed that relatively little change could be expected. During extended storage chemical reactions continued at a slow rate and would probably result in a reduction in the free acid content (if any), a reduction in unreacted phosphate rock, an increase in the proportion of soluble phosphate salts and an increase in hydration levels of component salts with reduction in free moisture level. In the light of this information it is felt that as far as possible the superphosphate used for the test programme was of similar chemical composition and properties.

Three duplex Avery cantilever rotating beam fatigue machines were used for the main testing programme. Each machine was powered by a ¾ h.p. a.c. synchronous motor running at a nominal speed of 3000 r.p.m. For each specimen a clock counter is provided to record the number of stress reversals. One revolution of the pointer of each clock indicates 10 million reversals, one small division equalling 100,000 reversals. Two cut-out contacts are provided, one under the centre of each load pan. Upon fracture of one specimen, the load pan suspended from it drops on to the cut-out contact breaking the circuit of its stress cycle counter. The second contact is operated by the fracture of the other specimen and stops the second counter and the motor simultaneously.

Each rotating beam (R.B.) machine held two specimens loaded as simple cantilever beams (wholer system). This system of loading gives a varying bending moment over the specimen and the actual stress at the centre of the specimen depends very much on the accuracy with which the specimen is machined. A modified loading system, based on the design of the N.P.L. rotating beam fatigue machine, was designed and this system produced a constant bending moment along the gauge length of the specimen. By using a waisted specimen, the maximum stress level was thus located at the smallest cross section regardless of the length of the specimen held in the machine chuck. The design of the modified system is shown in Figure 4/3.

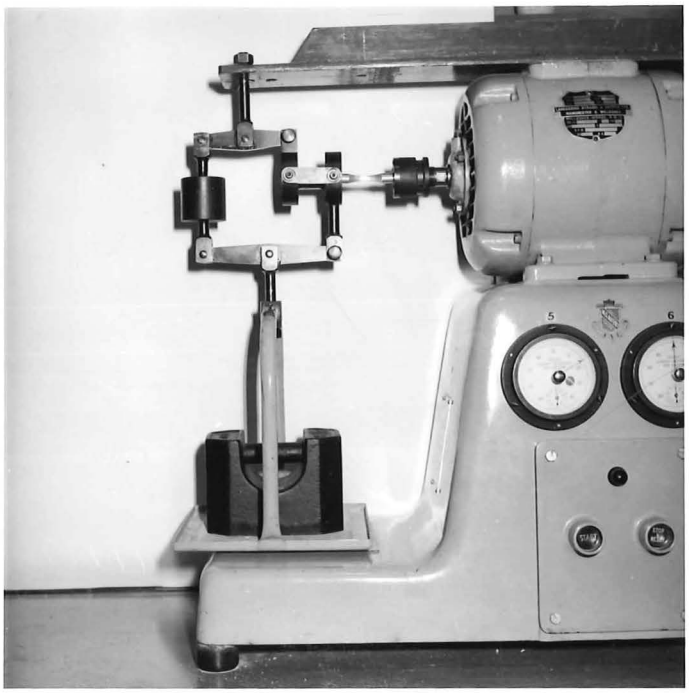

Figure 4/3: Rotating beam fatigue machine showing modified loading system.

In order to keep the corrodent from being splashed on to the actual machines and in later tests to keep the corrodent in contact with the specimen, a chamber was designed which fitted round the specimen. Several designs of chamber were tried and the final design was a chamber with hardboard ends and perspex sides. The perspex sides were removable but for normal testing they were sealed into the hardboard. The corrodent entered the chamber from the top and was lead to waste through a bottom tube. The chamber had to fulfil two purposes, namely, to contain the corrodent and to support the broken specimen without spillage of the corrodent. The broken specimen had to be supported so that it was clear of the specimen end remaining in the chuck of the machine as this end continued to rotate until failure of both specimens occurred. It was found necessary to place plastic splash guards on the specimen to prevent the corrodent entering the bearings of the loading rig, several bearing failure having occurred before the guards were fitted. The guards were initially fitted inside the chamber but in the final design they were placed outside the chamber, however, the presence of the guards in either position had no apparent effect on the results of the tests.

4.2 Fatigue Tests in Air.

In order to establish the fatigue curve in air for the 2024 - T4 alloy tests were made at a number of different stress levels. All three R.B. machines were used for this programme and specimens were tested in pairs, each pair on a machine

being tested at the same stress level. At least four specimens were tested at each stress level and where scatter occurred more specimens were tested. Considerable scatter did occur in some cases but from the literature it appears that this is a feature of this particular alloy. The resulting fatigue curve is shown in Figure 4/4 and actual test results tabulated in Appendix A. A feature observed was the appearance of a black deposit on the actual fatigue fracture surface but similar deposits have been reported by other workers and it appears that it is fretting debris possibly from the $CuAl_2$ particles present in the micro-structure of the alloy.

4.3 Fatigue Tests in Superphosphate.

In fatigue tests using a superphosphate environment, the original aim was to test the specimen in an atmosphere of damp superphosphate dust such as would be encountered in an actual aircraft. However, considerable experimental difficulties were encountered and three techniques were evolved to keep the corrodent in contact with the specimen. The experimental problems encountered were due in part to the nature of the R.B. fatigue test and in part to the nature of the corrodent being used. With the rotating specimen, any corrodent tended to be flung off and there was also the difficulty of sealing the chamber around the specimen. The superphosphate also, once it became damp, could not be made to flow into the chamber. All the work reported in the literature involving wet corrosive media in fatigue testing has been carried out using solutions,

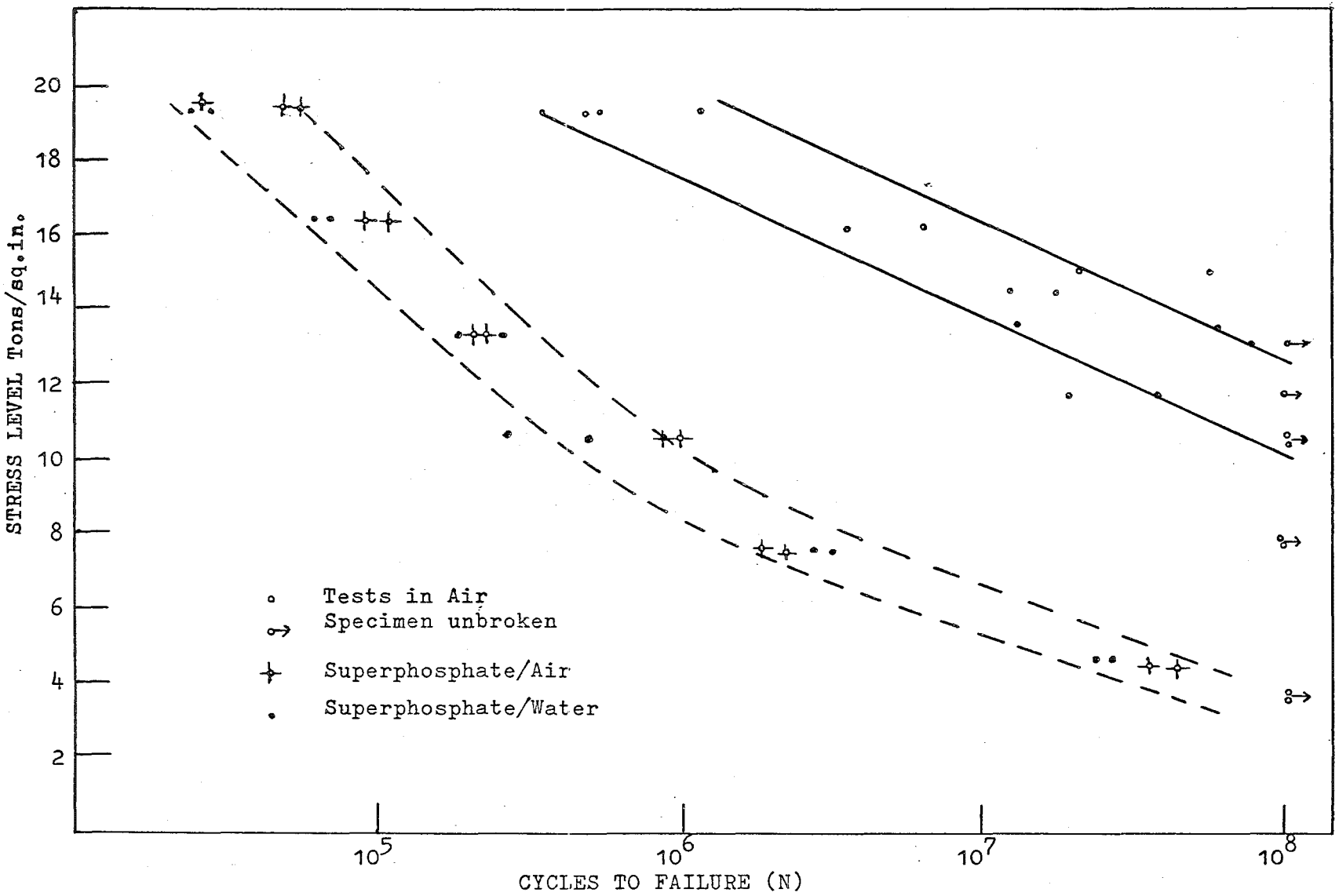

Figure 4/4: Results of fatigue tests in Air, Superphosphate/Water and superphosphate/Air.

no previous work has involved solid particles of corrodent.

The initial test programme used a solution of 25 grammes per litre of finely ground superphosphate in tap water, which was allowed to drip on to the centre of the specimen and was led to waste through the bottom of the chamber. The suspension of powder was kept agitated by a mechanical stirrer and the drip rate adjusted to give approximately 2 drops per second. It was found necessary to maintain this rate to prevent clogging of the feed tubes. A similar experimental set-up was used for tests involving tap water alone and a 3% NaCl solution. The tap water used was drawn from the Waimairi County supply and a typical analysis of the water is given in Table 4/II, together with an analysis of the actual superphosphate solution. The experimental conditions gave a partially immersed condition in that only the centre of the specimen received the drop of corrodent and the excess tended to be flung off as the specimen rotated. With the superphosphate solution the undissolved material was carried over with the liquor and in the long term tests a noticeable deposit built up on the actual specimen.

The results of the fatigue tests in the superphosphate/water solution are shown in Figure 4/4 together with the air curve for comparison, while actual test results are tabulated in Appendix A. The most noticeable differences between these corrosion fatigue tests and the air tests were firstly, the marked reduction in fatigue life and secondly, the markedly

different type of fracture produced. However, the black deposit on the fracture surfaces was again observed. The fractures will be discussed more fully under Fractography and Metallography in Chapter Seven.

TABLE 4/II - Analyses of Water and Corrodent[107]

	Waimairi County Water	Superphosphate Solution
Ph	6.6 - 7.0	4.5
Total Solids	75 p.p.m.	1260 p.p.m.
Calcium	34 "	188 "
Magnesium	7 "	38 "
Chloride	5 "	30 "
Silica	12 "	4 "
Alkalinity	35	60
Sulphate (SO_4)	*	570 p.p.m.
Phosphate (P_2O_5)	*	480 "
Fluoride	Trace	13 "

* Not analysed.

The second phase of the experimental work involved the use of solid superphosphate dust in a stream of moist air to simulate the conditions which would be encountered in an actual aircraft. It was hoped to supply the powder continuously and to draw the excess through the chamber by a suitable suction device, the moist air being drawn in with the powder at the top of the chamber. Unfortunately this system worked only so long as the powder remained dry, because as soon as moisture entered

the chamber the superphosphate powder clogged badly and it proved impossible to maintain a flow of powder through the chamber. An attempt was made to use the fluidised bed technique by blowing moist air in at the bottom of the chamber. This approach failed for two reasons, one being the clogging mentioned above and the other and more serious reason, was the contamination of machine bearings by superphosphate powder escaping from the chamber. It was virtually impossible to seal the chamber around the specimen and still be able to maintain this seal when the specimen fractured. The following procedure was then adopted. The chamber was packed with superphosphate powder until the specimen was covered completely. Air, from a compressed air cylinder, was then passed through a simple humidifier and blown into the chamber, passing through the superphosphate powder. The powder absorbed the moisture and thus moist superphosphate was maintained in contact with the specimen as required. If necessary, extra powder was fed into the chamber during the tests to ensure that the specimen was covered with superphosphate.

This technique proved satisfactory except that the actual moisture content of the superphosphate could not be controlled very easily. There was a tendency for free water to collect on the sides of the chamber and possibly around the specimen, although this latter point could not be very easily established. To avoid this, an intermittent flow of air was allowed to enter

the chamber although the humidifier was left connected to the chamber inlet. By these means it was possible to avoid free water accumulating in the chamber while still maintaining a moist atmosphere. It is realised that there are two serious objections to the above technique. One is the possibility of free water around the specimen together with variability of moisture content, especially in long term tests, and the other is the possible abrasion effects from the powder lying in contact with the rotating specimen. However, the test results obtained from using the above technique showed remarkable consistency and this would seem to indicate that the variability of moisture content and abrasion effects were not affecting the actual fatigue process to any marked extent. The results of fatigue tests using the chamber techniques are also shown in Figure 4/4 with the results of the air tests and the superphosphate/water tests. Actual test results are tabulated in Appendix A.

In later tests a different technique was used to keep the superphosphate in contact with the specimen. A series of fatigue tests were conducted with a paste of superphosphate and water held on to the specimen by aluminium foil and adhesive tape. These tests gave similar results to those obtained using superphosphate/water and the chamber technique. Various water contents of the paste, ranging from ½% to 10% by weight of the paste, were tested and all gave similar

results at the same stress level, thus confirming the suspicion that the actual moisture content of the superphosphate was not an important variable. However, in order to standardise, the moisture content was held at 5% which gave a paste of a very similar consistency to that produced by the chamber technique. When the specimen fractured the foil ripped apart allowing the broken half of the specimen to swing clear. The foil/paste technique was used for some later test work, but mainly on short term tests as the moisture tended to be centrifuged out of the paste after about 5×10^5 cycles. If the test was obviously going to last longer than this period, then the paste was renewed at regular intervals.

The fracture produced by the chamber technique and the foil/paste technique were identical to those from the superphosphate/water tests and the fatigue lives obtained were also very similar, as is shown by Figure 4/4.

During discussions with the Director and Staff of the New Zealand Fertilizer Manufacturers' Research Association, Auckland, it became apparent that a large bulk of the fertilizers being used in the North Island were of the potassic superphosphate type. These grades are based on one of the standard superphosphate types usually either ordinary superphosphate or the aerial type and contain either 25% or 33% potassium chloride. Fatigue tests were therefore run using the 33% potassic superphosphate with moist air, as the

corrodent. The results of these tests are shown in Figure 4/5 together with those for the standard aerial superphosphate. Actual test results are tabulated in Appendix B.

The results of previous experiments indicated that the presence of moisture is essential for the superphosphate to have any effect on the fatigue life of the alloy. To check this fact a series of tests were run using superphosphate which had been oven dried for 24 hours at 105°C. The dry powder was packed around the specimen in the test chamber in the same manner as described previously. The results of these tests showed that the dry superphosphate had no effect on the fatigue life of the specimens, the fatigue lives being the same as if the tests had been performed in air. Tests using the stock superphosphate powder without oven drying gave similar results to the oven dried material.

4.4 Fatigue Tests in Water and 3% NaCl Solution.

In order to check on the effects of other corrodents and to check on the effects of the tap water alone, two series of fatigue tests were run using

a) Waimairi County tap water, and

b) a 3% NaCl solution.

The technique for applying the corrodent was the same as that for the superphosphate/water series, namely, that the corrodent was allowed to drip on to the centre of the rotating specimen, the excess being led to waste through the

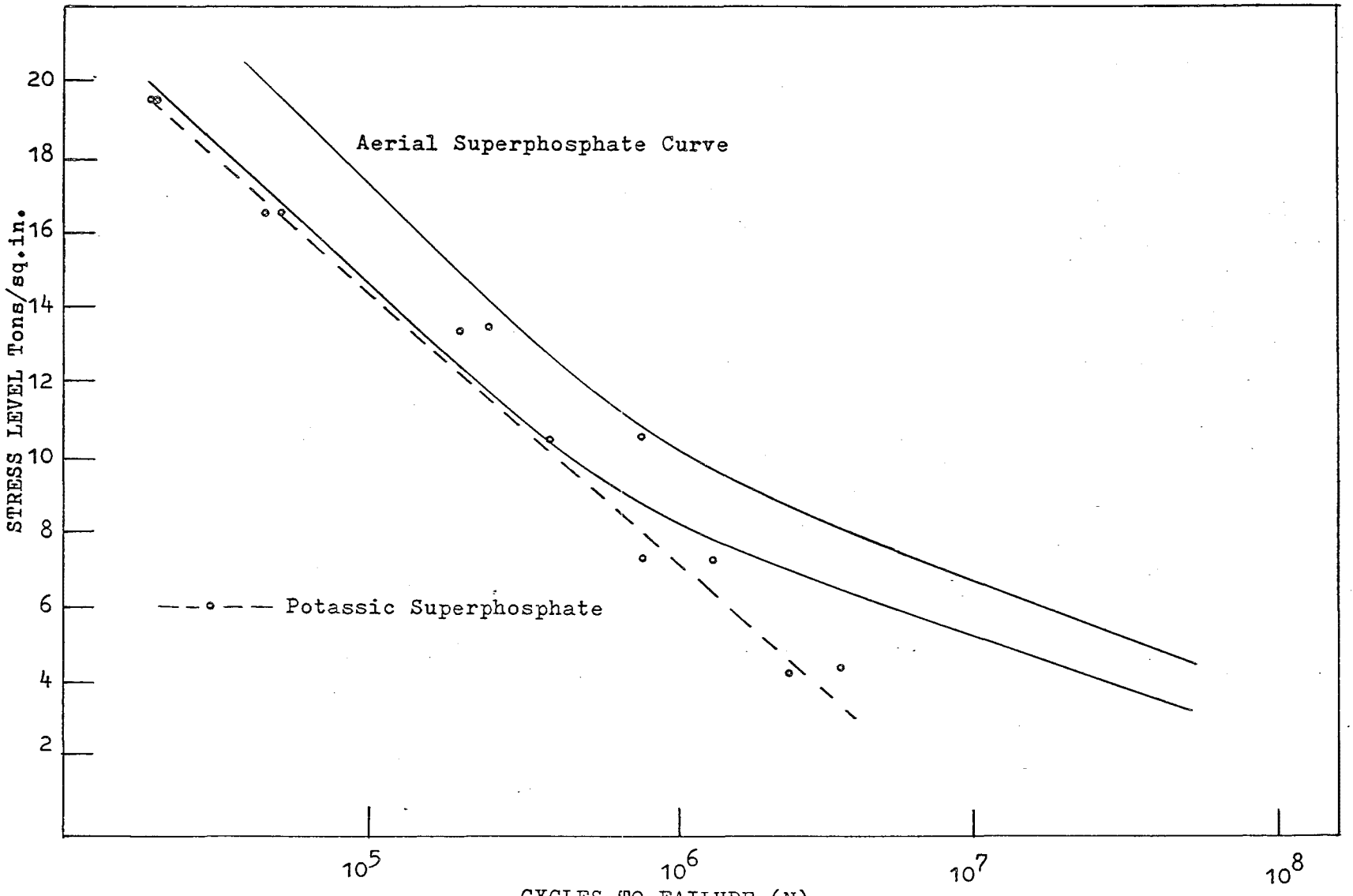

Figure 4/5: Fatigue curves for potassic superphosphate and aerial superphosphate.

bottom of the chamber. The results of the water tests are shown in Figure 4/6 together with the results of the superphosphate/water and air tests for comparison. Figure 4/6 is plotted from data tabulated in Appendix B.

Practically all other workers in the field of corrosion fatigue have used 3% NaCl solution as the corrodent and in order to have some degree of comparison between the results obtained using moist superphosphate as the corrodent and those obtained using 3% NaCl it was felt necessary to run a similar series of tests. During these tests it was noted that a considerable deposit of NaCl built up on the specimen especially during the longer tests. The results of these tests are shown in Figure 4/7 together with the superphosphate/moist air curve for comparison and the results of the 3% NaCl tests are tabulated in Appendix B.

The tests showed that the water alone gave fatigue lives slightly above the superphosphate curve, while the 3% NaCl curve lies below the superphosphate curve. Significantly, there is no difference in fracture mode between the tests conducted in the different corrodents.

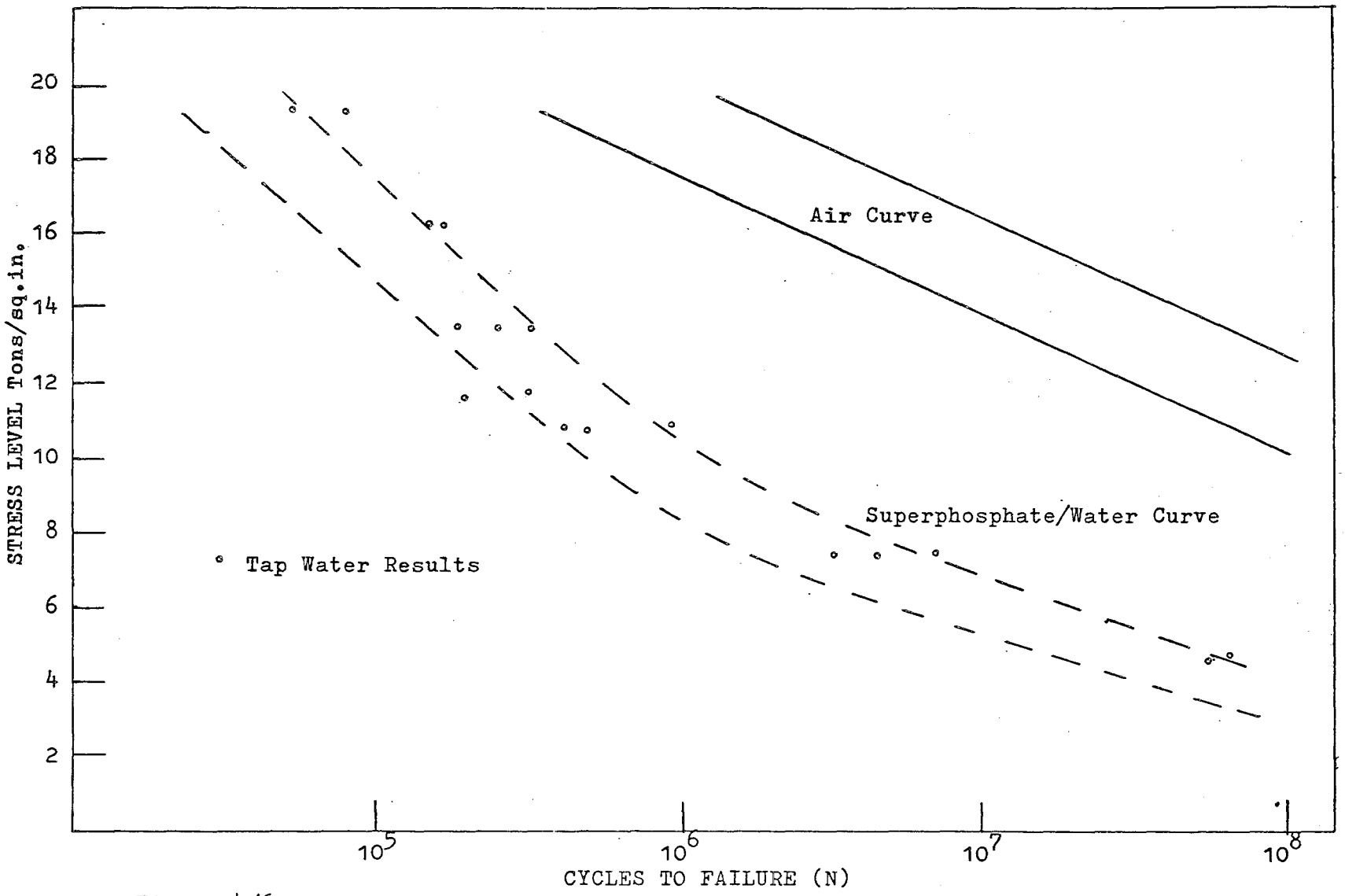

Figure 4/6: Fatigue curves for Tap Water, Superphosphate/Water and Air.

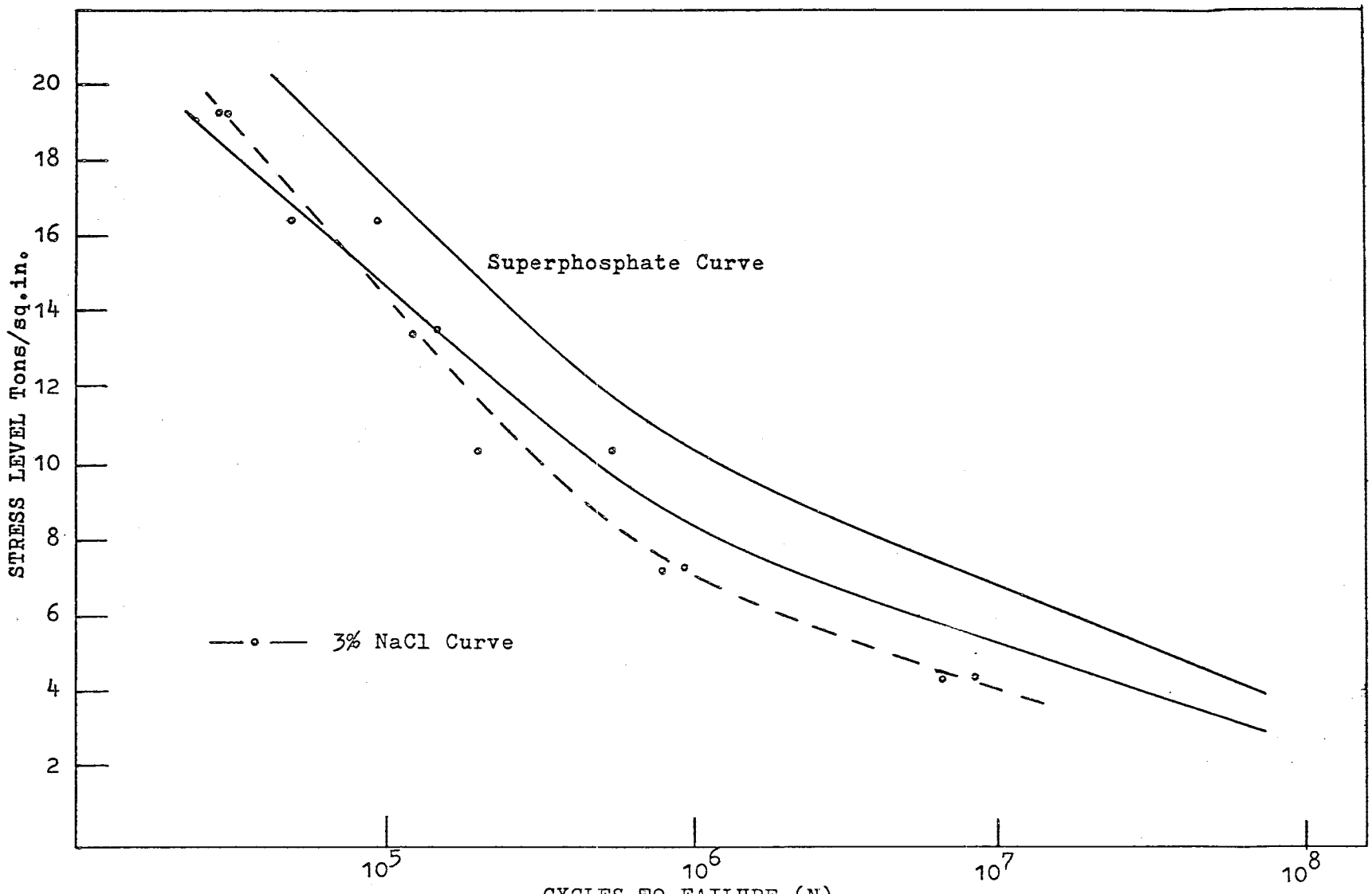

Figure 4/7: Results of fatigue tests in 3% NaCl compared with those for Superphosphate.

4.5 Two Stage Fatigue Tests.

a) Wet - Dry Tests. These tests were designed to discover the influence of the corrodent on crack propagation rates. The specimens were allowed to run for a pre-determined number of cycles in the superphosphate corrodent (using the foil/paste technique), and then the residual fatigue life in air determined. The specimens were carefully cleaned of all loose corrodent without damaging the surface, washed in alcohol, dried, inspected for cracks and surface corrosion damage and then placed in a different fatigue machine to determine the residual fatigue life in air. The use of a different machine for the air tests was because only one R.B. machine was set up for the corrosion fatigue tests, leaving two machines available for back-up air testing in order to speed the testing programme. The results of these tests are tabulated in Table 4/III.

b) Dry - Wet Tests. These tests were designed to check if the mechanisms of air fatigue and corrosion fatigue are the same. If the mechanism is the same in both cases, then a period of air fatigue followed by the corrosion fatigue stage should result in a reduced corrosion fatigue life.

According to most workers, fatigue damage occurs early in the life of a specimen tested in air and this should provide the initiation stage and the action of any corrodent should be to accelerate the crack propagation rates giving a shortened life. If the initiation of corrosion fatigue cracks is in fact due to cyclic slip and not the electro-chemical pitting mechanism suggested by Evans, then air fatigue followed by corrosion fatigue should eliminate the initiation stage and thus give a shortened corrosion fatigue life as only the crack propagation stage will be necessary. The period of air fatigue prior to the corrosion fatigue stage was varied during the tests, but in most cases it was of the order of 1% of the total expected life in air. This figure was chosen because many workers have reported the presence of micro-cracks at approximately this stage in air fatigue tests. In these dry - wet tests the foil/paste technique was used to apply the corrodent to the specimen. The results of these tests are tabulated in Table 4/IV.

TABLE 4/III: Results of Wet - Dry Tests.

Stress Level Tons/sq.in.	Cycles of Corrosion Fatigue.	% of C.F. Life.	Residual Life in Air.	Normal Life in Air.	Normal Corrosion Fatigue Life.
16.25	9×10^3	9	2.7×10^6	5×10^6	1×10^5
	1.7×10^4	17	6×10^5		
	3×10^4	30	6.8×10^5		
	4.5×10^4	45	2.5×10^4		
	5×10^4	50	3.5×10^4		
	6×10^4	60	2.1×10^4		
13.3	6×10^4	30	8.1×10^6	87×10^6	2×10^5
	1×10^5	50	4.5×10^5		
	1.5×10^5	75	2.5×10^5		
10.35	9×10^4	10	18.5×10^6*	10^8*	9×10^5
	2×10^5	22	1.5×10^6		
	3×10^5	33	5×10^5		
	3.5×10^5	39	5.5×10^5		
7.4	8.5×10^5	37	1.95×10^6	10^8*	2.3×10^6

* Specimen unbroken.

TABLE 4/IV: Results of Dry - Wet Tests.

Stress Level Tons/sq.in.	Cycles of Air Fatigue.	% of A.F. Life.	Residual Corrosion Fatigue Life.	Normal Life in Air.	Normal Corrosion Fatigue Life.
16.25	3×10^4	0.6	6×10^4	5×10^6	1×10^5
	5×10^4	1	4×10^4		
13.3	3×10^4	0.04	1.8×10^5	87×10^6	2×10^5
	6×10^4	0.08	1.6×10^5		
	1.5×10^5	0.2	1.5×10^5		
	1.8×10^6	2	6×10^4		
	21.5×10^6	24	5×10^4		
10.35	5×10^5	0.5	5.5×10^5	10^{8*}	9×10^5
	6×10^5	0.6	5×10^5		
	8×10^5	0.8	3×10^5		
7.4	1.8×10^6	2	1.5×10^6	10^{8*}	2.3×10^6
	3.3×10^6	3	1.3×10^6		
	14.1×10^6	14	8×10^5		

* Specimen unbroken.

4.6 Tests to Determine the Effects of Corrodent On Crack Initiation.

In experiments to determine the mechanism of corrosion fatigue, Evans developed a potentiometric method which was claimed accurately to detect the formation of a crack in specimens undergoing corrosion fatigue. This method is based on the corrodent being an electrolytic solution and thus could not be successfully utilised under the present experimental conditions, requiring a different method of detecting crack initiation to be devised. The only method applicable to the present work was visual examination of the specimen during an actual test. In these tests, the specimens were run in the corrodent for certain pre-determined numbers of cycles, the number being selected from the corrosion fatigue tests in superphosphate/moist air. The specimens were then very carefully cleaned of all loose corrodent particles, washed in alcohol, dried, and examined microscopically for surface damage, and likely areas subjected to metallographic examination. Typical results from these tests are tabulated in Table 4/V, but the main information is discussed in Chapter Seven under Fractography and Metallography. A number of specimens were polished with one micron diamond polishing paste and tested in air and superphosphate corrodent. These specimens were also examined for surface damage and crack initiation and the results of these particular tests are discussed in Chapter Seven also.

TABLE 4/V: Results of Crack Initiation Tests.

Stress Level Tons/sq.in.	Corrosion Fatigue Cycles.	Surface Cracks Detected	% of Estimated Fatigue Life.
16.25	1.7×10^4	Surface damage	17
	3×10^4	Small cracks	30
	6×10^4	Major cracks	60
13.3	1×10^5	Small cracks	50
	1.5×10^5	Major cracks	75
10.35	2×10^5	Small cracks	22
	2.5×10^5	Small cracks	30
	3.5×10^5	Major cracks	39
7.4	8.5×10^5	Major cracks	38

4.7 Fatigue Tests Using Notched Specimens.

From the literature survey, it appears that there has been no work done on notched specimens of the high strength aluminium alloys in a highly corrosive environment. Many workers have reported the results of fatigue tests on notched specimens in air but to date few references have been found covering notched fatigue tests in wet corrosive media and those reported deal with steel. In the normal aircraft structure, there are many built-in notches and it is therefore of considerable interest to the present investigation to

ascertain the effect of superphosphate corrodent on notched fatigue specimens. The specimen used for these tests had a theoretical stress concentration factor of 3 and the dimensions of the specimen and notch detail are shown in Figure 4/8.

Two series of tests were conducted, one in air and the other in the superphosphate corrodent, the results of these tests being plotted in Figure 4/9 and tabulated in Appendix C. Considerable difficulty was experienced in conducting the tests on the notched specimens using superphosphate as the corrodent. The chamber method was obviously not suitable because of the difficulty of ensuring that the corrodent penetrated to the root of the notch. An aqueous solution of superphosphate powder, as used in the original test series, was tried but this method also failed because the surface tension of the solution prevented the corrodent penetrating the notch root. The most effective method was the foil/paste technique and this method was therefore adopted for the test series.

A feature of the tests with the corrodent was the two different types of fracture produced. Some specimens had a very short life and gave a cup and cone type of fracture, but others at the same stress level, while having a shorter life than the air tests, gave a fracture at right angles to the specimen axis. It is possible that the topography of the notch was affecting the test results but this feature is

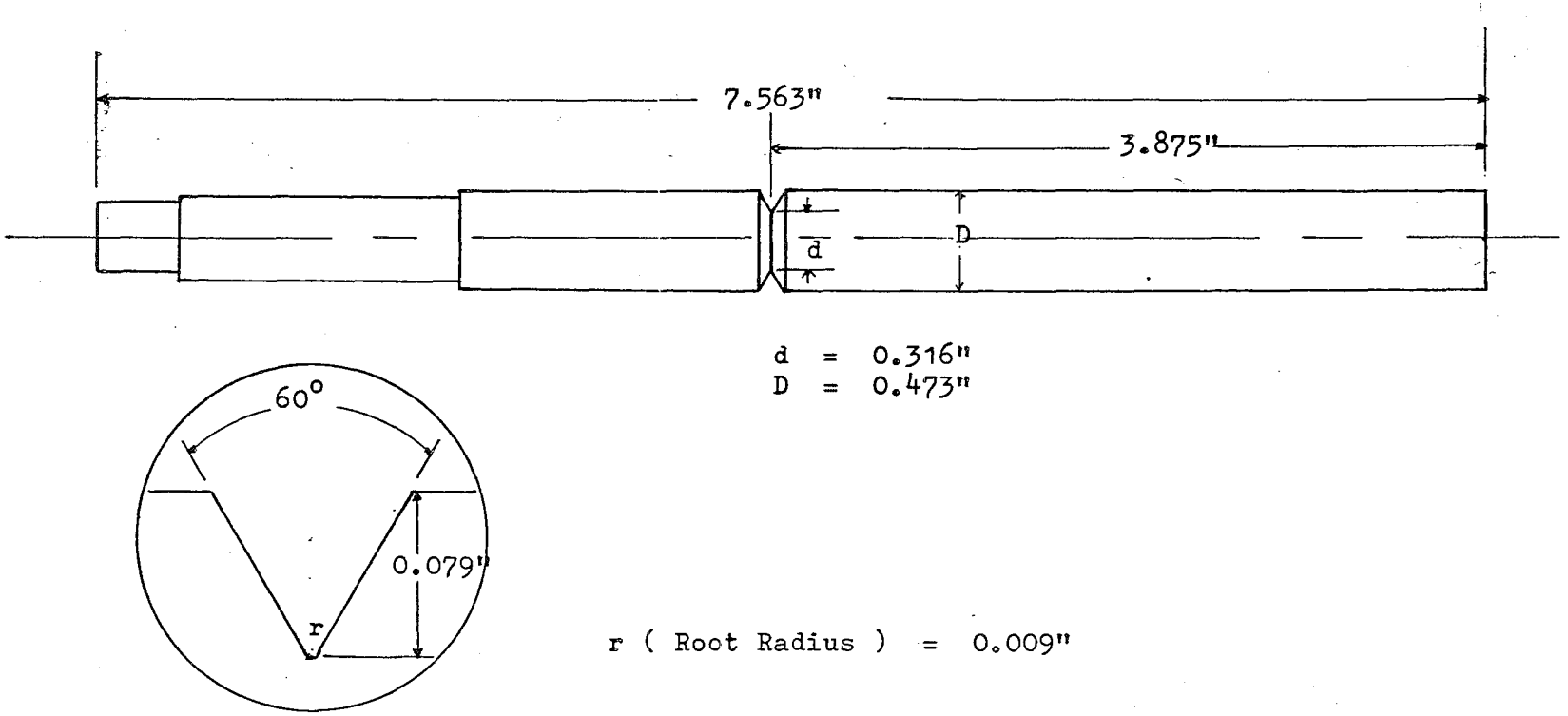

Figure 4/8: Details of notched rotating beam fatigue test specimen.

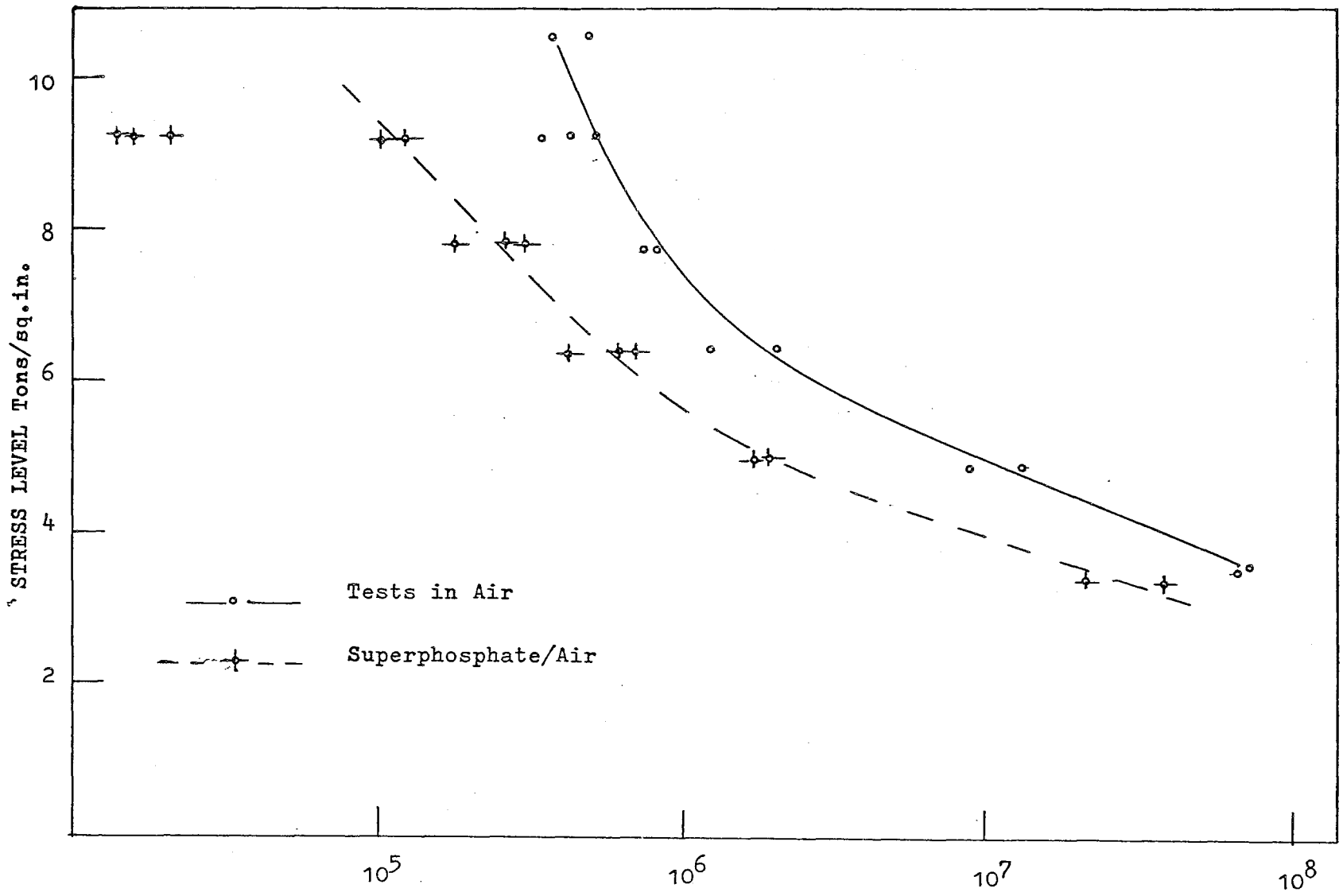

Figure 4/9: Fatigue curves for notched specimens in Air and Superphosphate/Air.

discussed more fully in the section dealing with fractography.

4.8 The Effect of a Painted Coating on Fatigue Life.

From a practical viewpoint one of the questions to be answered in the aerial top-dressing industry is the effectiveness of protective coatings in preventing the corrosion fatigue of 2024 - T4 aluminium alloy structural members of top-dressing aircraft. A number of standard rotating beam specimens were polished in the standard manner as outlined in Section 4.1 and were then treated by the National Airways Corporation Engineering Workshops, Christchurch Airport, through the courtesy of Mr. P. Clayton, Technical Supervisor. The specimens were given the standard treatment used by N.A.C., that is, anodising followed by a chromate etch primer coat, with a final top coat. These specimens were then tested in air and under corrosive conditions, using superphosphate/moist air as the corrodent. The results of these tests are given in Appendix D and plotted in Figure 4/10 with the two curves for the un-treated specimens for comparison.

The notable features of these tests were the drop in life at high stress levels in air compared to the untreated specimens, and the considerable gain in corrosion fatigue life at all stress levels. The gain in corrosion fatigue life was not quite as high as had been expected and it would appear that the coating was permeable to the corrodent allowing some corrosion attack to occur. The gain in corrosion fatigue life was only possible

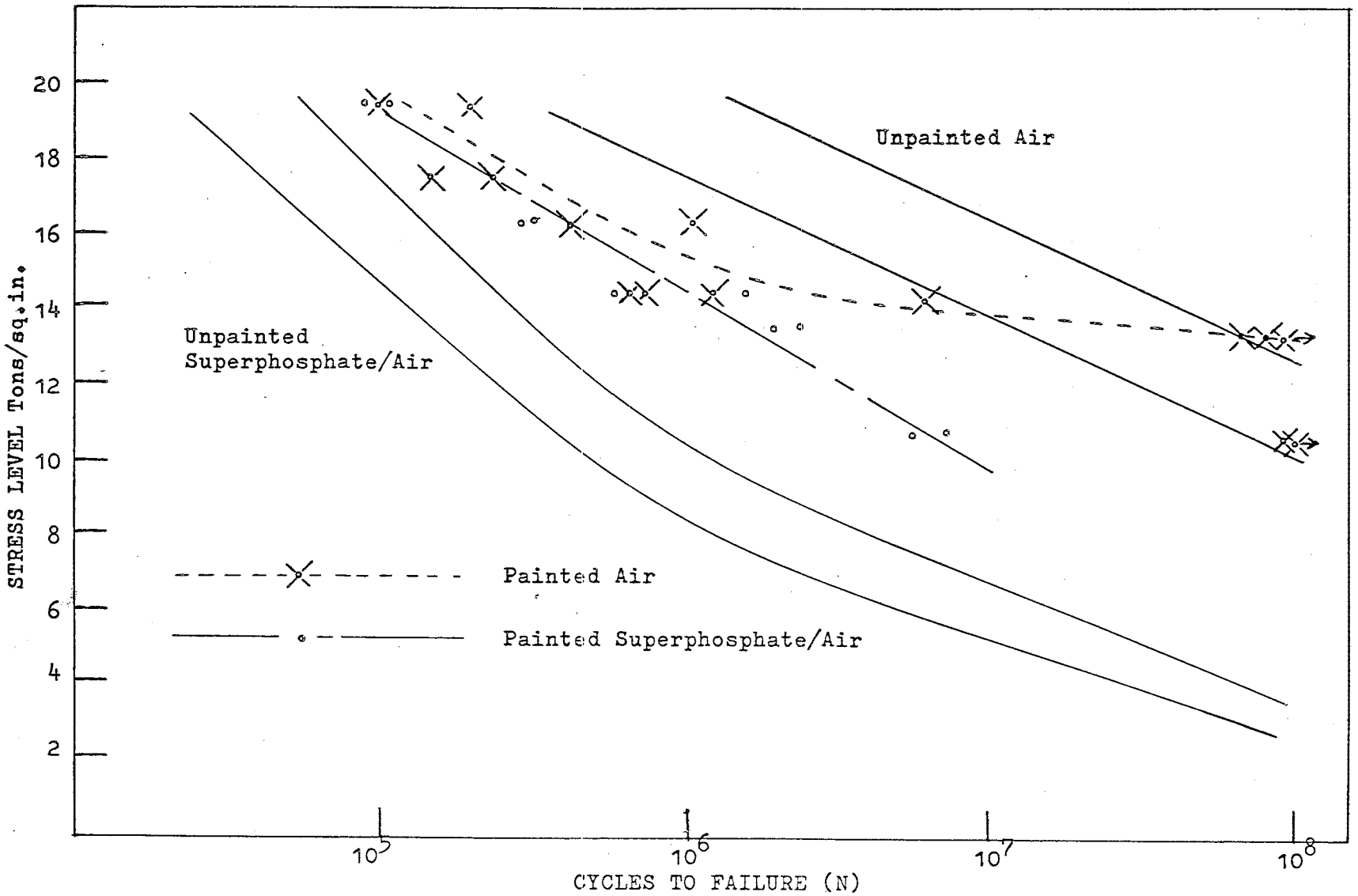

Figure 4/10: Fatigue curves for painted specimens compared with those for unpainted specimens.

so long as the painted coating remained intact. Specimens where the paint and anodised coatings were removed from small areas of the surface exposing bare metal to the corrodent had corrosion fatigue lives similar to un-treated specimens.

4.9 The Effect of Pre-Corrosion on Air Fatigue Life.

McAdam, and several later workers, had shown that pre-corrosion of specimens followed by fatigue testing in air gave lives very similar to those obtained in corrosion fatigue. This feature appears to be very marked in the case of aluminium and its alloys. From a practical viewpoint, it is thus of value in the present study to determine whether pre-corrosion by moist superphosphate causes a marked reduction in air fatigue life for the 2024 - T4 alloy. Corrosion of aircraft structural members due to moist superphosphate is a considerable problem in the aerial top-dressing industry and component inspection and replacement schedules would possibly have to be revised if the fatigue lives of components are drastically affected by the corrosion attack.

Standard specimens were placed in contact with superphosphate powder containing 5% tap water and left in contact for 24 hours. No load was applied to the specimens while they were in contact with the moist superphosphate. After 24 hours, the specimens were carefully cleaned of all loose corrodent, washed in alcohol, dried, and the fatigue life in air determined. The results of these tests are given in

Table 4/VI.

TABLE 4/VI: Results of Pre-Corrosion Tests.

Stress Level in Fatigue Test: Tons/sq.in.	Life in Air Following Pre-Corrosion	Normal Life in Air.	Normal Corrosion Fatigue Life.
19.2	2.0×10^5	6.0×10^5	4.0×10^4
	1.4×10^5		
	5.0×10^5		
16.25	4.0×10^5	5.0×10^6	1.0×10^5
	2.5×10^5		
13.3	7.0×10^5	87×10^6	2.0×10^5
	1.3×10^6		
10.35	1.0×10^6	10^{8*}	9.0×10^5
	1.3×10^6		
7.4	10^{8*}	10^{8*}	2.2×10^6
4.4	10^{8*}	10^{8*}	40.0×10^6

* Specimen unbroken.

4.10 The Effect of Over-Ageing on Corrosion Fatigue Life.

Work by Robertson[108] has shown that by over-ageing the 2024 aluminium alloy can be made extremely susceptible to stressless corrosion. From his published data it appears that heat treatment for four hours at 175°C. after natural ageing left the alloy in the most susceptible condition for corrosion attack. If the Evans electro-chemical mechanism for corrosion fatigue is correct, then any treatment which increases the susceptibility of the alloy to pitting corrosion attack should accelerate the initiation of corrosion fatigue cracks and thus shorten the corrosion fatigue life. Specimens were therefore heat treated for four hours at 175°C. and fatigue tested using superphosphate/moist air as the corrodent. The results of these tests showed no change in the corrosion fatigue life, indicating that the over-ageing had had no adverse effect.

CHAPTER FIVE.

5. DIRECT STRESS FATIGUE TEST PROGRAMME.

5.1 Materials and Equipment.

The direct stress fatigue specimens were machined from the same batch of extruded 2024 - T4 alloy rod as that used for the rotating beam test specimens. Two types of specimen were chosen, a waisted specimen and a notched specimen with a theoretical stress concentration factor, K, of 2.9. The shape and dimensions of both specimens are shown in Figure 5/1. Preparation of the waisted specimen was the same as that outlined for the rotating beam specimens, namely, they were machined oversize and hand polished in two stages to the final diameter. It had been planned to use the same diameter (0.25 in.) at the centre of the specimens in all test work but it was found necessary to reduce the direct stress specimen diameter to 0.20 in. in order to achieve sufficiently high stresses for failure to occur in a reasonable time. This was due to the limitations imposed by the fatigue testing machine. The notched specimens were designed so as to give a final diameter of 0.20 in. at the smallest cross section to give uniformity of cross sectional area in all tests whether with waisted or notched specimens.

The superphosphate used for these tests was that prepared for the rotating beam test programme and the foil/paste technique was used to apply the corrodent. Unlike the rotating beam tests, no problems were encountered in keeping the

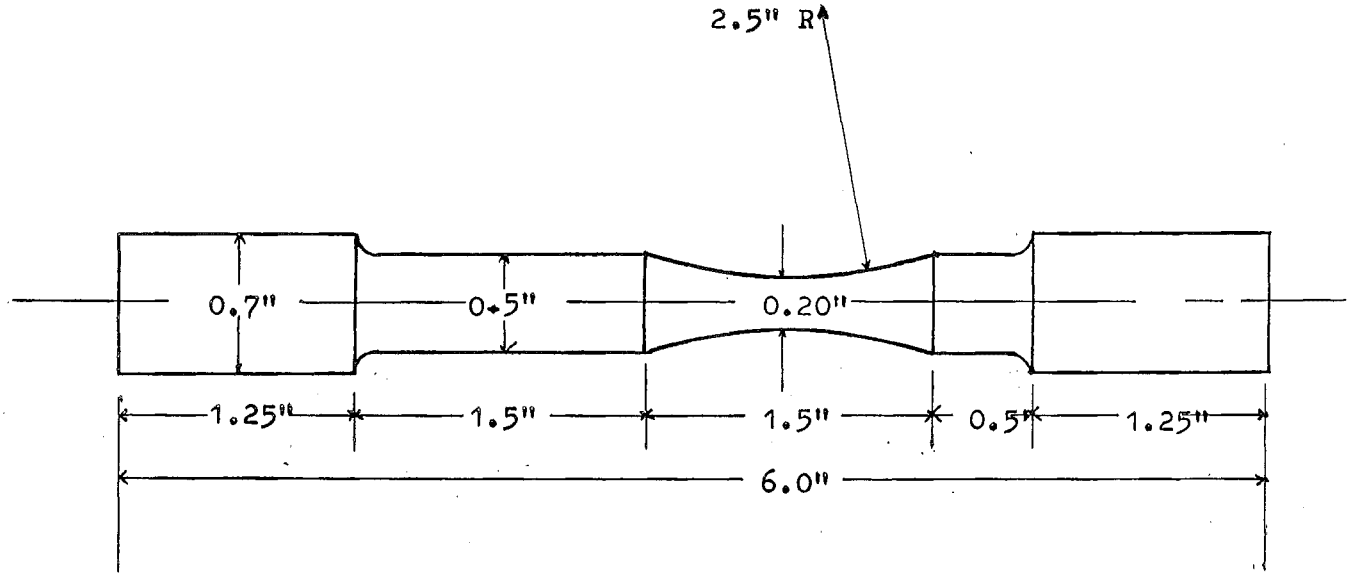

(a)

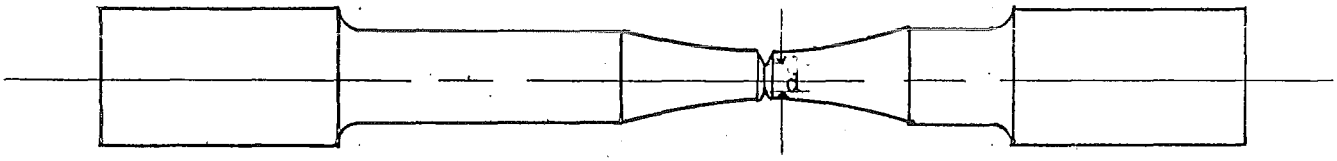

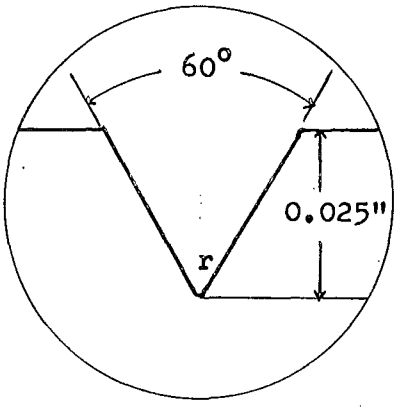

Root diameter (d) = 0.20"

Root radius (r) = 0.01"

(b)

Figure 5/1: Direct stress fatigue test specimens, (a) Un-notched specimen, (b) Notched specimen.

corrodent in contact with the root of the notch.

The direct stress fatigue machine was based on a "Savage V1000B" moving coil vibrator capable of delivering a peak thrust of ± 750 lb. over a frequency range of zero c/s to 5 Kc/s. The input current to the vibrator was controlled from a "Savage KM2Z" 1 kilowatt amplifier to which was connected the signal generator. The actual peak thrust of the vibrator was limited to ± 500 lb. because of the amplifier characteristics, and this posed several practical problems in achieving a sufficiently high stress level in the test specimen. Sine-wave loading was used in the fatigue machine to give loading characteristics similar to those used in the rotating beam fatigue tests.

Figure 5/2 shows the actual vibrator with the specimen in position, and Figure 5/3 shows the control instruments consisting of signal generator, amplifier, stress measurement and timing instruments. The actual test rig was designed to operate at resonance in order to achieve the desired stress levels. Resonate frequency varied from specimen to specimen and also altered once a fatigue crack was formed, but generally it was of the order of 175 c/s.

In the design of the moving head (lower grip) two flat leaf springs were used to hold the bottom specimen grip and the grip was attached to the vibrator by means of an aluminium

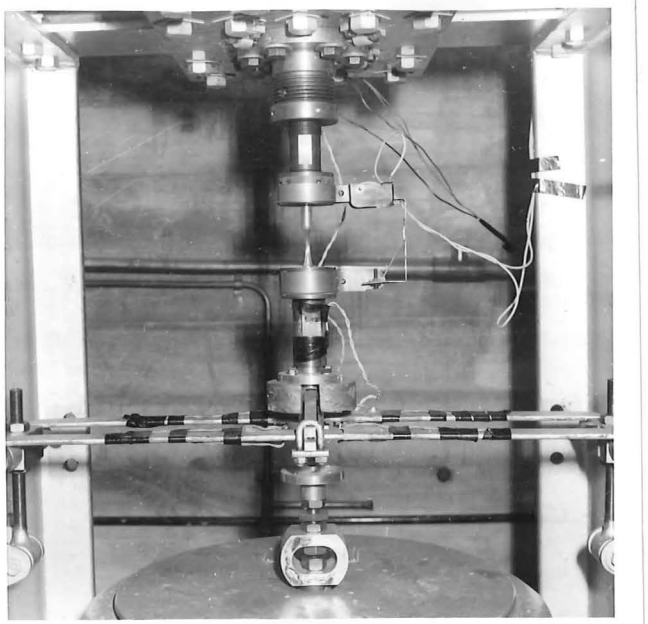

Figure 5/2: Direct stress fatigue machine with specimen in position.

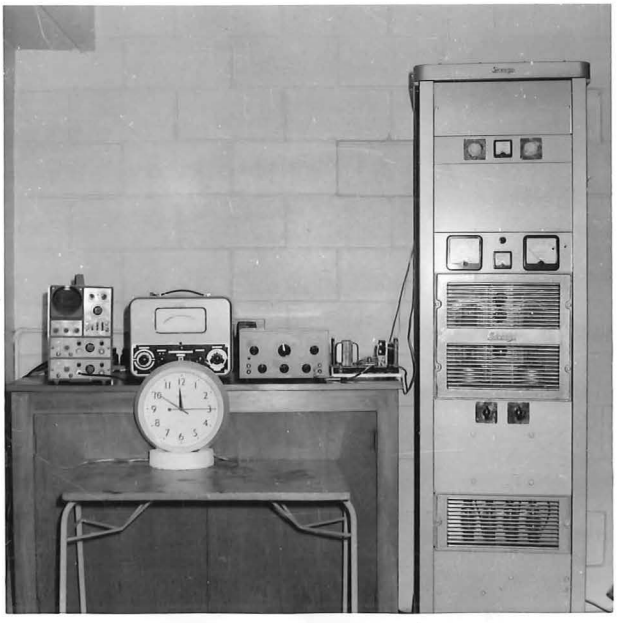

Figure 5/3: Control instruments for the direct stress fatigue machine.

alloy connecting piece. This design enabled the grip to be released from the vibrator for adjustment of the specimen without placing any strain on the moving coil of the vibrator. As the top grip was held in position by locking nuts (one above and one below the main frame) its position could be easily adjusted to give a small amount of mean stress on the specimen if required, and to allow for any possible variation in specimen length.

Gripping of the specimens was by means of split collets held in place by locking nuts. The specimen was a close fit in the grip and to avoid any possible binding during the test the specimen ends and the grips were coated with an anti-scuff paste containing molybdenum disulphide. The method of gripping the specimens and of attaching the bottom grip to the moving coil could possibly cause some bending on the specimen during the fatigue test. This point was carefully checked and no lack of uni-axiality was observed during actual tests.

To ensure that no bending stresses were imposed on the specimen during the fatigue test it was essential that the top and bottom grips be correctly aligned. The initial alignment was checked by placing a specimen in the lower grip and allowing the top grip to rest on the specimen. The position of the top grip was then adjusted until the grip slid down on to the specimen. The final alignment was checked by placing a

½ in. diameter specimen, to which was attached four strain gauges, in the grips. The four strain gauges were equally spaced around the diameter at the centre of the bar and diametrically opposite gauges connected together; all four gauges were then connected to form a wheatstone bridge circuit. Any bending strain was shown up as a departure from zero reading of the bridge circuit. By then reading the strain on each pair of gauges separately the direction of bending was established and so corrected. This method was periodically used to check the alignment of the grips during the test programme but no adjustment was found to be necessary after the initial setting up.

Calibration of the test rig also caused some problems but the method finally adopted appeared to give satisfactory and consistent results. The output from a resistance strain gauge on the bottom grip was fed through a "Philips" strain bridge to an oscilliscope and the strain shown on the screen in the form of a sine wave, the amplitude of which was a measure of the degree of strain. In order to calibrate the machine the bottom grip was loaded statically and the shift in oscilliscope reading correlated to the actual stress applied. The shift in oscilliscope reading under static loading correlated with the amplitude of the sine wave shown on the oscilliscope during dynamic loading. A similar method to this, developed by the National Physical Laboratory, only using a specially built

d.c. amplifier instead of the strain bridge is described by Dowell.[109] The calibration method was also used to measure the actual stress applied during fatigue tests and was found to be reasonably satisfactory although electrical interference picked up by the oscilliscope sometimes made it difficult to ascertain the exact amplitude of the sine wave.

Cycle counting during tests was by means of an electric clock which drew its power from the amplifier. This method assumes that the cycle frequency remains constant and that no drift of the signal generator occurs. All test work was monitored and the generator adjusted to keep the test rig at resonance, no test work being continued unless the author was personally on the premises. Some drift of the generator undoubtedly did occur but it was generally corrected and an effort made to allow for it in calculating the number of stress reversals. A micro-switch was attached to the upper grip and actuated by a lever attached to the lower grip. When the specimen failed the bottom grip dropped slightly and the lever tripped the switch which then actuated a relay which in turn switched out the input current from the amplifier to the moving coil. When the amplifier cut out the timing clock also stopped thus giving the total time of the test.

One of the major problems encountered was that of achieving sufficiently high stress levels to cause failure of the standard waisted specimens within reasonable times

(0 - 8 hours). The specimen diameter was reduced from 0.25 in. to 0.20 in. in an effort to overcome this but use of a notched specimen was the only real answer. While reasonably high stresses could be achieved at resonance with full input current, a lowering of input current gave a marked drop off in stress level and thus prevented a full investigation of the lower stress ranges for the waisted specimens. Higher stress levels could possibly have been achieved by aiming for resonance at higher frequencies but there were two major objections to this. One was that frequency has an effect on the corrosion fatigue life and in order to have some comparison with the rotating beam tests the lower the test frequency the better and the other was the noise level of the vibrator at the higher frequencies. At lower frequencies, of the order of 60 - 100 c/s, which were nearer the frequency of the rotating beam tests (50 c/s) the stress levels dropped off markedly preventing failure within reasonable times.

5.2 Notched Specimen Test Programme.

Fatigue tests in both air and superphosphate/air were conducted using the notched specimens. The corrodent was applied to the specimen using the foil/paste technique and no difficulties were encountered in keeping the superphosphate in contact with the root of the notch. Due to the size of the specimen used and the limitations of the fatigue machine, the very low stress levels (circa 6 tons/sq.in.) could not be fully

investigated, especially for the tests in air. However, it is felt that sufficient data is available to indicate the general trend of results, and this data is given in Figure 5/4 and tabulated in Appendix E, for both air and corrosion tests. The fractography of the specimens is discussed in Chapter 7.

5.3 Un-Notched Specimen Test Programme.

As in the case of the notched specimen test series, the experimental circumstances prevented a full investigation at all stress levels in tests using superphosphate corrodent and no results were obtained for tests in air. At the highest stress levels obtainable the specimens tested in air remained unbroken after some 5×10^6 cycles, representing approximately 8 hours testing. In the tests using superphosphate corrodent, failures did occur at the highest stress levels but no failures occurred at the lower stress levels after 8 hours testing. If the specimen was still unbroken at this stage the test was discontinued. The results from the corrodent tests did show the general trend expected and these results are shown in Figure 5/5 and are tabulated in Appendix E. The fractography of these specimens is discussed in Chapter 7.

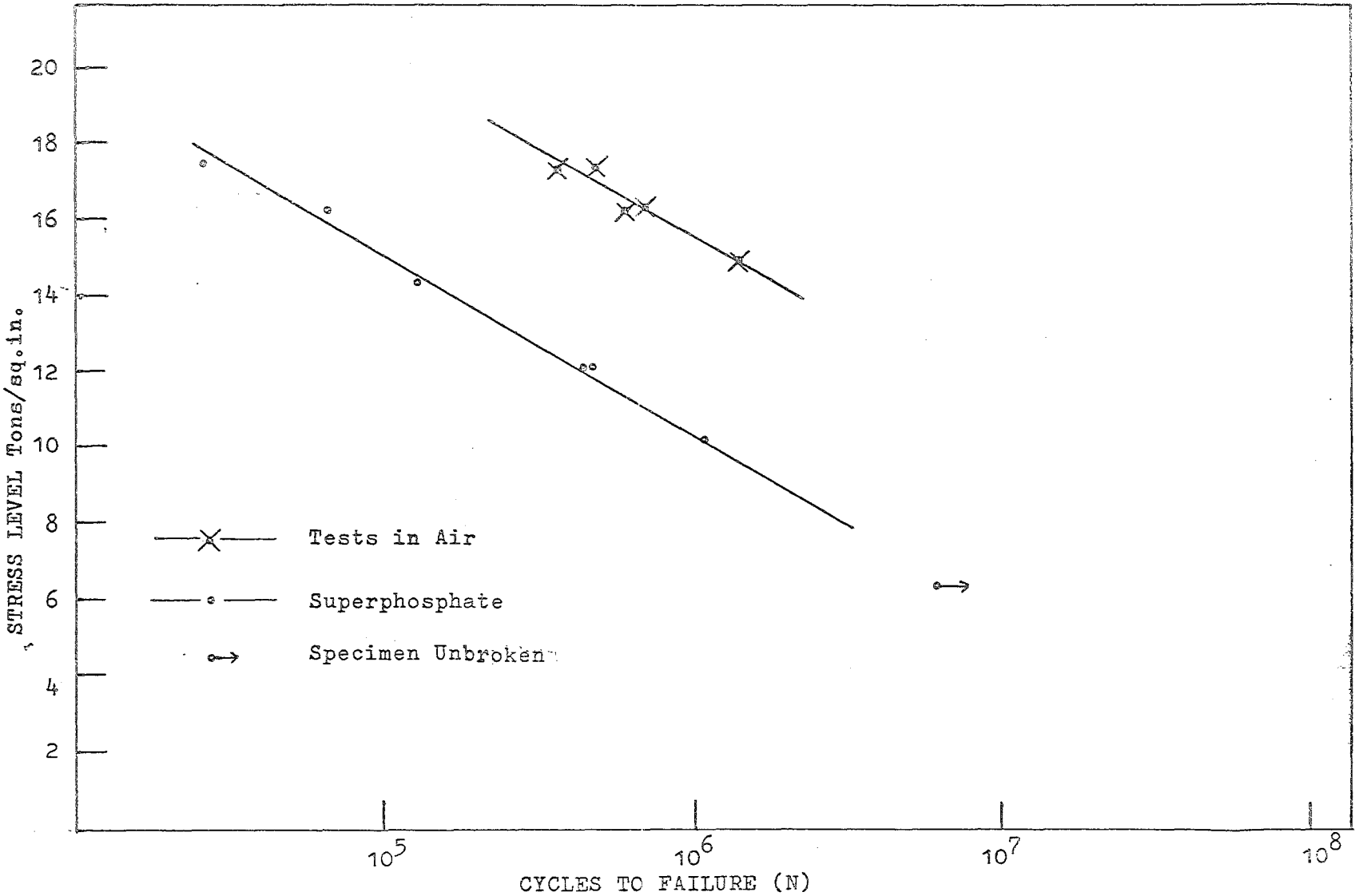

Figure 5/4: Fatigue curves for notched direct stress tests.

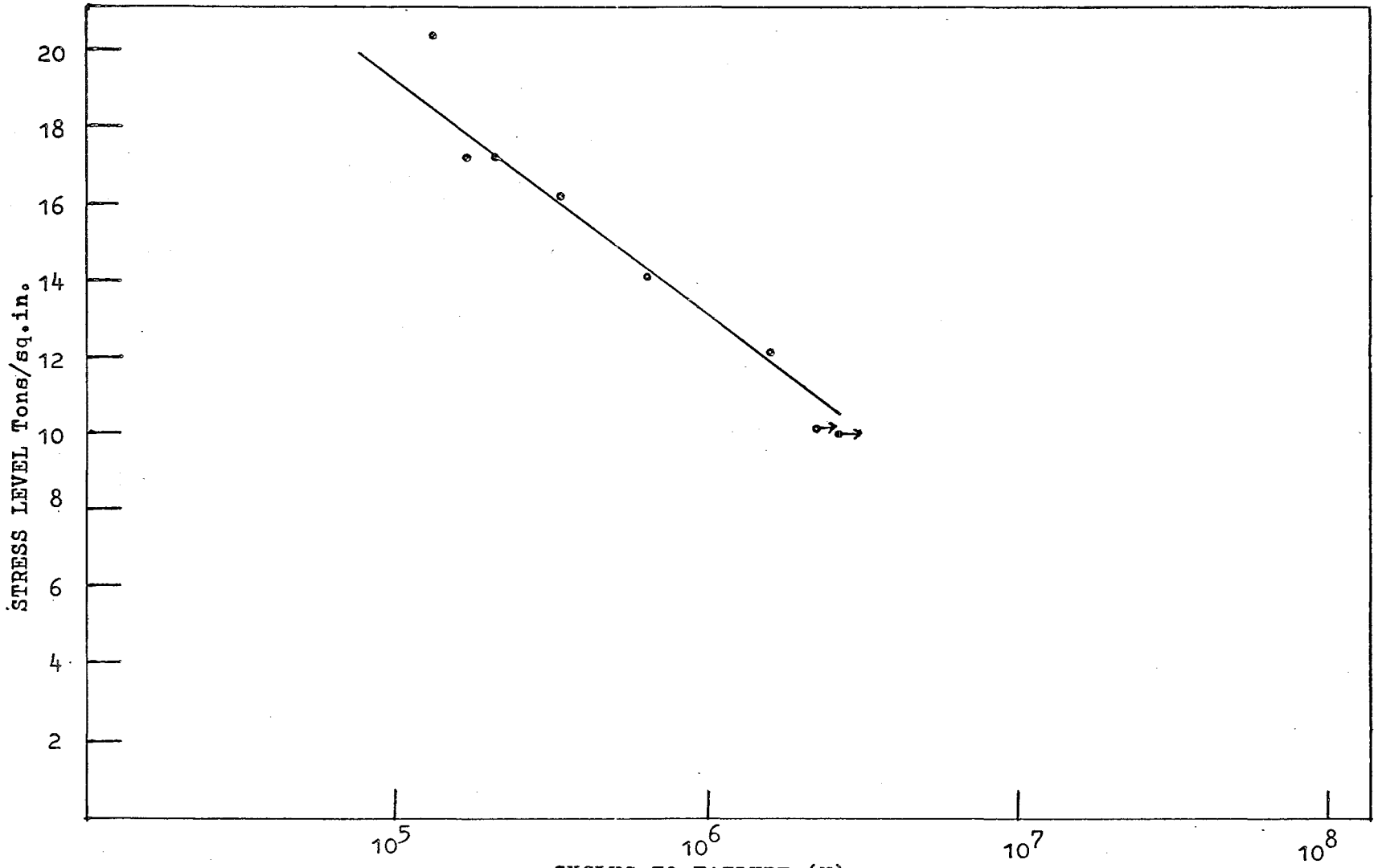

Figure 5/5: Fatigue curve for un-notched direct test specimens in superphosphate.

CHAPTER SIX.

6. REVERSE BEND FATIGUE TEST PROGRAMME.

A Limited programme of reverse bend fatigue testing was conducted by the author in the laboratories of Chemistry Division, D.S.I.R., Gracefield. The materials used for the test work were the same as those used in both the rotating beam and direct stress work, that is 2024 - T4 aluminium alloy and aerial superphosphate as the corrodent. The shape and dimensions of the test specimen are shown in Figure 6/1, and it will be noted that the specimen diameter was 0.30 in. not 0.25 in., this being the standard specimen for the machine used.

The machine used for the test work was an Amsler resonance type reverse bend fatigue tester in which the stress amplitude is controlled by placing out-of-balance weights on a fly wheel suspended from cantilever leaf springs. Two pins on the fly wheel held the weights but owing to errors in the instruction manual and lack of markings on the fly wheel it was not discovered until the end of the programme that the weights had to be placed on particular pins to achieve the desired stress level. This means that the actual stress levels in the test work are somewhat suspect and that they could in fact differ from those supposedly set on the machine. Cycle frequency of the machine was 1500 c.p.m.

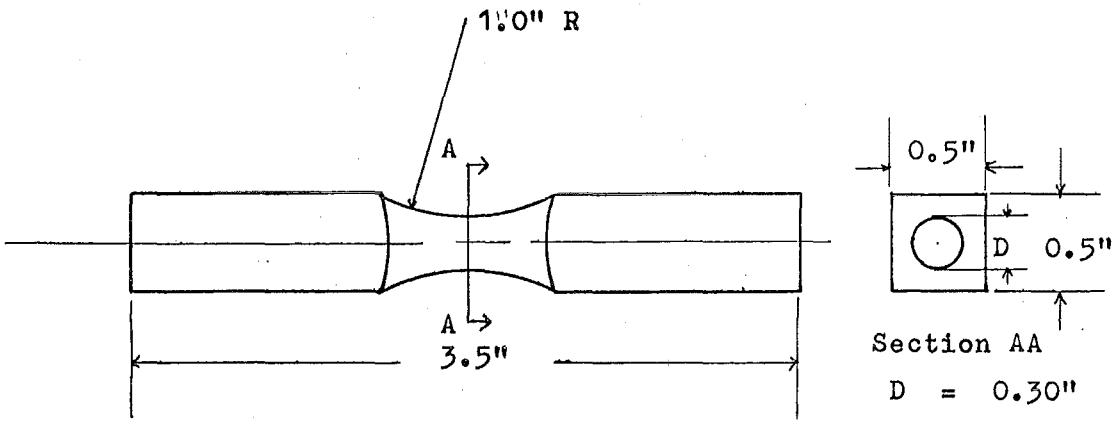

Figure 6/1: Reverse bend fatigue test specimen.

Tests were conducted in air and superphosphate corrodent using the foil/paste technique to apply the corrodent. While typical results are tabulated in Table 6/I it must be remembered that the stress levels given are those supposedly set on the machine and may not necessarily be the actual stresses acting on the specimens in the tests. Main interest however, was centred on the fractography of these specimens as compared to the other test work using rotating bending and direct stress systems, and this is discussed in Chapter 7.

As the results of the fractographic studies were in line with those from the other test programmes and as the fatigue machine used was suspect, no major programme of reverse bend fatigue testing was undertaken. A further consideration was the necessity for the author to spend considerable time at Gracefield to complete a major test programme.

TABLE 6/I: Reverse Bend Fatigue Test Results.

Stress Level Tons/sq.in.	Air Fatigue Life.	Corrosion Fatigue Life.
18	1.08×10^5	3.34×10^4
		6.08×10^4
16.4	7.1×10^4	-
12.5	-	1.49×10^5
10.9	-	3.26×10^5
7.6	7.48×10^5	3.2×10^5
6.3	-	6.77×10^5

CHAPTER SEVEN.

7. FRACTOGRAPHY AND METALLOGRAPHY.

A study of the fractures obtained from the various fatigue tests revealed several striking features, the most obvious being a change in actual fracture morphology between those tests made in air and those made under corrosive conditions. All three stress systems used in the fatigue testing programmes gave similar results as regards the fracture morphology and it would appear that the features observed could apply in general to the high strength aluminium alloys.

7.1 Un-Notched Rotating Beam Air Fractures.

The fractures obtained in air showed two major modes of crack propagation. Initially, the direction of crack propagation was at 90^{o} to the maximum tensile stress direction, but after the crack had travelled only a short distance into the specimen, the direction of propagation changed to lie at about 35^{o} to the tensile stress. The length of the crack formed at 90^{o} to the tensile stress varied with stress level, the lower the stress level the greater the length of crack. This mode of cracking at 90^{o} will be called the tensile mode for the purposes of this discussion.

That part of the fracture running at 35^{o} to the tensile stress, i.e., near the maximum shear direction, was remarkably flat in that the crack surface was a plane inclined at 35^{o} to

the specimen axis. This type of cracking will be called shear mode cracking. Figure 7/1 shows a typical air fatigue fracture while Figure 7/2 shows a close-up photograph of an air fatigue crack in its initial stages. In all the air fractures the tensile mode of cracking always preceded the shear mode. The final fracture of the specimen took place on a 45^{o} plane. All three stages of a typical air fatigue failure are shown in Figure 7/3.

The air fractures showed a river pattern marking on the shear mode fracture face with the pattern branching out from the transition area. A noticeable feature was the absence of the conchoidal markings normally associated with a fatigue failure. Also prominent was the appearance of a black powdery deposit on the fatigue fracture faces. This deposit is thought to be fretting debris possibly from the $CuAl_2$ phase present in the alloy and similar deposits on fatigue fractures in high strength aluminium alloys have been reported in the literature.

The transition of crack propagation from 90^{o} to 45^{o} to the maximum tensile stress is also a well recognised phenomenon in high strength aluminium alloys and several authors refer to it, especially in research involving sheet specimens.[19, 104, (105, 110 - 112)].

Figure 7/1: Typical air fatigue fractures in un-notched specimens.

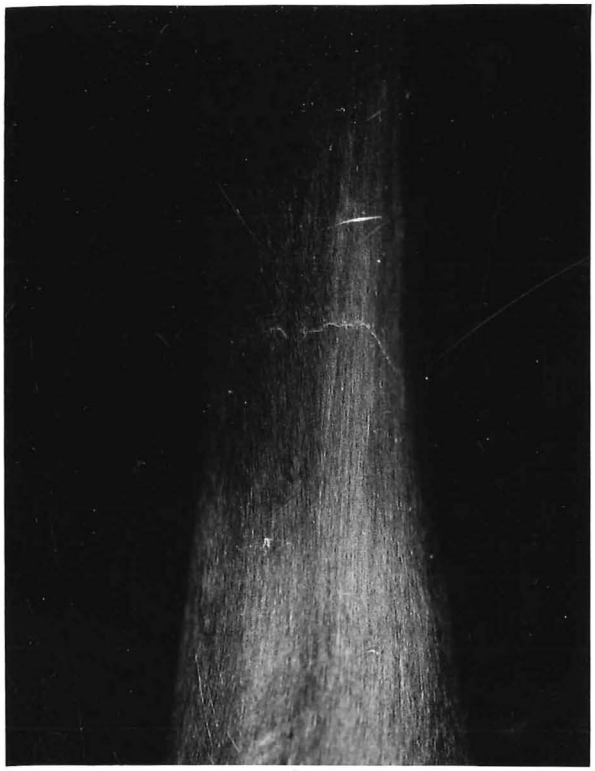

Figure 7/2: A close-up photograph of an air fatigue crack, showing both tensile and shear mode systems.

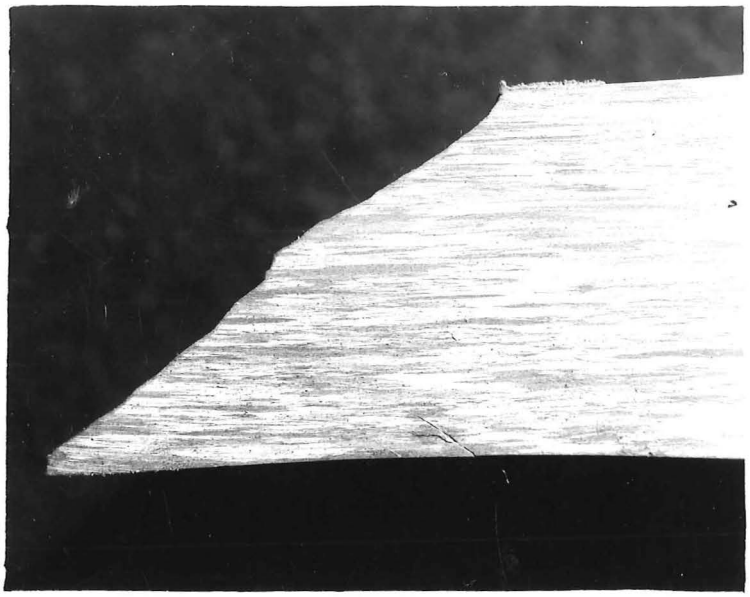

MAXIMUM TENSILE STRESS

Figure 7/3: A macro-photograph showing the three stages of failure in an air fatigue crack.

Several specimens were tested until cracks appeared, the tests were then discontinued and the specimens sectioned. Figure 7/4 - 7/6 show typical features of these cracks. Figure 7/4 shows the highest stress level crack and Figure 7/5 a crack at a lower stress level. The influence of stress level on the degree of tensile mode cracking can be clearly seen. Figure 7/6 shows a tensile mode crack before the transition to the shear mode has begun. A feature is the way the crack moves in certain places in short bursts at 35^{o} to the tensile stress, but the overall effect is to produce a fracture surface at 90^{o} to the specimen axis. A further feature shown in Figure 7/6 is the way the crack has initiated at 45^{o} to the specimen axis. This correlated with Forsyth's Stage I cracking and in fact Figure 7/6 shows several of the early stages of cracking discussed by Forsyth[19] and reproduced in Figure 2/2.

At the transition of the tensile mode to the shear mode of crack growth, the crack has two possible 35^{o} planes (at 90^{o} to each other) on which it can propagate. Under these circumstances it should be possible for two shear mode cracks to be formed and in several sectioned specimens this feature has in fact been observed. However one crack normally becomes dominant and propagates rapidly while the other crack apparently becomes non-propagating. Which crack becomes dominant is probably determined by local stress and micro-structural details. Figure 7/5 shows the formation of two shear mode cracks with

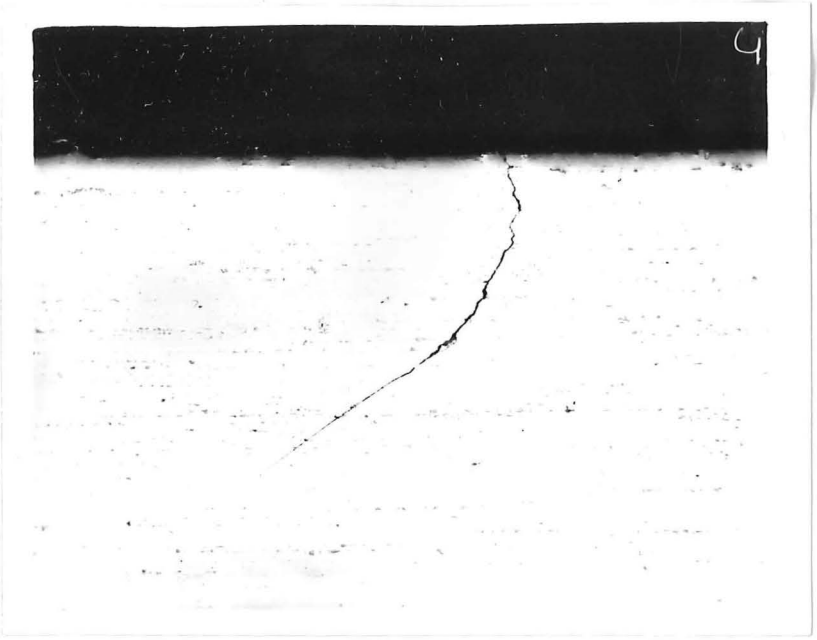

MAXIMUM TENSILE STRESS ⟷

Figure 7/4: Photograph (x50) showing an air fatigue crack. Stress level 19 tsi, cycles 1 x 10^5

MAXIMUM TENSILE STRESS ⟷

Figure 7/5: Photograph (x50) showing an air fatigue crack. Stress level 16 tsi, cycles 2.2 x 10^6

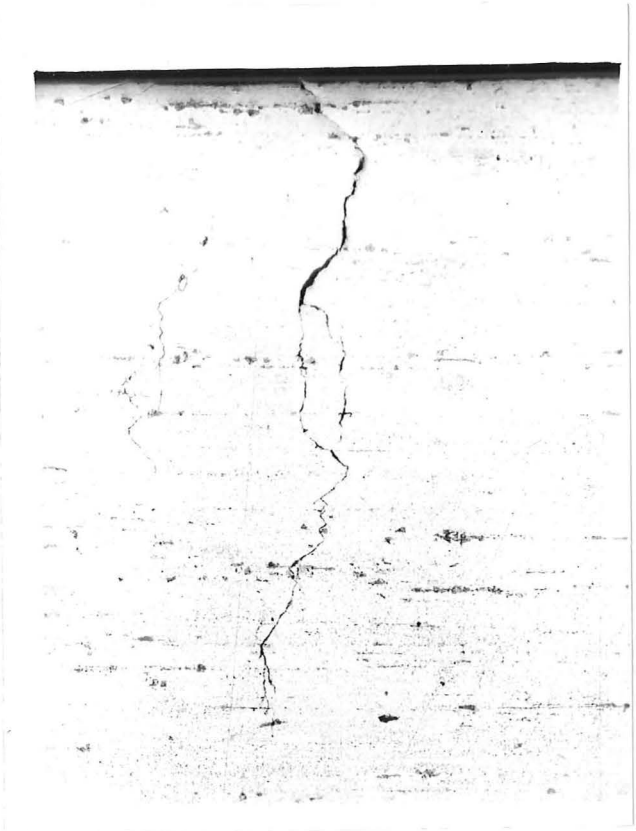

MAXIMUM TENSILE STRESS ⟷

Figure 7/6: A photomicrograph of an air fatigue crack showing the tensile mode of cracking. x150.

the non-propagating crack to the right of the major shear mode crack.

The tensile mode of cracking occupies the major part of the fatigue life of the specimen and rapid crack propagation occurs once the transition to the shear mode has taken place. In a paper by Broek and Schijve,[112] crack propagation rates in the two stages are quoted and transition points giving the number of cycles after which shear mode crack propagation occurs are shown graphically. The influence of mean stress on the length of the tensile mode cracking is also discussed.

In order to study the crack initiation stage and the initial stages of crack propagation several standard test specimens were polished using 1 and ¼ micron diamond paste. This treatment gave a surface finish equivalent to that of a metallographic section and thus enabled a closer study of the surface than was possible with the standard specimen preparation. These polished specimens were then fatigued for varying numbers of cycles until surface cracks appeared. These cracks were then studied using a metallurgical microscope and relevant areas photographed. This study showed that the surface cracking was often associated with a $CuAl_2$ particle (Figure 7/7) and that the crack zig-zagged around the specimen circumference (Figure 7/8). The transition from the tensile to shear mode cracking could also be clearly distinguished as is shown in Figure 7/9.

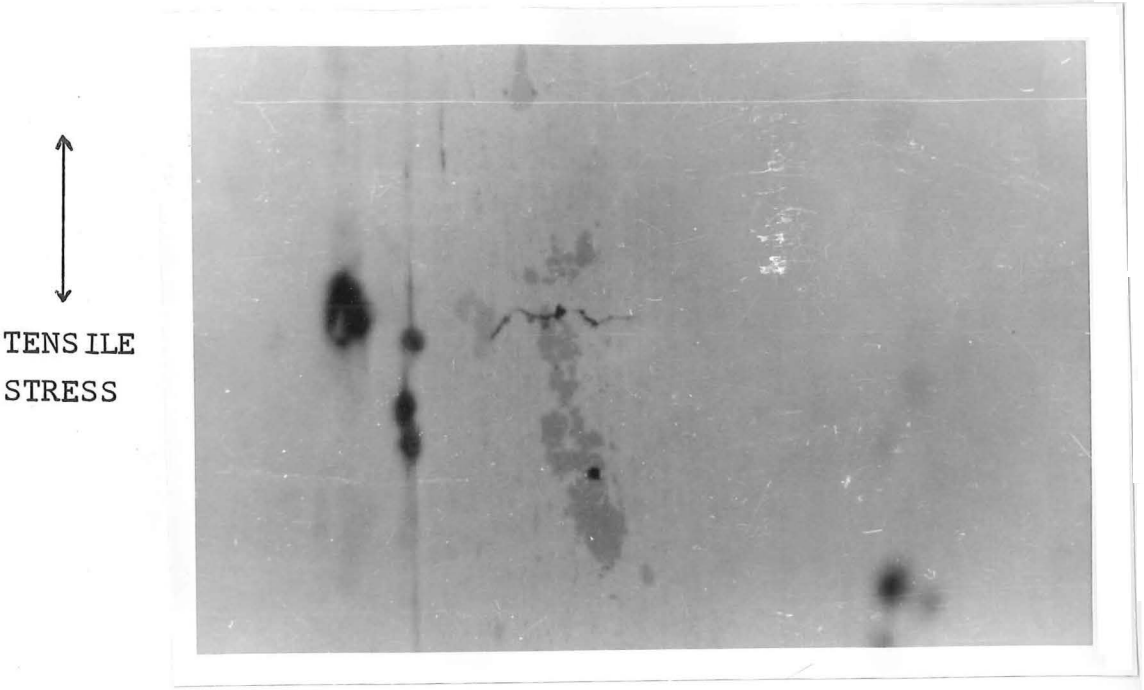

Figure 7/7: Initiation area of air fatigue crack on polished specimen. Crack initiates from $CuAl_2$ particle. x150.

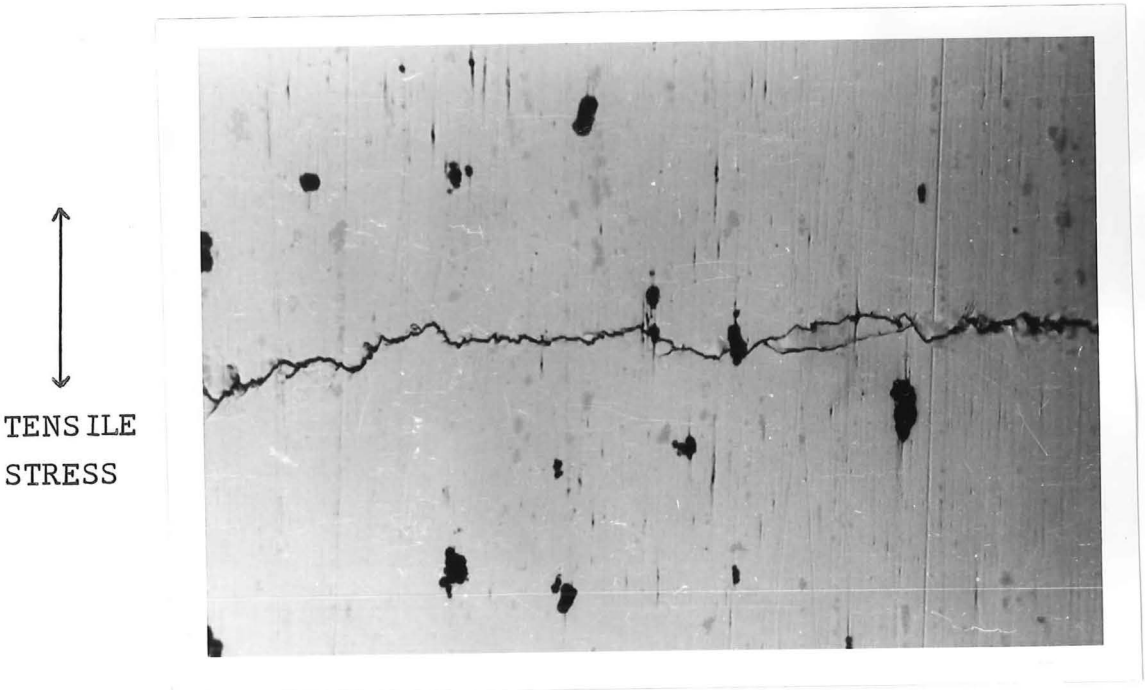

Figure 7/8: Typical air fatigue crack in polished specimen. x40

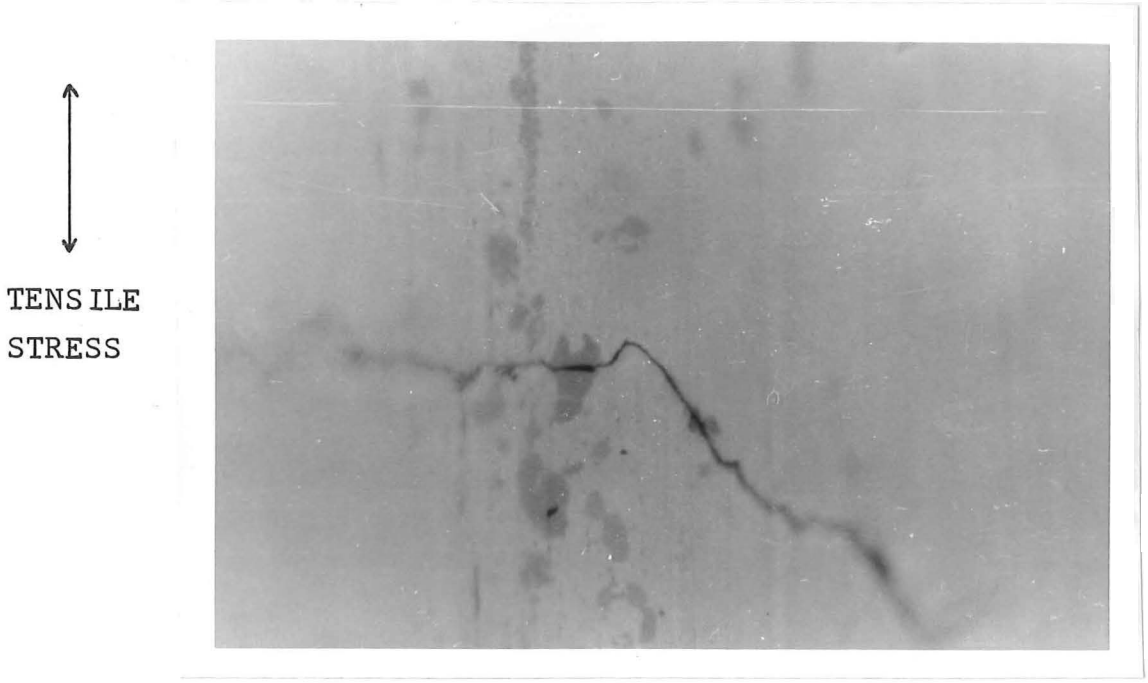

Figure 7/9: Air fatigue crack in polished specimen showing transition to shear mode. x150

7.2 Un-Notched Rotating Beam Corrosion Fatigue Fractures.

The fractures in the corrosion fatigue tests differed quite markedly from those obtained in air, in that the tensile mode was absent and the shear mode was apparently the only crack propagation system operative. Although all the corrosion fatigue fractures showed the same essential features there were some differences observed between the tests made with the various corrodents. These were, however, not differences in the basic crack morphology but were more a matter of the extent of crack formation and the number of cracks formed.

Basically, the fractures appeared to initiate at a single point and to propagate across the specimen at 35^{o} to the tensile stress direction, i.e., at 35^{o} to the specimen axis. This propagation in the shear mode differed from that observed in the air fatigue fractures in that the corrosion fatigue crack lay on the surface of a cone of 70^{o} included angle to give a "valley" fracture. Multiple cracking was also a marked feature in the corrosion fatigue tests especially at the lower stress levels where time became an important variable. The lower the stress level, the longer the time of test and the greater the degree of multiple cracking. This was especially the case in the superphosphate/moist air tests.

In the lower stress level tests it appears that several cracks form and propagate simultaneously until ultimate failure

occurs. This mechanism results in small crack facets and gives a zig-zag pattern around the specimen circumference. In the very low stress tests (4.4 tons/sq.in.) in superphosphate/moist air a large number of cracks were formed and the final fracture appeared to be at 90^{o} to the specimen axis. Closer examination of the fracture however, revealed the multiplicity of crack facets each one showing the features described above. Similar features were observed in tests with 3% NaCl as corrodent.

At higher stress levels two cracks often initiated in the same surface area but propagated in opposite directions. As there are two maximum shear stress directions, the formation of two cracks from the same area is highly probable. Normally, however, one crack becomes dominant and propagates to failure. Figure 7/10 shows typical corrosion fatigue fractures with the stress levels decreasing from top to bottom of the photograph. The specimen second from the top shows two cracks initiating from the same area but only one has propagated to failure. Both the lower specimens show multiple cracking around the whole specimen circumference. Also observable in the photograph is the build-up of superphosphate corrodent which occurred in the longer tests.

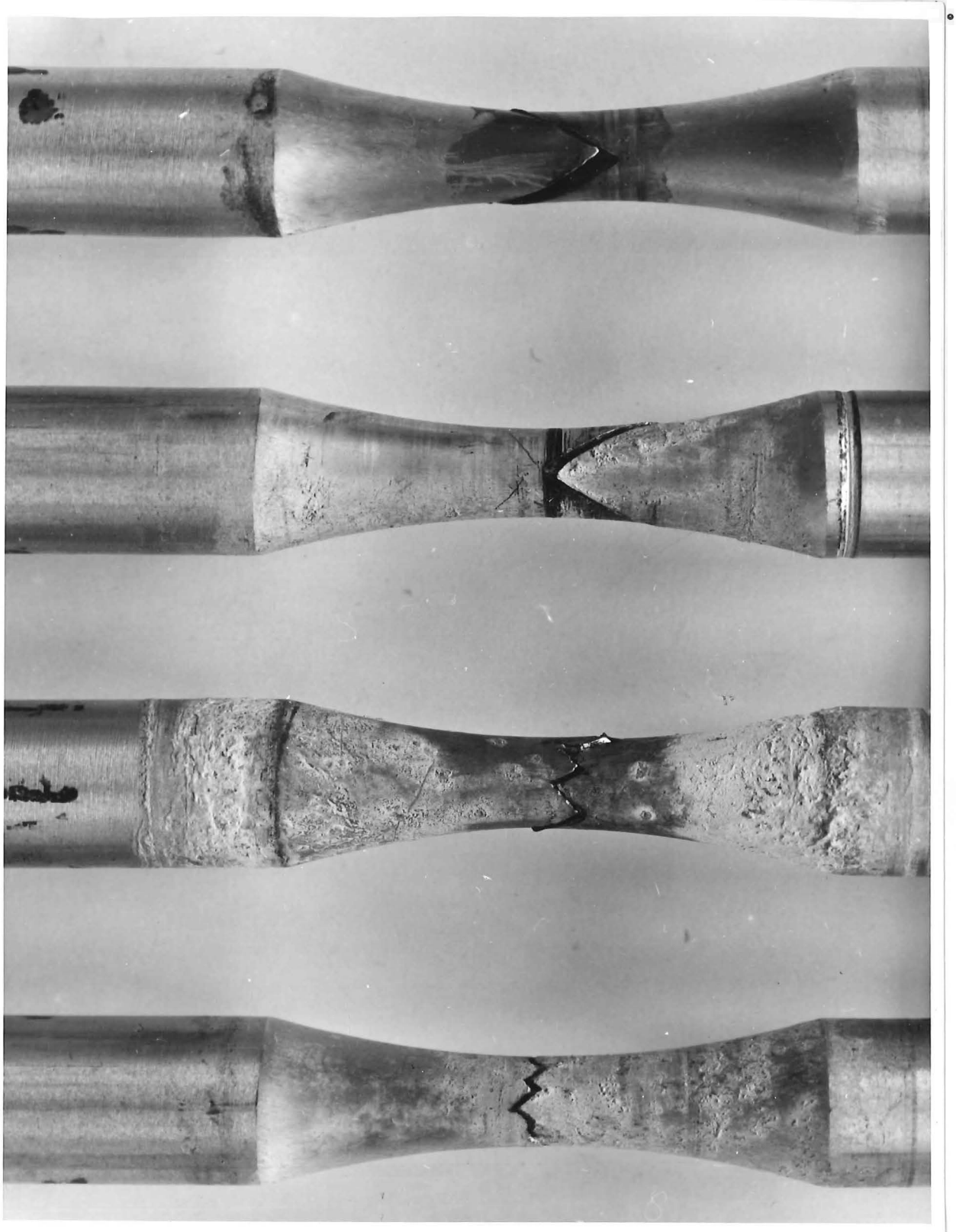

Figure 7/10: Corrosion fatigue fractures. Stress level highest at top of the photograph and lowest at the bottom.

Features which the corrosion fatigue fractures hold in common with the air fatigue fractures are the black fretting debris and the river pattern striations on the shear mode fracture faces. Details of the striations were however destroyed by corrosion especially in long term tests or where the specimen had failed overnight and had remained in contact with the corrodent.

A detailed study of the corrosion fatigue crack morphology showed that the crack propagates faster along the surface of the specimen than in the centre. The crack on the surface follows the maximum shear plane and its path resembles a helix. This faster crack growth on the surface means that the crack front is in the form of a V with the apex pointing back towards the point of crack initiation. This observation is illustrated in Figure 7/11 where an actual fracture surface is shown. Metallographic sections taken near the extremities of corrosion fatigue cracks showed how the crack advances into the centre of the specimen from the surfaces with crack growth in the centre lagging behind.

As with the air tests a number of corrosion fatigue tests were conducted until surface cracks were detected visually. These specimens were then sectioned and examined metallographically. Figures 7/12 - 7/15 show features of the corrosion fatigue cracks revealed by metallographic examination. Figures 7/12 and 7/13 which are sections along the specimen axis

Figure 7/11: Photograph of a corrosion fatigue fracture, showing how the crack propagates faster at the edges of the specimen than in the centre.

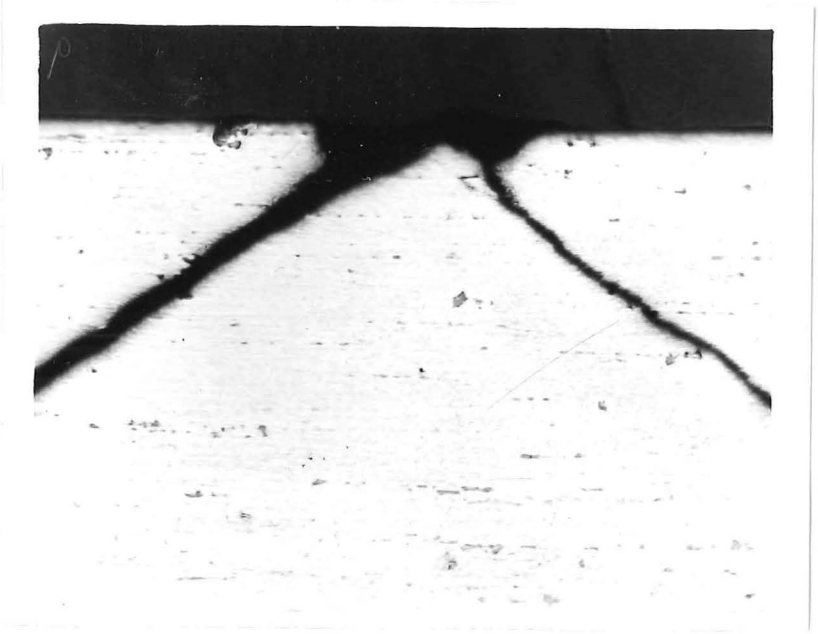

MAXIMUM TENSILE STRESS ⟷

Figure 7/12: Photomicrograph of two corrosion fatigue cracks initiating from same point. x150.

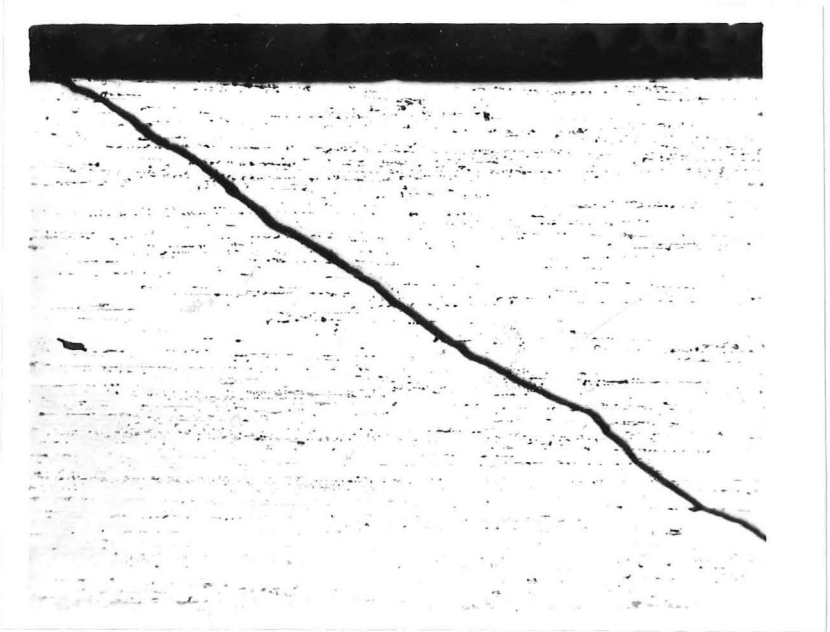

MAXIMUM TENSILE STRESS ⟷

Figure 7/13: Photomicrograph of a typical corrosion fatigue crack, showing shear mode of failure. x50.

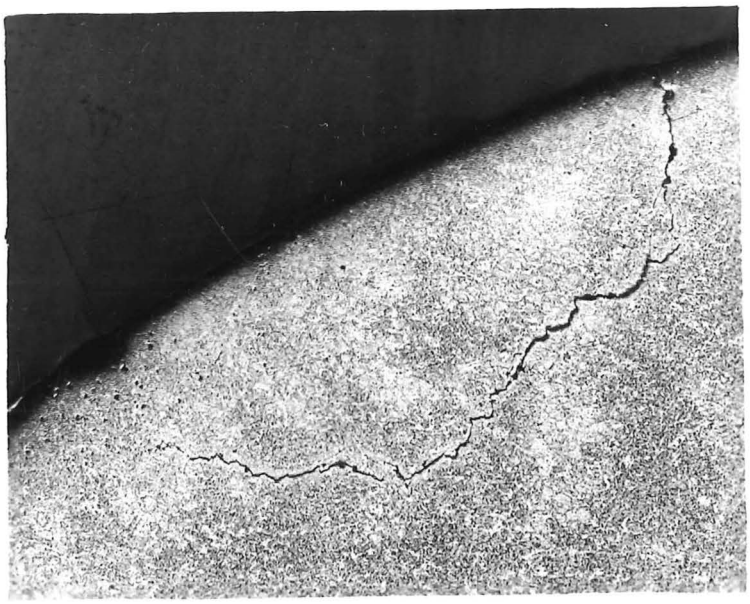

Figure 7/14: View of a section through a corrosion fatigue crack at right angles to the longitudinal axis of the specimen. The crack front forms part of the surface of a cone. X50.

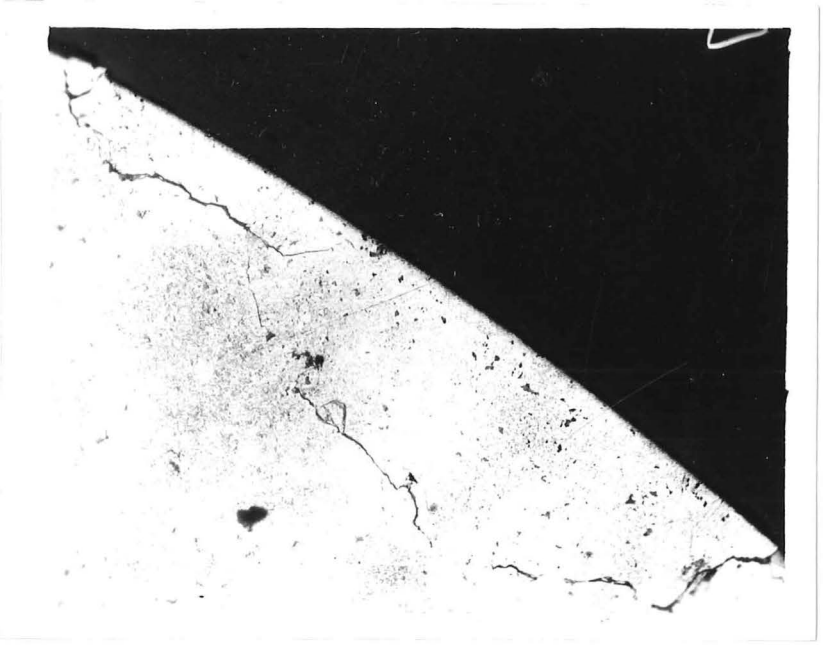

Figure 7/15: A similar view to Figure 7/14 but showing two corrosion fatigue cracks. x50.

show the cracks propagating at 35° to the specimen axis, i.e., in the shear mode. The absence of any tensile mode cracking is most noticeable. Figure 7/13 shows two shear mode cracks initiating at the same point. This double cracking was a common feature especially at higher stress levels. In addition to the longitudinal sections, sections were taken at right angles to the specimen axis to examine the nature of the crack front. Typical views of such sections are shown in Figures 7/14 and 7/15. These sections show clearly how the crack front lies on the surface of a cone to give the typical valley fracture.

In the metallographic studies careful note was taken as to whether corrosion pits had been formed on the specimen surface and whether or not the corrosion fatigue cracks were associated with these pits. Exfoliation corrosion was the main form of corrosion attack in the lowest stress level tests but very few of these areas of attack were associated with corrosion fatigue cracking. At the higher stress levels the only evidence of corrosion attack was discolouration of the specimen surface. There was some indication that corrosion pitting was in fact occurring in the lowest stress level tests in superphosphate corrodent and that the corrosion fatigue cracks appeared to be associated with this pitting. However, there was considerable doubt as to whether the pitting came first and the cracks initiated from it or whether the cracks

formed first and the pits were due to corrosion attach on the crack initiation areas resulting in widening of the cracks to give apparent pits.

In order to study this aspect of corrosion fatigue crack initiation, specimens were polished with 1 and ¼ micron diamond paste and these specimens tested in superphosphate/mois air corrodent for varying numbers of cycles. The surface of each specimen was examined using a metallographic microscope and the initiation areas photographed. No corrosion pitting was observed in these tests although corrosion fatigue cracks were formed. The initiation of these cracks showed a marked resemblance to the early stages of the air fatigue cracks on similarly prepared specimens except that the shear mode became dominant much earlier. Figures 7/16 and 7/17 show typical initiation areas of corrosion fatigue cracks and these can be compared with similar areas for air fatigue cracks shown in Figures 7/7 - 7/9. It was noted that the $CuAl_2$ particles appeared to be preferentially attacked by the corrodent and evidence of this attack is visible in both Figures 7/16 and 7/17. The corrosion fatigue cracks, like the air cracks, appeared to be associated with the $CuAl_2$ particles.

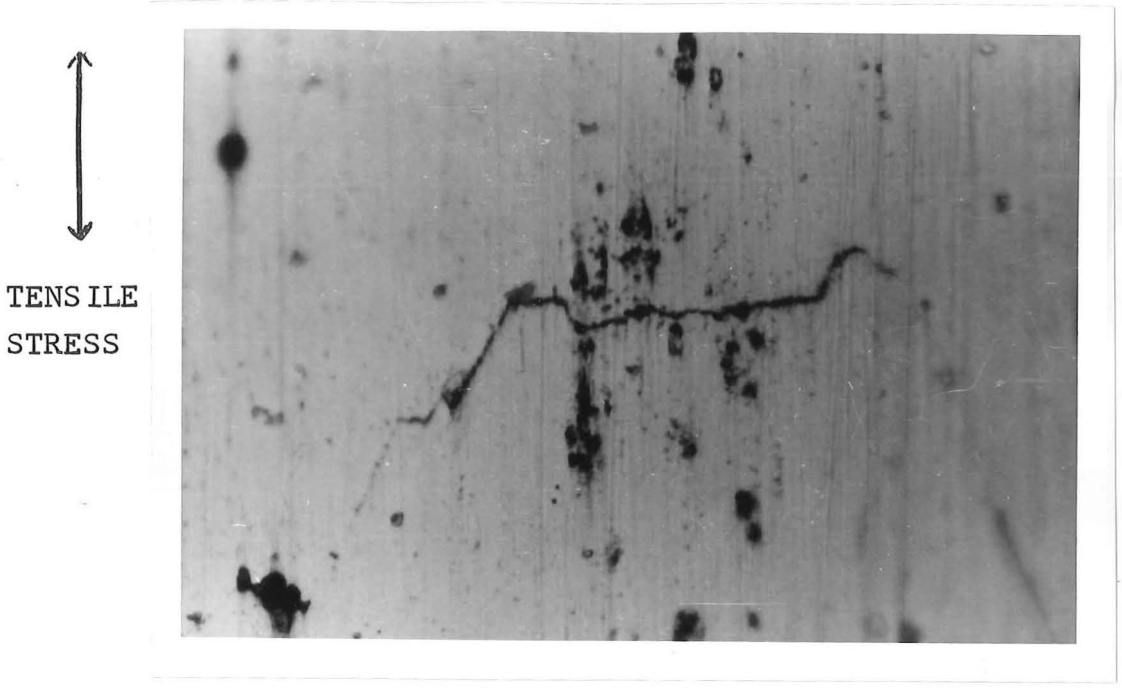

Figure 7/16: Initiation area of corrosion fatigue crack on polished specimen. Initiation associated with corroded $CuAl_2$ particles. x150

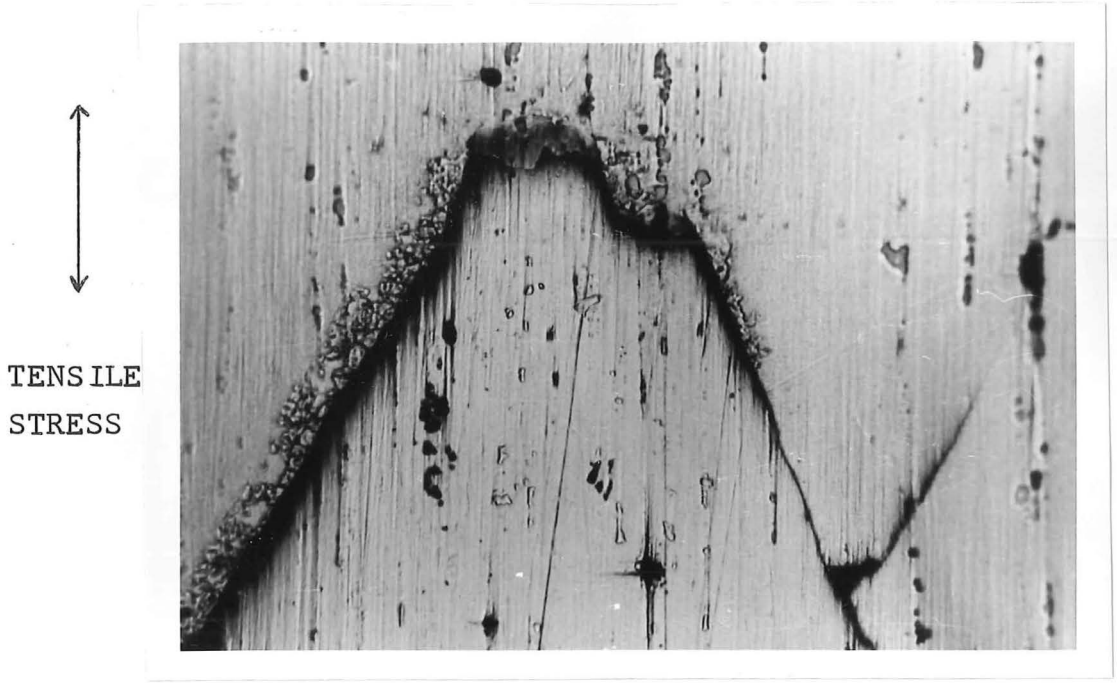

Figure 7/17: Corrosion fatigue crack in polished specimen. x40

7.3 Notched Rotating Beam Fractures.

At first glance the notched rotating beam tests in air gave an entirely new type of fracture compared with those already described, the fractures tending to be somewhat cone shaped especially at high stress levels. However, a closer and more detailed study including metallographic sections, showed that the same modes of crack propagation were operative here as in the un-notched tests. The fatigue crack initially propagated in the tensile mode as is the case with the un-notched specimens, but in the notched specimens fatigue cracks were initiated around the whole circumference rather than in a limited area. This gave continuous tensile mode crack propagation around the whole specimen circumference. After the appropriate number of cycles, which depended on stress level, the shear mode of fatigue crack propagation became operative. The extent of tensile mode cracking was dependent on stress level, as in the un-notched specimens, and the lower the stress level the greater the proportion of tensile mode cracking. The continuous tensile mode cracking around the notch circumference meant that the shear mode fracture face formed the surface of a cone of included angle of approximately 70^{o} rather than the planar fracture normally associated with shear mode fractures.

Very little, if any, shear mode cracking occurred in the lower stress level tests, as the specimen diameter was sufficiently reduced by the tensile mode cracking for complete failure to occur before the transition to shear mode cracking took place. This feature was not observed in the un-notched specimens where only limited tensile mode cracking occurred and the transition to shear mode cracking could take place. Figure 7/18 shows typical air fractures obtained with notched rotating beam specimens, and Figure 7/19 shows how the tensile and shear crack propagation modes operate in these notched specimens.

Finney[110,111,113] has observed similar cone-shaped fractures in notched specimens of high strength aluminium alloys and has also shown that the extent of shear mode cracking is dependent on cycle frequency[113] as well as stress level. High cycle frequency (12000 c.p.m.) together with high stress levels (above 35,000 lb./sq.in.) gave almost perfect cone-shaped fractures.

Two types of fracture were observed in the notched rotating beam tests with superphosphate corrodent. One type was similar to the air fractures of the notched specimens, i.e., tensile mode followed by shear mode cracking. In some instances, shear mode cracking became operative for a very short period at the start of fatigue cracking but then changed back to the tensile mode. The other type of fracture observed

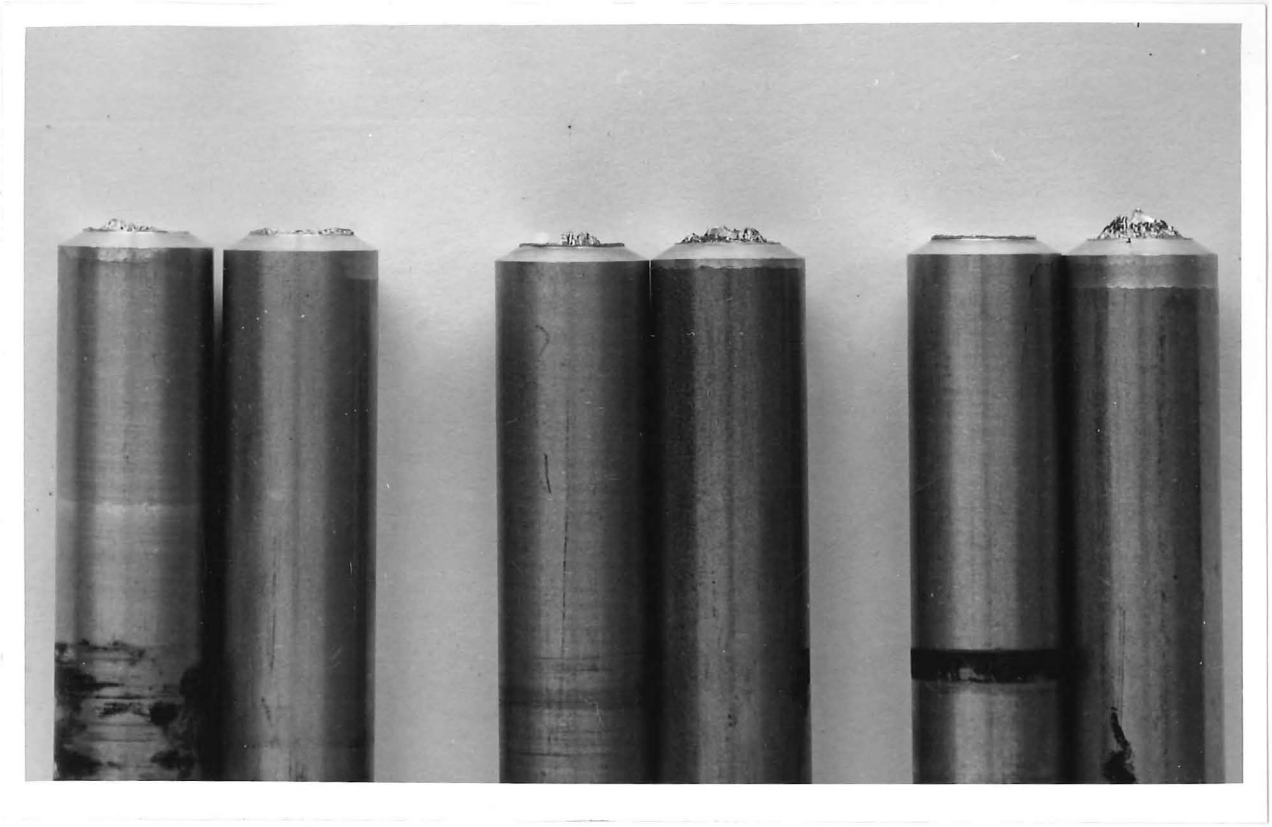

Figure 7/18: Air fatigue fractures in notched rotating beam specimens. Stress level lowest at left and highest at right.

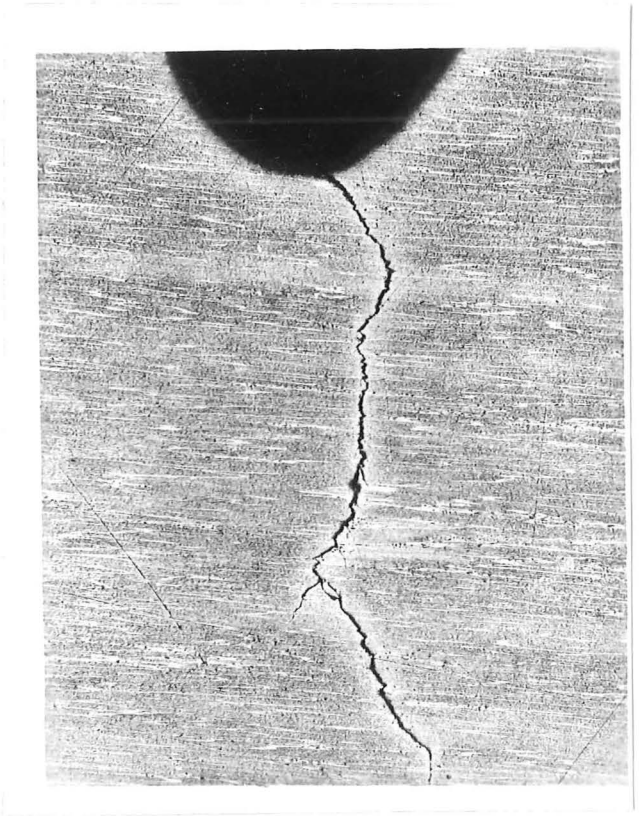

MAXIMUM TENSILE STRESS ⟷

Figure 7/19: Photomicrograph of air fatigue crack in a notched rotating beam test specimen. Initiation at 45°, followed by tensile mode cracking and transition to shear mode cracking. Two shear mode cracks formed at end of tensile mode cracking. x60.

was pure shear mode cracking and gave almost perfect cone-shaped fractures on a cone of included angle of approximately 70^{o}. It is highly probable that this latter type of fracture is nearer the true case of corrosion accelerated fatigue cracking as specimens showing this mode of failure had very short fatigue lives and similar fractures were consistently obtained in the direct stress tests (see Section 7.6). A cross section of a shear mode type of failure is shown in Figure 7/20 and the cone-shaped fracture can be clearly seen. This type of fracture is identical to that described by Finney in his work on notched specimens in air.

7.4 Fractures Observed in Two Stage Wet-Dry Tests.

In the two stage wet-dry fatigue tests the type of fracture observed depended on stress level and the length of the wet fatigue stage. At high stress levels a shear mode crack usually existed prior to the dry fatigue stage and crack propagation in the dry stage continued in the shear mode. The crack propagation rate however, was apparently determined to some extent by the length of the wet stage. Where this was less than about 40% of the normal corrosion fatigue life, i.e., the total life if the test was continued in the corrodent, then crack propagation rates were slower in air than if the test had been continued in the corrodent. If the wet stage exceeded 40% of the normal corrosion fatigue life, the crack propagation

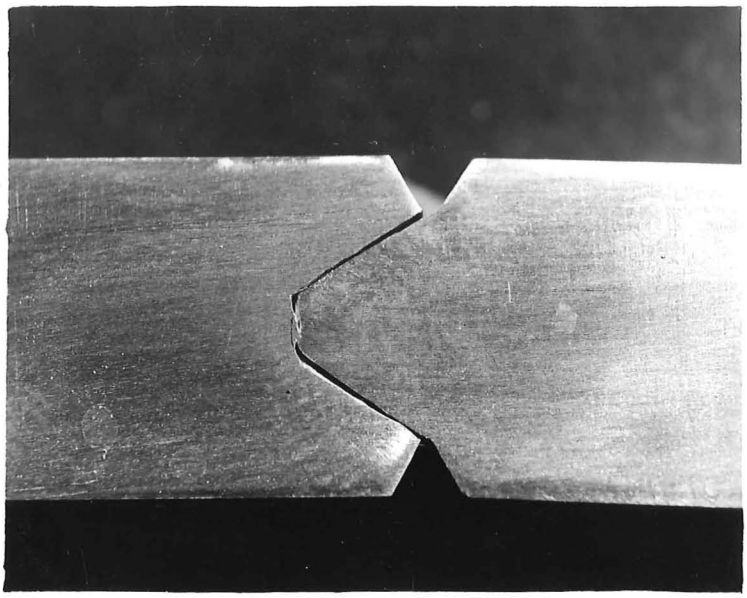

MAXIMUM TENSILE STRESS ⟷

Figure 7/20: Shear mode fatigue failure obtained in corrosion fatigue test of a rotating beam specimen. Corrodent superphosphate, stress level 9.2 tons/sq.in.

rates in the dry stage were apparently unaltered compared to those in the wet stage and the total fatigue life (wet plus dry stages) was the same as the normal corrosion fatigue life.

At lower stress levels the type of fracture obtained was very dependent on the length of the wet stage. If a shear mode crack was initiated in the wet stage then two possible effects were observed. Where the wet stage was less than 40% of the normal corrosion fatigue life then the shear mode crack did not continue to propagate in the dry stage. Instead, the tensile mode of cracking occurred and often continued until ultimate failure took place. Fractures obtained in this type of test typically showed a small shear mode fracture face with a large tensile mode failure initiating from it. (Figure 7/21) Where the wet stage of the test exceeded 40% of the normal corrosion fatigue life, crack propagation in the dry stage was normally a continuation of the existing shear mode crack.

In the lower stress level tests where a shear mode crack was not initiated in the wet stage, tensile mode cracking initiated in the subsequent dry stage. However this tensile mode cracking occurred around a large part of the circumference, unlike the limited cracking observed in completely dry tests. This extensive tensile mode cracking in the dry stage of the two stage tests resulted in fractures resembling those obtained with notched specimens in air.

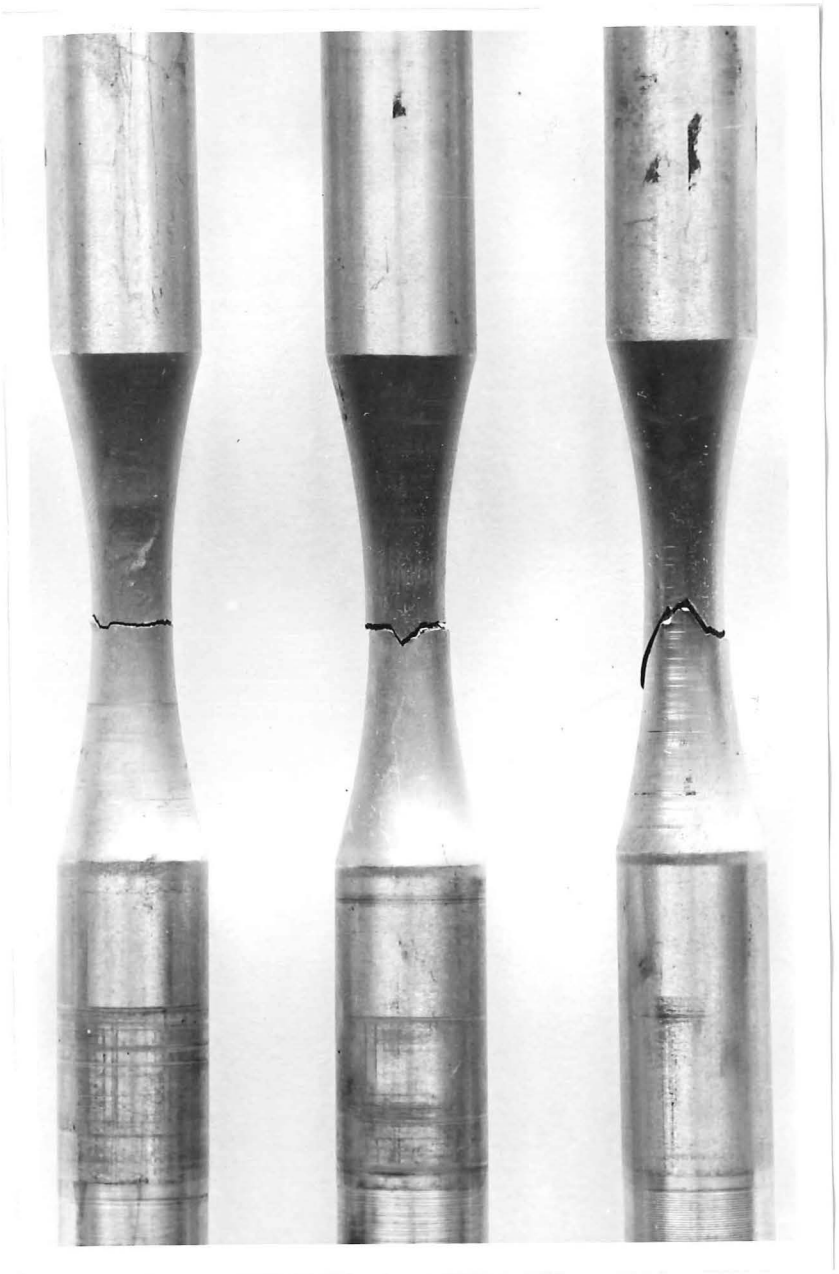

Figure 7/21: Fractures obtained in Wet-Dry two stage fatigue tests showing effect of corrodent on crack propagation mode. Specimen at left shows tensile mode cracking that occurred after a wet stage less than 20% of the corrosion fatigue life. Middle specimen shows initiation in the shear mode but with reversion to the tensile mode after removal from the corrodent. Specimen on right shows crack propagation continuing in shear mode after removal from the corrodent.

The two stage dry-wet tests gave similar shear mode fractures to those obtained in the corrosion fatigue tests (see Section 7.2). One notable feature however, was that the incidence of multiple cracking increased especially at high stress levels, and the longer the dry stage the greater the number of shear mode cracks initiated during the wet stage.

7.5 Fractures in Pre-Corroded Specimens and in Painted Specimens.

The pre-corrosion tests gave fractures which displayed many of the features already discussed for the notched tests and the two stage wet-dry tests. Basically the fractures were typical air fractures showing crack propagation in the tensile mode with subsequent transition to the shear mode. The tensile mode cracking was initiated around a greater proportion of the specimen circumference than was usual for non-corroded air specimens. This extensive tensile mode cracking was similar to that found in wet-dry and notched specimens and it produced a rounded shear mode fracture surface rather than the flat planar fracture found in normal air fractures of un-notched specimens. In many instances, especially at low stress levels, tensile mode cracking occurred in diametrically opposite areas of the specimen and where this was observed no shear mode fracture was seen. This feature, while also

observed in the two stage wet-dry tests was never found in normal air fatigue tests.

With the painted specimens, somewhat similar features to those described for the pre-corrosion tests was observed. The usual fracture modes of tensile cracking followed by shear mode cracking were noted in the air fatigue tests. As in the pre-corrosion tests, however, the tensile mode cracking was generally more extensive than in the unpainted air tests and this produced a rounded (semi-cone) shear mode fracture surface similar to those found in the pre-corrosion tests.

A very surprising feature of the tests of painted specimens in superphosphate corrodent was that the fractures produced were identical to those found in un-painted specimens, i.e., shear mode valley fractures. The only difference was that multiple cracking was absent in the painted specimens. Typical air and corrosion fatigue fractures of painted specimens are shown in Figure 7/22. In some corrosion fatigue tests the painted coating was deliverately damaged exposing the bare metal to the corrodent. With these specimens, fractures always initiated in the exposed metal.

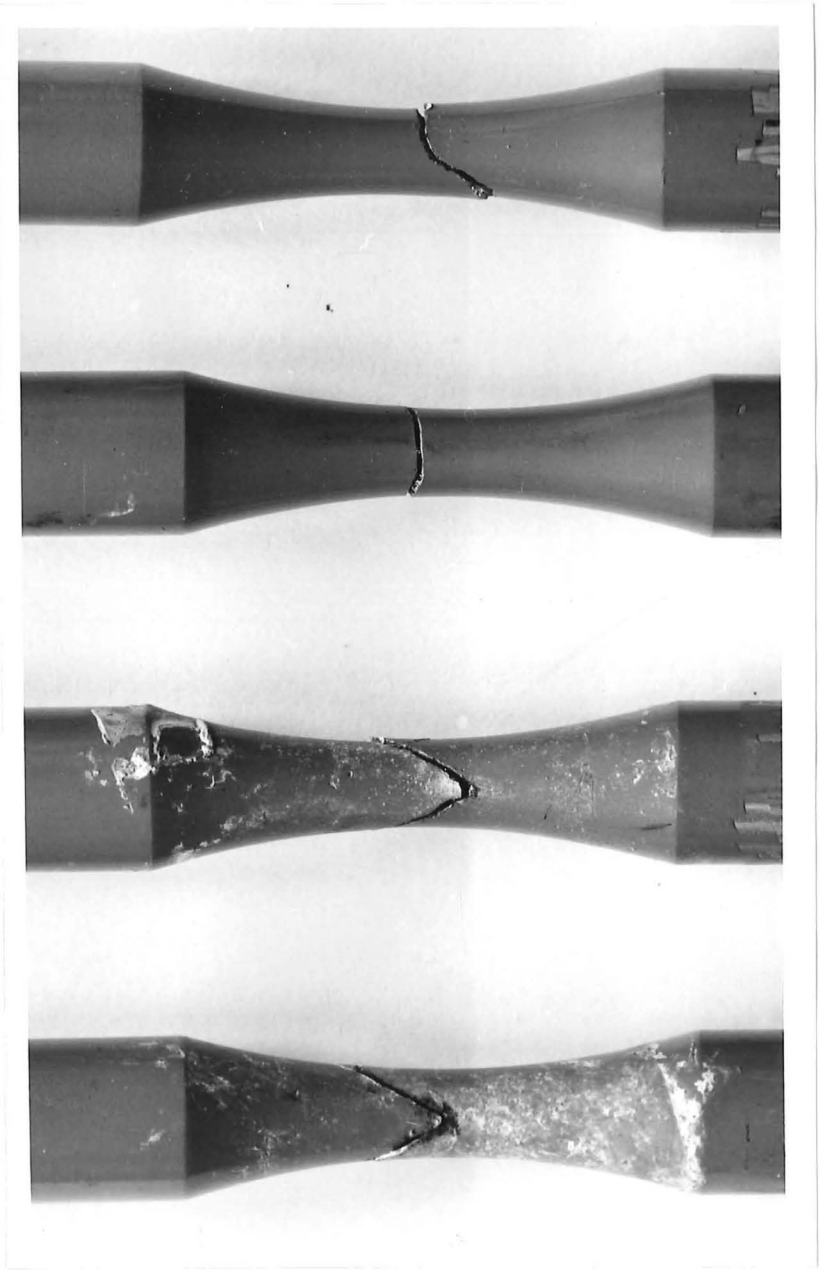

Figure 7/22: Fatigue fractures in painted rotating beam test specimens. Upper fractures obtained in air, lower fractures in superphosphate corrodent.

7.6 Direct Stress Fractures.

The fractures in the notched direct stress fatigue tests resembled those from the notched rotating beam tests. In air the cracks initiated in the tensile mode and the normal transition to the shear mode took place. As was normal, the length of the tensile mode depended on stress level and the lower the stress level the greater the degree of tensile mode cracking. One difference however, was that the shear mode cracking was much more definite in the direct stress tests than in the rotating beam tests. Distinct cone-shaped fractures were produced in the direct stress tests at all stress levels at which fractures occurred.

In the superphosphate corrodent tests of notched direct stress specimens the fractures were cone-shaped shear mode failures and no tensile mode cracking was observed. These cone-shaped fractures were similar to those described as occurring in some of the rotating beam tests. The included angle of the cone was approximately 70°.

Typical notched direct stress fractures are shown in Figures 7/23 and 7/24.

With the un-notched direct stress specimens in the superphosphate corrodent shear mode fractures identical to those found in un-notched rotating beam tests occurred. Figure 7/25 shows a typical fracture and one feature to be noted is the absence of multiple cracking. This was a

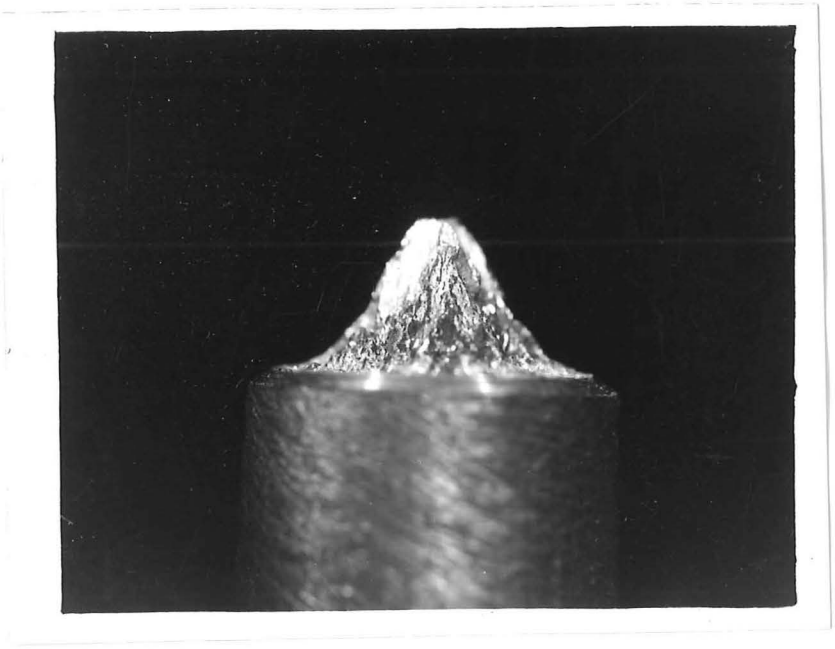

Figure 7/23: Air fatigue fracture in notched direct stress specimen. Fracture starts in tensile mode but then changes to shear mode.

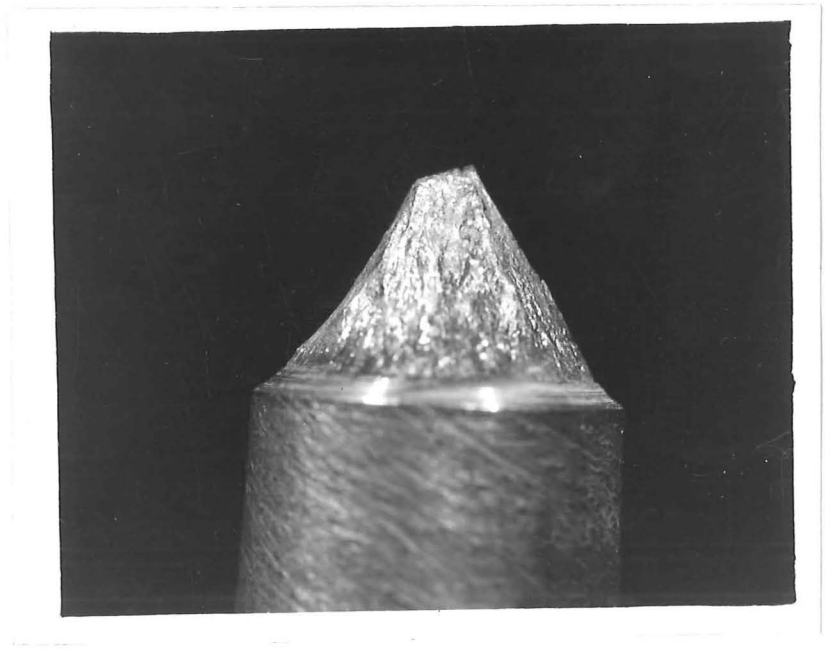

Figure 7/24: Corrosion fatigue fracture in notched direct stress specimen. Tensile mode absent and only shear mode operative.

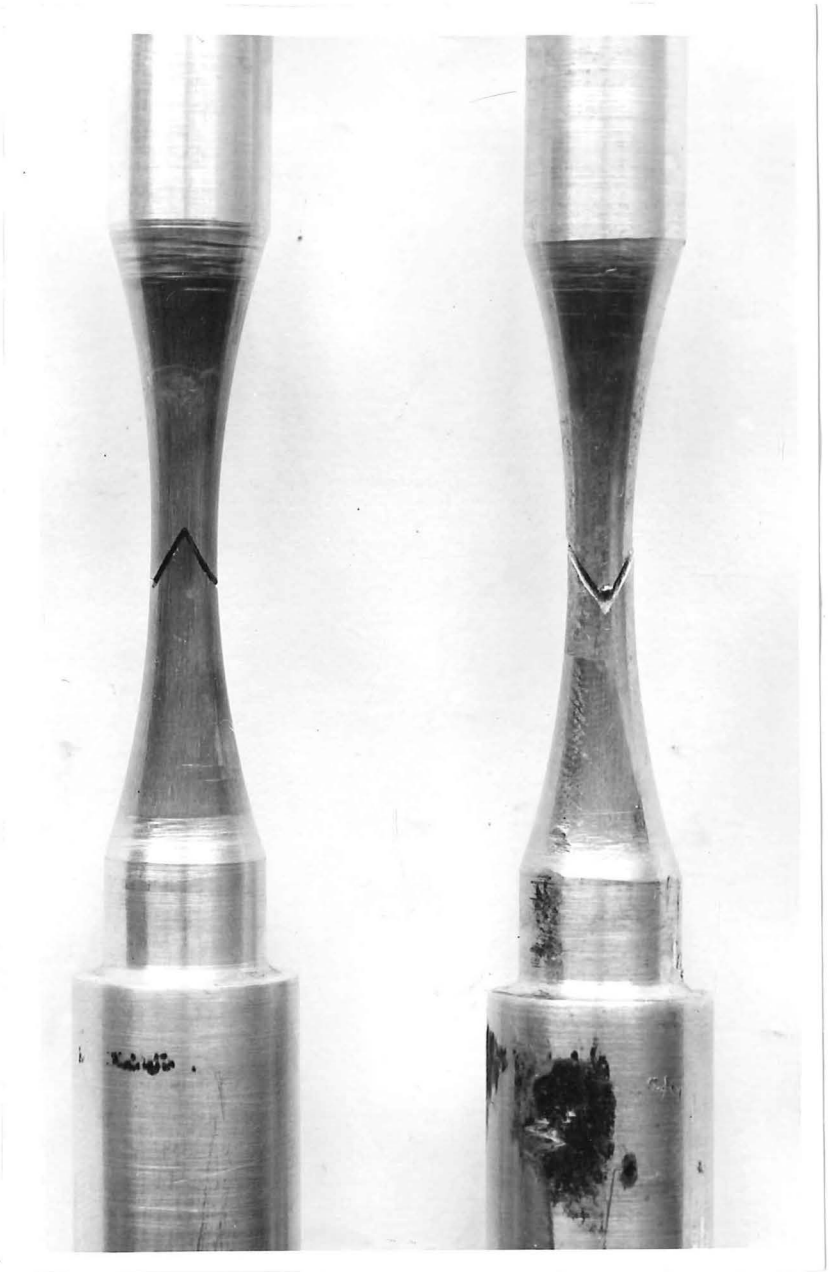

Figure 7/25: Typical corrosion fatigue fractures in un-notched direct stress test specimens with superphosphate corrodent.

feature of the un-notched direct stress tests in contrast to the rotating beam tests where multiple cracking at all but the highest stress levels was the rule rather than the exception.

7.7 Reverse Bend Fractures.

All the features of the un-notched rotating beam tests were reproduced in the reverse bend tests. Tests in air showed tensile mode cracking followed by transition to planar shear mode cracking. One difference was the initiation of tensile mode cracking on diametrically opposite sides of the specimen but this would be expected from the mode of stressing.

Tests conducted in superphosphate corrodent showed the typical valley shear mode failures. Normally two such cracks were initiated on opposite sides of the specimen but multiple cracking also occurred. This multiple cracking was very similar to that described as occurring in the rotating beam test work. Typical reverse bend fractures are shown in Figure 7/26.

7.8 Summary of Fractographic Studies.

With the un-notched specimens in air, for all stress systems studied, fatigue failure occurs in two main stages. The first or tensile mode is at 90^{o} to the applied tensile stress and the length of this stage depends on stress level, the lower the stress level, the longer the stage. The

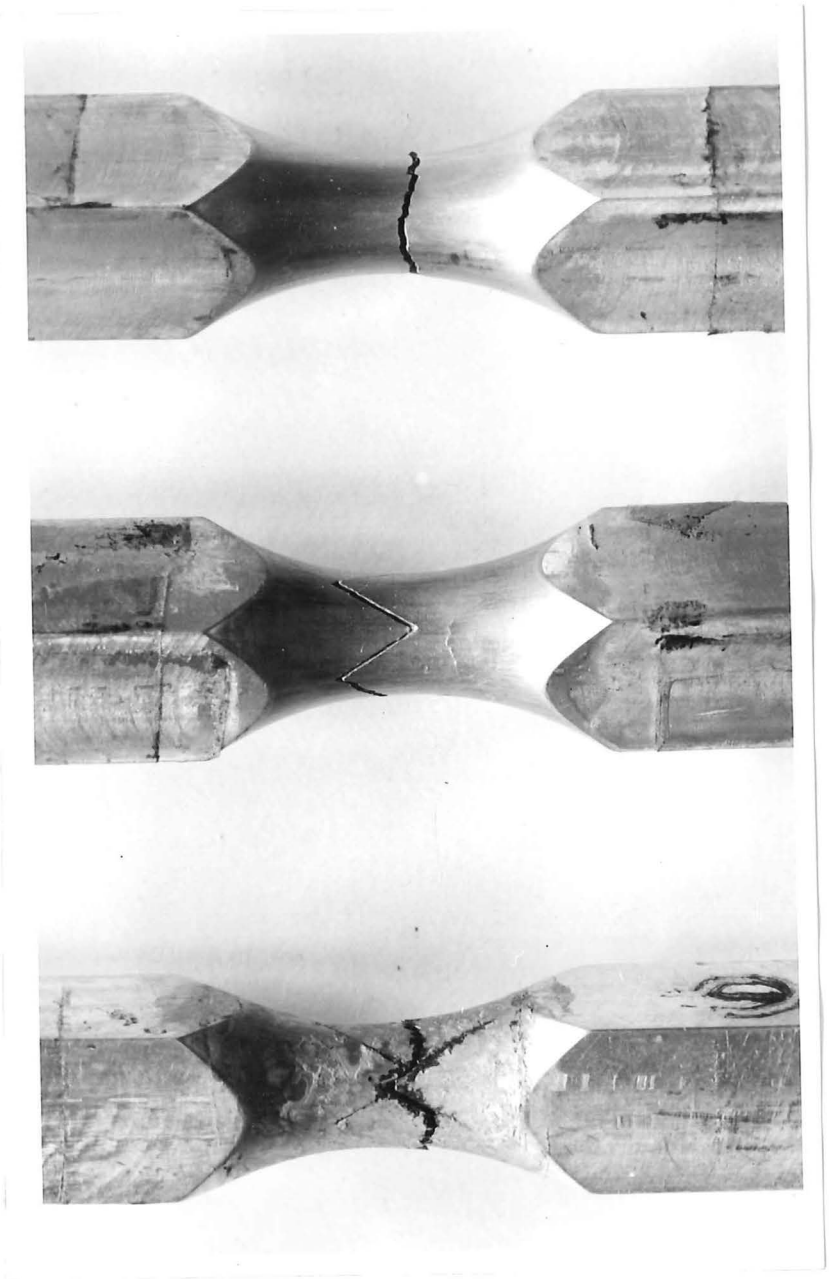

Figure 7/26: Reverse bend fatigue fractures. Upper fracture obtained in air, middle and lower in superphosphate corrodent.

second or shear mode is at about 35^{o} - 40^{o} to the applied tensile stress and produces either a planar or a semi-cone surface depending on the extent of tensile mode cracking around the specimen circumference. Final fracture occurs on a 45^{o} shear plane. The bulk of the fatigue life of a specimen (up to 90%) is spent in the tensile mode stage and very rapid crack propagation rates occur in the shear mode.

Under corrosive conditions shear mode cracking only is operative in un-notched specimens with very rapid crack propagation rates. The fracture surfaces lie on part of the surface of a cone of included angle of 70^{o} to give a valley fracture. Multiple cracking is a feature of these tests especially at low stress levels.

For notched specimens, the same crack propagation modes operate as for the un-notched specimens. In air, tensile mode cracking is followed by shear mode cracking. The degree of shear mode cracking is influenced by stress level and cycle frequency and at high stress levels and high cycle frequencies cone-shaped shear mode fractures are produced. Under corrosive conditions cone-shaped shear mode fractures are produced and the fracture surface forms a cone of 70^{o} included angle.

C H A P T E R E I G H T.

8. DISCUSSION OF RESULTS.

8.1 Un-notched Specimens.

The test results from the present investigation follow the general pattern reported in the literature in that fatigue tests made in a highly corrosive environment showed a marked reduction in life compared to equivalent tests in air. While the S-N curve in air for the rotating beam tests showed no definite shape, the S-N curves obtained under corrosive conditions tended to follow the general shape of the idealised S-N curve suggested by Wood[22] and shown in Figure 2/2. A remarkable feature of the corrosion fatigue test work was the reproducibility and lack of scatter in test results compared to equivalent tests in air. This feature was first observed by McAdam[43 - 47] and appears to be a feature of corrosion fatigue testing. Results were so reproducible that the result of a test could be accurately predicted and this was of extreme value when deciding on the length of the wet stage in the two-stage wet-dry test series.

A further feature of the corrosion fatigue work was the multiplicity of cracking and this again has been commented on by many workers and is a well recognised feature. The fractography of corrosion fatigue failures has however received comparatively little attention from research workers, most interest being taken in the loss in fatigue

life, and as a result descriptions of corrosion fatigue fractures are lacking in the literature. It is thus not clear whether the fractures observed in the present investigation are the normal type of fractures obtained in corrosion fatigue. In view of the fact that all the corrodents used in the test work gave similar fractures it is felt that the valley fracture is the usual type of fracture for high strength aluminium alloys for fatigue loading under highly corrosive conditions.

In the rotating beam tests in air there was considerable scatter in results and the resulting S-N curve (Figure 4/4) shows no definite shape. At stress levels below 12 tons/sq.in. specimens had fatigue lives in excess of 10^8 cycles. Of the various corrodents used in the corrosion fatigue test work, tap water produced the least drop in fatigue life, 3% NaCl and potassic superphosphate the greatest and aerial superphosphate values intermediate between tap water and 3% NaCl. At stress levels above 10 tons/sq.in. all corrodents gave very similar results and the fatigue lives showed only small differences. At stress levels less than 8 tons/sq.in. fatigue lives in excess of 10^6 cycles were obtained and at this stage the difference between the various corrodents became more apparent with the potassic superphosphate and 3% NaCl producing the greatest drop in fatigue life. These differences are shown clearly in Figures 4/4 - 4/7.

The decrease in fatigue life produced by a given corrodent is apparently related to the severity of corrosion attack on the 2024 - T4 alloy by the corrodent. If the corrodents are arranged in order of increasing severity of attack then tap water should produce the smallest reduction in fatigue life, followed by aerial superphosphate, 3% NaCl and potassic superphosphate. This is in fact the case as shown by the results of the corrosion fatigue tests.

The presence of moisture is necessary to produce corrosion attack by the various grades of superphosphate. Dry aerial superphosphate has no effect on the fatigue life of the 2024 alloy but the presence of even small amounts of moisture produces a marked reduction in fatigue life. The amount of moisture present does not appear to be critical in that similar reductions in fatigue life were produced by a slurry of 25 grams/litre of superphosphate and pastes of superphosphate containing various amounts of water ranging up to a maximum of 10%.

A standard painted coating on the alloy had some effect in improving the fatigue life under corrosive conditions. The treatment of anodising followed by a chromate etch with a final top coat of paint did however affect the fatigue life in air at high stress levels. At stress levels above 14 tons/sq.in. the protective treatment gave quite a marked

reduction in fatigue life in air compared to unpainted specimens (Figure 4/10). At lower stress levels however, an improvement in air fatigue life became apparent. Under corrosive conditions the painted specimens gave a marked improvement in fatigue life over unpainted specimens but a disturbing feature was that the type of fractures produced were identical to those found in unpainted specimens. While the painted specimens showed an improved corrosion fatigue life over unpainted specimens, they did show a drop in fatigue life compared to painted specimens in air. Thus in Figure 4/10 the painted specimen S-N curve in superphosphate is lower than the corresponding air curve. The similarity of fracture morphology together with the lowering of fatigue life in superphosphate indicates that the corrodent is permeating through the painted coating causing accelerated fatigue failures.

When the fatigue curves obtained in tests with the various corrodents are considered it is apparent that even a mildly corrosive medium such as tap water causes a marked reduction in fatigue life. The most serious aspect of the test results with superphosphate is the very poor fatigue lives at stresses as low as 4.4 tons/sq.in. This means that fatigue failures are highly probable in aircraft components made from 2024 alloy at stresses well below those that would be considered safe, if superphosphate is present. In fact

these stress levels are around normal design stresses and thus the question of whether superphosphate can cause accelerated fatigue failures in aircraft components can be answered in the affirmative. Painting of the component can produce a marked improvement in the fatigue life providing the coating remains intact. Once the protective coating has been damaged in any way permitting superphosphate to come into contact with bare metal, then a rapid fatigue failure can be expected. This emphasises the need for careful and continued inspection of aerial topdressing aircraft for evidence of either corrosion attack or damaged paintwork.

The effects of pre-corrosion on the aluminium alloy was expected from the results reported by McAdam, and Panseri[65]. The reduction in fatigue life after 24 hours corrosion attack was not as high as that produced by combined fatigue loading and corrosion attack but is still sufficient to be of practical concern to the aerial topdressing industry. It is felt that the reduction in fatigue life by pre-corrosion is probably due to the notch effect of the corrosion pits formed on the specimen surface. In the pre-corrosion tests a certain amount of ex-foliation corrosion attack was noted and these areas would act as stress raisers of low stress concentration factor and would thus produce an accelerated fatigue failure.

From the fractographic studies it is evident that two major modes of crack propagation operate in the air fractures. In the first, or tensile mode, the crack runs at right angles to the tensile stress (Figure 7/5). During this stage, the length of which depends on the stress level, the crack moves in short bursts at about 35^{o} to the tensile stress, the length of each burst being of the order of the grain size of the alloy. Each burst propagates until it is halted by a barrier such as an unfavourably oriented grain, plastic working ahead of the crack tip, grain boundaries or by dislocation pile-up. A combination of several of these factors is highly probable. As the specimens were machined from extruded rod which had been solution treated and naturally aged there will be a marked tendency for the grain structure to be oriented along the specimen axis. It would thus be possible for a single burst of crack propagation to continue across several suitably oriented grains before being halted. This is the most probable explanation for the uneven-ness of length of the crack propagation bursts shown in Figure 7/6. When crack propagation is blocked on one 35^{o} plane, then because of the grain orientation in the alloy it is to be expected that the 35^{o} plane at 90^{o} to the original one could become active. This would explain the type of crack propagation that occurs in the tensile mode and which is illustrated in Figure 7/6, where the crack runs in short

bursts at 35° to the tensile stress, and zig-zags across the specimen. The overall effect however, on a macroscopic scale is that the crack propagates at right angles to the maximum tensile stress, i.e., at right angles to the specimen axis. This type of crack propagation bears a close resemblance to that designated Stage II by Forsyth.[19] Metallographic studies of air fatigue cracks in the present work have indicated that these cracks initiate at 45° to the tensile stress which confirms Forsyth's Stage I cracking. This Stage I cracking occupies only a very small portion of the total fatigue fracture surfaces of the specimens.

The tensile mode crack spreads transversely across the specimen surface at the same time as it propagates into the specimen interior. The length of the tensile mode crack is very dependent on the stress level, being of short duration at high stress levels but occupying an appreciable portion of the total fatigue life at low stress levels (around 14 tons/sq.in.). Broek and Schijve[112] in their work state that up to 90% of the total fatigue life can be taken up in the tensile mode of crack propagation. Once the transition to the shear mode of crack propagation has occurred very rapid crack propagation rates are observed and it seems that transition to the shear mode of failure heralds the end of the specimen's fatigue life.

Work by Finney[114] on DTD 683/3 aluminium alloy, describes similar fractures in air to those described above. In his work he measured the depth of tensile mode cracking at various stress levels and found that the depth of crack increased with decreased nominal stress level. However, the transition to the shear mode cracking was most abrupt, unlike in the present work where gradual curving of the crack front was noted (Figures 7/4 and 7/5). As in the present investigation, two shear mode cracks developed at the end of the tensile mode in Finney's work but only one propagated to failure. The tensile mode cracking in Finney's work gave a chord fracture front unlike in the work with 2024 alloy where the fracture front followed the curvature of the specimen surface and was convex.

At the end of the tensile mode crack growth stage, the crack changes direction and propagates on a plane inclined at 35^{o} to the specimen axis, i.e., near the plane of maximum shear stress. This shear mode of crack propagation would appear to be one of rapid crack movement and it would seem that it represents a relatively small part of the total fatigue life. This shear mode system is an extension of the tensile mode in that the last tensile mode burst often continues to propagate along the 35^{o} plane instead of reversing direction. This indicates that the stress level at the crack tip is sufficient to overcome the barriers which would normally stop

crack growth. There are two possible explanations for the case where two shear mode cracks are formed at the end of the tensile stage. One is that the crack reverses direction from one 35° plane to the other just at the time when the stress level at the crack tip is sufficient for shear mode crack propagation to occur on either plane, with the resultant formation of two shear mode cracks. The one that becomes dominant probably would have the path of easiest crack propagation. The other explanation is that at the end of the tensile mode the last burst at 35° continues under the action of the applied stress but there is sufficient time for a second shear mode crack to be initiated and to propagate as well. The more dominant crack would be that which has the easiest path of crack propagation. This latter explanation infers that the lower the stress level the greater the likelihood of a second shear mode crack being formed and in fact where secondary shear mode cracking has been observed it has been in the lower stress level tests.

At high stress levels the tensile mode is of short duration because the stress concentration at the crack tip reaches the value required for shear mode propagation very rapidly. At lower stress levels the opposite holds and the tensile mode operates for a longer period before sufficient stress concentration is achieved. At very low stress levels it would be probable that the tensile mode would operate for

practically the entire life of the specimen. This has not been observed in the present study but could hold for tests conducted for large numbers of cycles (in excess of 10^8). A corollary of the above is that should a sufficient stress concentrator exist prior to the fatigue test in air then the tensile mode would be eliminated and the shear mode only operate. This could be expected to produce in air, the same type of fracture as shown in high stress level corrosion fatigue tests.

Finney does not accept that stress concentration effects alone explain the transition from tensile to shear mode cracking. In a mathematical analysis[114] of the stress level at the crack front in a rotating beam fatigue test specimen he shows that the nominal tensile stress decreases in the early stages of cracking rather than increases, but then rapidly increases as the crack propagates deeper into the specimen. In his analysis he appears to neglect any stress concentration effect of the actual crack and thus the present writer feels that the mathematical analysis does not present the full picture. In view of the very marked correlation between stress level and depth of tensile mode crack the writer favours the theory that once a critical stress level at the crack front is reached then shear mode cracking becomes operative. Further evidence to support this stress concentration theory comes from both Finney's

own work on notched specimens in air and the present investigation of notched specimens in air. In Finney's work in particular, pure shear mode fractures were produced in air in notched specimens indicating that if a sufficiently high stress level is achieved at the root of the notch then tensile mode cracking is eliminated and only shear mode crack propagation takes place. This would result in very short fatigue lives.

Liu[115] in discussing the fatigue crack mode transition from a 90^{o} to a 45^{o} orientation with the tensile direction in sheet material proposed that this may be explained as a transition from plane strain to plane stress plasticity conditions. This proposal is based on his continuum mechanics approach to the problem of fatigue crack propagation (see References 10 and 11). Plane stress conditions may be expected to initiate when the plastic region at the crack tip becomes sufficiently large so that 45^{o} shearing is kinematically possible. The size of the plastic region at the crack tip will depend on the stress level at the crack tip, the higher the stress the larger the plastic region. While his results are worked out for sheet material, the ideas proposed are also applicable to round specimens although in this case the transition is to 35^{o} orientation not 45^{o}.

When the corrosion fatigue cracks are considered it appears that an entirely different system of crack propagation is operative. Typically the fracture initiates at a point and propagates across the specimen at an angle of 35^{o} to the tensile stress, with the resulting fracture surface forming part of the surface of a cone of included angle of 70^{o}, as shown in Figure 7/11, the apex of the cone being at the point of initiation. This valley fracture was observed in all the test work and with all the corrodents used. Multiple cracking was a feature of the corrosion fatigue failures and two basic forms of multiple cracking were observed, one where two cracks initiated in the same area but propagated in opposite directions (Figures 7/10 and 7/13), and the other where several cracks were initiated apparently simultaneously around the circumference of the specimen (Figure 7/10) and all propagated until failure of the specimen occurred.

The metallographic studies showed that the tensile mode of crack propagation was absent in the corrosion fatigue fractures and that only the shear mode at 35^{o} to the tensile stress was operative. Sections taken at right angles to the tensile stress confirmed that the fracture surface formed part of a cone (Figures 7/14 and 7/15) and also that crack propagation was faster at the surface of the specimen than in the centre. The crack front formed a Vee with the apex pointing back to the point of initiation.

The classical theory of corrosion fatigue as put forward by Evans[56] divides the process into two distinct stages. In the first stage electro-chemical corrosion attack takes place assisted by the applied stress. This attack produces narrow pits extending down into the metal. Normal fatigue cracks are then initiated at the bottoms of some of these pits and one of these cracks then propagates to failure. Thus the only action of the corrodent is in producing the pits which act as notches or stress concentrators, it plays no part in the propagation of the fatigue crack which forms at the bottom of the notch.

Most of the research workers using wet corrosive media for corrosion fatigue work have noted the presence of pits or crevices on the specimen surface and also that the fatigue cracks are associated with these pits. In the present work careful note was taken as to whether pitting attack had in fact occurred and if so whether the fatigue cracks were associated with these pits. Corrosive attack in the form of ex-foliation corrosion did in fact take place in the long term tests (in excess of 10^7 cycles) and the fatigue cracks appeared to be associated with this attack. However, at corrosion fatigue lives less than 10^7 cycles very little, if any, pitting attack occurred but specimen lives were as short as 4×10^4 cycles, i.e., about 14 minutes. Even at stresses as low as 10 tons/sq.in. the corrosion fatigue lives were as

short as 9×10^5 cycles, i.e., about 5 hours. With such short periods in the corrodent it is difficult to see that sufficient time is possible for the pitting attack to occur followed by the normal initiation and propagation of a fatigue crack.

In his research on corrosion fatigue at Cambridge University, Evans showed that anodic protection could prevent the corrosion fatigue of steel and on the basis of his experimental results he advanced his electro-chemical theory of corrosion fatigue. Various workers since have shown that anodic protection of other metals and alloys can indeed prevent corrosion fatigue and in the main these workers have accepted Evans' explanation of corrosion fatigue. The recent Russian work[58] has however thrown doubt on the interpretation of the results of potentiostatic measurements such as those carried out by Evans and others. The work of Kitagawa[59] showing that the corrodent has a significant effect on the crack propagation rate and that of Cornet and Behrsing[60] which produces evidence of the presence of persistent slip bands in both air and corrosion fatigue casts further doubts on the validity of the Evans two stage process of corrosion fatigue. Gough and Sopwith in work on aluminium bi-crystals[50] have reported that cracking occurred at slip bands where preferential corrosion had taken place. They noted the occurrence of pitting but this apparently had nothing to do with the fatigue cracking. Stubbington and Forsyth[61 - 62]

from the results of their work on corrosion fatigue also appear to disagree with the electro-chemical mechanism of corrosion fatigue.

Much recent research work has shown that tests in vacuum and various gaseous environments can also affect the fatigue life of metals and alloys. In this work however, the same mechanisms of crack initiation and propagation operate in both gaseous environments and vacuum and the main effect of the environment is on crack propagation not crack initiation. While many workers admit that air fatigue is a mild form of corrosion fatigue there is the tendency to treat fatigue tests under wet corrosive media and those in air as two separate and distinct phenomena. The present writer's view is that corrosion fatigue is but one extreme case of metal fatigue and that fatigue tests under vacuum represent the other extreme. The same mechanisms of crack initiation and crack propagation will operate in both cases.

It is felt that any theory of corrosion fatigue must take into account the results of modern research covering the general problem of metal fatigue. A great deal of attention has been paid over recent years to the problem of the initiation of fatigue cracks. These researches have shown that persistent slip bands are formed in certain grains within the metal under test and that these persistent slip bands develop into fatigue cracks. These persistent slip bands or

micro-cracks have been observed to form in the very early stages of the fatigue life and reported figures range between 2% and 0.5% of the total air fatigue life. Various other phenomena such as extrusions and intrusions, cavities, holes in slip bands, etc., have also been reported at early stages of the fatigue life of a specimen. All the available evidence indicates that the bulk of the fatigue life is taken up by crack propagation, often in the Stage I mode of cracking.

The continuum mechanics approach to the problem of fatigue crack propagation ignores the question of crack initiation and concentrates on producing formulae which can predict the crack propagation rates in metals undergoing fatigue loading. These formulae relate crack propagation rates to crack length, area of plastic working at the crack tip and the applied stress. The more recent formulae utilise the idea of the stress intensity factor. These continuum mechanics formulae are generally of the form of either $\frac{d\ell}{dn}$ = Constant x $(\sigma\sqrt{\ell})^4$ where σ is the applied stress and ℓ is the crack length; or $\frac{d\ell}{dn}$ = Constant x $f(\sigma)$ x $f(p)$, where $f(\sigma)$ is a function of the applied stress and $f(p)$ is a function of the plastic zone size (p) at the crack tip. Thus it can be seen that to cause shorter fatigue lives $\frac{d\ell}{dn}$ must be increased and this could be possible by increasing the effective length of the crack for the same function of stress level.

Taking the above factors into account together with the results from the present investigation, the writer considers that corrosion fatigue is simply an accelerated fatigue failure due to the effect of the corrodent on crack propagation rates. It is felt that the crack initiation is relatively little affected by the corrodent. As the bulk of the fatigue life is taken up in crack propagation this is the stage where any accelerating effect will be most noticeable. If, as experimental evidence suggests, persistent slip bands and micro-cracks are present after as little as 0.5% of the air fatigue life then similar persistent slip bands will have time to form in corrosion fatigue tests and these offer sites for corrosive attack which would accelerate the crack propagation rates.

To test the validity of the above proposition, studies of corrosion fatigue crack initiation and propagation were undertaken. The studies of crack initiation took two forms, one using highly polished specimens to check on the influence of corrosion pitting on crack initiation and the other using two stage dry-wet tests to check on the influence of dry fatigue on corrosion fatigue crack initiation. Crack propagation was studied by the two stage wet-dry tests and the effect of the corrodent on crack propagation rates determined by this means.

In the tests on the highly polished specimens, no evidence of pitting attack was found although corrosion fatigue cracks were initiated. As shown in Figures 7/7 - 7/9 and 7/16 - 7/17, the initiation areas of the corrosion fatigue cracks showed a marked similarity to the initiation areas of the cracks in air on similarly polished specimens. No evidence for the formation of persistent slip bands was found in these tests but the studies did show that the corrosion fatigue cracks were not initiated from corrosion pitting and in fact very little evidence of corrosion attack was noted.

More direct evidence for the mechanism of the initiation of corrosion fatigue cracks came from the two stage dry-wet tests. If as postulated above, the same mechanism of fatigue crack initiation, i.e., persistent slip band formation and micro-cracking, occurs under all environments whether vacuum, gaseous or wet corrosive, then by running the specimen in air for say an estimated 1% of its air fatigue life and then testing under corrosive conditions a reduced corrosion fatigue life should result. By running the specimen in air first the initiation stage should be completed and thus only the crack propagation stage will occur in the corrodent. If the main effect of the corrodent is on crack propagation then a greatly reduced corrosion fatigue stage should result. The results of the two stage dry-wet tests are given in Table 4/IV and it can be seen that running in air prior to

the corrosion fatigue stage does in fact result in a reduced corrosion fatigue stage. Thus at 13.3 tons/sq.in. running in air for 2% of the air fatigue life reduces the corrosion fatigue life from 2×10^5 cycles to 6×10^4 cycles. Similar effects were found at other stress levels and the longer the stage in air the shorter the corrosion fatigue stage.

In view therefore of the work reported by other research workers, notably Gough and Sopwith, and Cornet and Behrsing, that persistent slip bands have been observed in corrosion fatigue and the results discussed above, it is considered that the evidence points to the same crack initiation processes operating for fatigue loading under vacuum, gaseous environments and wet corrosive media. It must be mentioned that the results of the dry-wet tests in the present investigation are at variance with the results of similar tests on steel wires reported by Whitwham and Evans.[57]

From studies of crack propagation using the two stage wet-dry tests it was found that the corrodent had a marked effect on crack propagation up to about 40% of the total corrosion fatigue life. Thus if a test was run in the corrodent for times less than about 40% of the total corrosion fatigue life and then tested to destruction in air, crack propagation rates were slower in air than in the corrodent and longer overall lives (corrosion plus air) resulted. If the wet stage was over 40% of the corrosion fatigue life then

crack propagation rates in air were found to be the same as if the corrodent had been present. These trends are shown in Table 4/III and if the results at 10.35 tons/sq.in. are studied it can be seen that for a wet stage of 22% of the total corrosion fatigue life the residual life in air is 1.5×10^6 cycles, while for a wet stage of 33% the residual life in air is 5×10^5 cycles giving an overall life of 8×10^5 cycles which is very similar to the normal corrosion fatigue life of 9×10^5 cycles. The results at other stress levels show similar trends. This test series confirms the results of Kitagawa[59] who reported that after a certain percentage of the total corrosion fatigue life the overall life of corrosion fatigue stage plus air stage is constant.

If, as the evidence of the wet-dry tests suggests, the corrodent has a marked effect on the crack propagation rate then two features should be observed. Firstly, the shorter the time in the corrosion fatigue stage the longer the stage in air, with very short times in the corrodent having virtually no effect on the air stage. Secondly, as a corollary to the former statement, the longer the time in the corrosion fatigue stage the shorter the test in air. The fact that these features are shown in the results of the wet-dry tests as given in Table 4/III confirms that the corrodent is playing a major part in the crack propagation stage.

The concept that corrosion fatigue failures occur by the same mechanisms as normal air and vacuum fatigue failures, namely by cyclic slip with the corrodent merely facilitating the crack propagation stage, can be used to explain the results of the corrosion fatigue test work in the present investigation.

When considering the initiation of fatigue cracks it is felt that the work of Wood et al[22] provides the most detailed descriptions of the phenomena that occur. Thus the corrosion fatigue curves obtained in the work using superphosphate corrodent can be divided into the H, F, and S ranges suggested by Wood. As discussed in Chapter 2, in the H range (lives up to 10^5 cycles) pores are formed after 1/200th of the specimen life and these pore develop into fatigue cracks, while in the F range (10^5 - 10^8 cycles) persistent slip bands form after about 1/1000th of the specimen life and these slip bands develop into fissures and thus into fatigue cracks. The H range of the corrosion fatigue curves cover stress levels above 16 tons/sq.in. while the remainder of the curve down to 4.4 tons/sq.in. comes within the F range. Table 8/I gives the number of cycles for both air and corrosion fatigue that would be necessary for crack initiation to occur according to the figures suggested above. One problem which does arise is the question of whether the crack initiation time is the same in both air and

corrosion fatigue as it can be seen from Table 8/I that at high stress levels the time for crack initiation in corrosion fatigue is extremely short.

TABLE 8/I: Cycles for Crack Initiation (After Wood)

Stress Level Tons/sq.in.	Range in S-N Curve.	Cycles for Crack Initiation Air.	C.F.	Corrosion Fatigue Life.
19.2	H	6×10^2	2×10^1	4×10^4
16.25	H	5×10^3	5×10^2	1×10^5
13.3	F	8.7×10^3	2×10^2	2×10^5
10.35	F	10^{5*}	9×10^2	9×10^5
7.4	F	10^{5*}	2.3×10^3	2.3×10^6
4.4	F	10^{5*}	4×10^4	40×10^6

* At these stress levels in air persistent slip bands form early in the specimen life.

From Table 8/I it can be seen that even if the crack initiation in corrosion fatigue occupied the same time as in air at a given stress level, the number of cycles for crack initiation are still less than the overall corrosion fatigue life at that stress level. For stress levels below 13 tons/sq.in. in air the S-N curve comes within Wood's S range but even in this range persistent slip bands were observed to form early in the fatigue life and formation continued up to about 10^7 cycles. From the figures given in Table 8/I it is suggested that crack initiation in air and

corrosion fatigue occupy about the same length of time and that the remainder of the corrosion fatigue life, as in air, is spent in crack propagation with the corrodent causing greatly accelerated crack propagation.

The corrodent will act to assist crack propagation as soon as a micro-crack is formed, that is it will accelerate the onset of Stage I cracking. With the corrodent assisting in crack propagation in the corrosion fatigue tests it thus seems likely that these failures are due to a form of continued Stage I cracking and that Stage II cracking does not in fact occur under highly corrosive conditions. This is borne out by the fractographic studies which showed the absence of the tensile mode of crack propagation.

Other research workers have reported that pits or crevices are formed in corrosion fatigue and that the fatigue failures initiate from them. It is suggested that these pits or crevices could simply be the fissures or pores which form in the early stages of fatigue and that they have been enlarged by corrosion attack during the test. That is to say the pits are a side effect of the corrosion fatigue process and are in fact formed concurrently with or after the initiation of the actual fatigue cracks and in fact have nothing to do with the initiation of the cracks. Gough and Sopwith, in their work on aluminium bicrystals reported that although pits were present these apparently had nothing to

do with the initiation of the actual fatigue crack. Ham notes that intrusions up to 1000 Å deep are formed in a very few cycles in air. These intrusions would form sites for corrosive attack producing the pits observed in corrosion fatigue testing.

Alternatively, the corrodent could attack the persistent slip bands which are formed in the early stages of fatigue cracking thus enlarging the fissures which are formed in these bands as a result of fatigue damage. This form of attack would assist in the formation of micro-cracks and thus could possibly accelerate the initial stages of crack growth. This form of attack is probable in the longer corrosion fatigue tests with specimens lives greater than 10^7 cycles and would explain why specimens which give lives in excess of 10^8 cycles in air fail rapidly in corrosion fatigue. In both the cases outlined above cyclic slip forming persistent slip bands and other fatigue damage is the prime cause of the initiation of the corrosion fatigue crack.

Questions to be answered for the initiation of corrosion fatigue cracks are the two types of multiple cracking observed and why multiple cracking should occur more readily at low stress levels. The most common type of multiple cracking observed was that where several cracks initiated around the circumference of the rotating beam and reverse bend fatigue test specimens. The probable explanation for this type of

cracking is that at the lower stress levels more potential fatigue crack initiation areas are formed, i.e., at lower stress levels, with larger numbers of cycles prior to crack initiation there is a greater chance of fatigue damage in the form of persistent slip band formation at a number of sites around the specimen circumference. This is especially so in the case of rotating beam tests where each point on the circumference undergoes one complete stress cycle each time the specimen completes one revolution. It is less likely in the reverse bend tests where only two areas of the specimen undergo the maximum stressing each stress cycle and is even less likely in direct stress tests where damage is likely to continue in the slip system which first becomes operative. Thus it could be expected that multiple cracking would be the normal form of cracking in low stress level rotating beam and reverse bend tests but not as likely in direct stress tests. This trend was in fact observed in the present investigation.

When dealing with the question of two cracks initiating in the same general area but propagating in opposite directions the problem is more difficult. This type of cracking was found to occur mainly in the stress range 13-16 tons/sq.in.. A possible explanation for this is that there are two possible shear planes on which Stage I cracks can form. At high stress levels it is possible that both

could become active and crack propagation could be assisted on both planes by the corrodent. It was usual in this form of multiple cracking to find that one crack was dominant and propagated to failure indicating that the less dominant crack either initiated some time after the first or that crack propagation conditions were more favourable for the dominant crack.

Once the fatigue crack has been initiated the corrodent facilitates crack propagation in the shear mode. When the crack is halted at the first barrier and would normally reverse direction, the corrodent will act to remove this barrier or to weaken it and thus enable the crack to continue on the original plane. As the crack becomes deeper the stress concentration effect will increase and thus the actual stress level at the crack tip will ultimately reach the level where shear mode propagation is possible without the action of the corrodent to remove barriers being required. This would represent the end of the tensile mode in air fatigue tests. The fact that the effect of the corrodent on crack propagation is most marked up to about 40% of the total corrosion fatigue life can be explained in terms of the stress concentration effect suggested above. Thus below 40% of the corrosion fatigue life the stress level at the crack tip is not sufficient for crack propagation in the shear mode to continue unaided and it would be expected that the tensile

mode of cracking would become operative should the specimen be removed from the corrodent. This was borne out by the results of the two stage wet-dry tests as discussed in Section 7.4 of Chapter 7. Above 40% of the corrosion fatigue life crack propagation continued in the shear mode regardless of whether the corrodent was present or not.

If, as seems most probable, the shear mode cracking in corrosion fatigue is a continuation of Stage I cracking then the marked reduction in fatigue life is understandable. Various workers have reported that Stage I cracking represents a large portion of the overall fatigue life, especially at low strain amplitudes, reported figures being as high as 90%. If this stage is accelerated by the effects of a corrodent then reduced fatigue lives can be expected. One problem is the mode of failure under corrosive conditions. As there are only two modes of failure possible in metals, shear and cleavage, one of these modes must operate in corrosion accelerated fatigue. McEvily and Boettner[13] suggest that Stage I cracking is a continuation of the cyclic shearing responsible for crack initiation. Thus if the fracture under corrosive conditions is due to a continuation of Stage I cracking it could be expected to be due to shear failure along planes close to the maximum shear plane. This was in fact the observed direction of failure in the present investigation. Cleavage failure is most unlikely in fcc aluminium alloys

although Forsyth does suggest that it occurs under corrosive conditions. What is more likely is that the corrosive attack reduces the amount of plastic work necessary for shear failure to occur thus giving the apparent cleavage described by Forsyth. The river pattern of striations noted both under corrosive conditions and in the final shear mode failure in air is probably due to the very rapid crack propagation rates that occur under these conditions. When a bcc metal or alloy is tested under corrosive conditions some cleavage may take place as these metals will fail by cleavage under the appropriate conditions.

It has been noted that the corrosion fatigue crack moves along the specimen surface faster than it propagates in the interior of the specimen. This would be expected in that the corrodent will be able to continue attack on the portions of the crack near the specimen surface more readily than those in the specimen interior due to easier access to the specimen surface. Near the end of the fatigue life of the specimen, when the corrodent has no marked effect on crack growth rate it would be expected that the Vee shape of the crack front would tend to change, with the centre of the crack catching up with the outer edges and such a tendency has been observed from the fractographic studies.

The fact that the crack moves faster along the specimen circumference than in the interior, and that the crack actually moves into the specimen interior from the specimen surface explains the form of the valley fracture observed in the corrosion fatigue test work. It is suspected that the use of a round specimen facilitates the formation of a valley fracture and it is highly probable that in square or flat specimens the fracture surface would tend to be more planar and would form on a plane at an angle of between 35^{o} and 45^{o} to the tensile stress. This point would however require to be checked by actual test work.

One problem to be solved is exactly how does the corrodent assist in crack propagation. From studies of fatigue tests in gaseous environments it has been postulated that a process of corrosive attack, probably by water vapour or water vapour and oxygen acting together, at the crack tip weakens the metal bonds there and thus accelerates the crack propagation rates. With wet corrosive media a similar hypothesis seems likely and possibly something similar to the mechanism proposed for stress corrosive cracking in metals occurs. In the stress corrosion mechanism as outlined by Cottrell in his book "An Introduction to Metallurgy"[116] it is postulated that anodic dissolution of plastically deformed metal at the crack tip is responsible for crack propagation under the applied static stress. It is suggested that the yield stress is locally

exceeded in the region ahead of the crack tip. The metal there deforms plastically slightly opening the crack and a highly anodic metal surface where dissolution can occur readily at dislocations, is thereby exposed at the tip. Most of the anodic reaction, which balances the cathodic conversion of oxygen and hydrogen to hydroxyl ions on the outer surface, then occurs at the tip, the weakly anodic sides of the crack remaining fairly inactive. Concentration polarization in the solution at the tip, which would oppose this effect, might be overcome by the gradual opening of the crack due to the plastic yielding at the crack tip so that fresh liquid is continually sucked in.

In corrosion fatigue a very similar effect probably occurs. At the crack tip during each cycle the metal is plastically deformed and a plastic region develops. This region would become anodic to the metal surface as suggested above allowing dissolution at the dislocations in the plastic region and thus increasing the effective length of the crack per cycle. A certain amount of crack sharpening could also result from this corrosive attack. The corrosive attack would also weaken the metal bonds in the plastic region allowing easy crack propagation in the next tension cycle and furthermore allowing crack propagation to continue on the same plane instead of reversing direction on to another plane as occurs in the tensile mode of crack propagation. During

each fatigue cycle the specimen undergoes a tensile cycle which would open the crack allowing fresh corrodent to enter the crack and in the following compression cycle corrosive attack could continue. This explanation covers the case of a liquid corrodent such as 3% NaCl or a slurry of superphosphate in water. In the case of a paste of superphosphate the moisture in the paste would be able to diffuse into the crack and thus provide a corrodent at the crack root. Once the crack becomes deeper and its opening wider, particles of the superphosphate can enter the crack and thus also assist in the corrosive attack. This would infer that the paste of superphosphate should not cause as great an acceleration in crack propagation rates as the slurry of superphosphate, especially at the higher stress levels where there would be less time for diffusion of the moisture to the crack tip. Such a trend was observed as can be seen from a study of the data given in Appendix A.

There is no evidence available to indicate which one of the several chemicals present in the superphosphate is the actual corrodent. However, the marked similarity between tests made with aerial superphosphate in the form of a slurry; as used in the chamber technique; in the form of a paste with water and water alone would tend to indicate that the water itself could be the main corrodent and that the superphosphate is simply the medium by which it comes into

contact with the specimen. Any moisture in the superphosphate will probably pick up the free phosphoric acid and some of the soluble phosphate compounds and this combination could act as the corrodent.

Any theory of corrosion fatigue must be able to explain the effects of anodic protection in preventing corrosion fatigue. In view of the above discussion the explanation of this is quite simple. It has been shown that the major effect of the corrodent is in accelerating crack propagation rates. Any factor which can prevent this will therefore prevent an accelerated fatigue failure. Thus when anodic coatings are applied to the metal these will corrode preferentially to the crack tip and will thus prevent the corrosive attack at the crack tip. By preventing this attack at the crack tip, the fatigue life in the corrodent is prolonged. Any coating which will exclude the corrodent from the metal surface and which remains intact after a fatigue crack has formed will similarly prevent corrosive attack at the crack tip and will prolong the fatigue life in the corrodent. Thus a coating which is impervious to water vapour will improve the air fatigue life of a specimen.

In the present investigation the painted coating was only partially successful in preventing corrosive attack at the crack root and thus it must have been permeable to the

moisture in the superphosphate. However, for all practical purposes it does at least alleviate the problem of superphosphate attack on the 2024 aluminium alloy.

Since the corrodent has little effect on the initiation of corrosion fatigue failures the reason why over-ageing of the 2024 aluminium alloy failed to produce accelerated corrosion fatigue failures is simple. Although the alloy was in a condition that was highly susceptible to corrosive attack the fatigue cracks would actually be initiated before the corrosive attack had time to form sufficiently deep pits to initiate fatigue cracks. Once the crack had initiated then the normal corrosion accelerated crack propagation would occur and thus very similar lives would be found in the over-aged and naturally-aged specimens. Panseri et al[65] reported that in their work on aluminium-magnesium alloys heat treatment, including over-ageing, also had no significant effect on the corrosion fatigue lives.

Several research workers, notably McAdam, and Panseri have reported that test frequency affects the corrosion fatigue life, the higher the test frequency the longer the corrosion fatigue life. The explanation for this feature is probably that with increased test frequency while more fatigue damage occurs there is actually less time for the corrodent to enter the crack and for corrosive attack to take place at the

crack tip. Thus the corrosive attack is stifled by the speed of cycling and this results in slower crack propagation rates with a subsequent increase in corrosion fatigue life.

8.2 Notched Specimens.

With the notched specimens, the S-N curves obtained showed similar trends to those for un-notched specimens. For the rotating beam tests both the air and corrosion S-N curves have the shape of the idealised S-N curve suggested by Wood. One feature of these curves is that at the lower stress levels the curves are converging. One possible explanation for this is the difficulty of retaining the corrodent in the notch of the rotating beam specimens. Because of this it is highly probable that the results of the fatigue tests in superphosphate do not give the true fatigue lives under highly corrosive conditions. This is confirmed by the tests at 9.2 tons/sq.in. where two groups of results were obtained. One group of specimens had very short fatigue lives and pure shear mode fractures were obtained. In the other group, where longer lives were obtained, the fatigue test results lie on the S-N curve but the fractures tended to be in the tensile mode.

In the direct stress tests there were no problems in keeping the corrodent in contact with the root of the notch and thus the results of the corrosive tests give a more accurate picture than is the case with the rotating beam

tests. As only the higher stress levels could be investigated it is not certain whether the S-N curves would have similar shapes to those for the rotating beam tests but it is highly probable that at the lower stress levels the curves would tend to become asymptotic to the axis. In the direct stress tests pure shear mode fractures were obtained under corrosive conditions at all stress levels. Figure 5/4 shows clearly the difference between the direct stress tests made in air and superphosphate and the reduction in fatigue life that occurs due to the corrodent. Both the fatigue curves have similar slopes and there is no tendency for the convergence that is apparent in the rotating beam tests.

When the fractography of the notched specimens is considered it is found that the same modes of crack propagation operate here as in the un-notched specimens. Thus in air for both rotating beam and direct stress tests the crack initiates in the tensile mode and then transition to the shear mode takes place once the stress level at the crack root reaches a sufficiently high level. One difference between the notched and un-notched tests is that with the former the fatigue crack initiates around the whole circumference and propagates inwards around the whole circumference. Two fractographic features result from this. At low stress levels it is possible to obtain fractures which are at right angles to the tensile stress, i.e., the shear mode is absent. This is due

to the crack propagating into the specimen interior in the tensile mode to such a depth that failure of the specimen occurs before transition to the shear mode takes place. With crack propagation taking place around the whole specimen circumference it means that there is considerable overall reduction in cross sectional area at a stage at which the stress level at the crack tip is less than that necessary to cause transition to the shear mode. This reduction in area is such that the remaining area cannot withstand the stresses imposed on it and final fracture results.

The other feature observed from the continuous cracking around the specimen circumference is the occurrence of cone shaped shear mode fracture surfaces. This is due to shear mode cracking being possible at all points around the reduced specimen diameter, and as each portion of the shear mode fracture surface lies on a 35^{o} plane the resulting fracture surface forms a cone of included angle of 70^{o}.

In the discussion of the un-notched specimens it was postulated that if a sufficient stress level could be achieved at the root of a stress concentrator, i.e., the notch, then pure shear mode cracking should be possible in air. There was a trend towards this in the present investigation for the rotating beam tests and a marked trend towards this in the direct stress tests. A puzzling feature here is that test frequency has a marked effect on whether a pure shear mode

failure is achieved in air or not and it also has a marked effect on the degree of shear mode cracking in all air tests. Thus in this research the direct stress tests were made at a frequency of around 10,500 c.p.m. while the rotating beam tests were made at a frequency of 3000 c.p.m. It was found that only the highest stress levels in the rotating beam tests showed the trend to the shear mode cone shaped fracture (Figure 7/18) while this feature occurred at all stress levels used in the direct stress tests (Figure 2/23).

In the work of Finney[113] a similar frequency effect was observed for rotating beam tests and he did in fact obtain pure shear mode fractures at 12,000 c.p.m. identical to those obtained with notched rotating beam specimens in superphosphate (Figure 7/20), in the present investigation.

It is difficult to see why test frequency should have such a marked effect on the transition to shear mode crack propagation in air and why increasing the test frequency should assist in the production of a pure shear mode crack in air. A possible explanation is that the higher test frequency, by increasing the speed of application of stress, is assisting the dislocations to break through the barriers which would normally halt their progress. Thus at high stress levels crack propagation is able to continue in the Stage I mode at high frequencies, beyond the stage where it would

normally change to Stage II or tensile mode crack propagation. After a relatively short time in this Stage I cracking the stress level at the crack tip would reach the level where shear mode cracking can continue unaided thus producing the cone shaped fractures observed in air by Finney.

For tests made in an environment of superphosphate with the notched specimens two types of fracture were observed. In the rotating beam tests a group of specimens tested at 9.2 tons/sq.in. gave pure shear mode fractures (Figure 7/20) but another group at the same stress level gave tensile mode failures similar to those found in air at the same stress level. Tensile mode failures similar to those in air were observed at all other stress levels. It is felt that the first group of specimens, with the pure shear mode cracking, represent the true picture of notched specimens under corrosive conditions. With the direct stress tests all specimens that failed gave pure shear mode fractures, no tensile mode cracking being observed in any of these tests. The fact that the fracture surfaces formed the surface of a cone is due to initiation and propagation of shear mode cracking around the entire specimen circumference and as each section of the crack propagates on a 35^{o} plane the resulting fracture surface lies on a cone of included angle of 70^{o}.

In view of the marked effect of cycle frequency on the fracture modes in notched specimens in air the question must be raised as to why the cycle frequency should have the opposite effect in un-notched specimens in a corrosive environment. With un-notched specimens it will be recalled that increasing the cycle frequency improved the fatigue life in a corrosive environment. It would be thought that the increased speed of stress application would increase crack propagation rates and thus balance the decrease in crack propagation due to stifling of the corrosive attack. However it would appear that the accelerating effect of the corrosive attack at the crack tip is much greater than the accelerating effect on crack propagation rates due to the increase in cycle frequency and thus when the corrosive attack is stifled the actual crack propagation rate is in fact lowered giving a longer life for the un-notched specimen.

In Section 8.1 it has been shown that the main effect of the corrodent is to assist crack propagation. This poses a problem with notched specimens in that the corrodent must remain in contact with the notch root in order for it to be able to reach the crack tip. In the un-notched specimens the corrodent is in contact with a considerable area of the specimen surface and thus the corrodent has ready access to the crack opening and hence to the crack tip. With the

notched specimens however, the crack is entirely in the specimen interior and the only access for the corrodent is via the root of the notch. This limited access for the corrodent will result in slower crack propagation rates and this is reflected in the fact that the reduction in fatigue life due to superphosphate is not as great in the notched specimens as in the un-notched specimens. The fact that the corrodent must remain in the root of the notch to have access to the crack root explains the convergence noted in the rotating beam fatigue curves. With these tests there was a tendency for the corrodent to be flung out of the notch and thus corrodent could not reach the crack root. This means that at low stress levels especially, where longer fatigue lives were usual,corrosive attack would be limited resulting in lives that would approach those found in air. With the direct stress tests this problem did not occur and thus there is no convergence of the fatigue curves.

8.3 The Practical Implications of the Research.

This investigation into the effects of superphosphate fertilizers on the fatigue properties of 2024 aluminium alloy arose out of a concern as to whether superphosphate would affect the fatigue lives of aircraft engaged in top dressing work. It is thus of interest to see what practical implications the results of the investigation have in terms of the fatigue lives of actual aircraft. This is however a

difficult question to answer and any suggestions must of necessity be very limited in their scope.

The load spectra for various types of aircraft engaged in aerial top dressing work are set out in the paper by Labett[1] which is based on work done by the New Zealand Department of Civil Aviation. In Table 2 of this paper the actual recorded 'G' values for three Fletcher FU24 top dressing aircraft are given. The longest period of recording is for 400 hours and these figures are reproduced in Table 8/II. This particular aircraft had a life of 11,130 hours at the time the recordings were taken. The average time of each flight was 4 minutes 11 seconds and it can be seen that 400 hours represents a considerable number of flights. In the recorded 'G' values only in-flight loads are given and landing and taxi-ing loads are ignored. It is however, estimated that the loading cycle imposes a load of -0.39 'G' on the aircraft.

TABLE 8/II: Recorded 'G' Values for a Fletcher FU24 (From Labett).

'G' Level:	-0.5	0.1	0.5	1.5	1.9	2.5	2.9	3.5
Average Counts/Hour:	0.01	0.63	13.5	46.3	27.0	9.7	4.69	1.44

Average Landings/Hour at -0.39 'G' = 14.34

From Table 8/II it can be seen that the highest recorded 'G' level was 3.5. The datum for all recordings was 1 'G' representing straight and level flight. Thus a value of 3.5

'G' means that the aircraft experiences a stress fluctuation of amplitude 2.5 'G'. For fatigue loading purposes this could be represented by a fluctuating stress of 1.25 'G' with a superimposed mean stress of 1 'G'. From private information given by Mr. Labett it appears that the stress level represented by 1 'G' is 2.5 tons/sq.in. for the Fletcher aircraft and this means that a 'G' value of 1.25 is equivalent to 3.125 tons/sq.in. Taking the most severe test condition in the present research, that given by a notched specimen in superphosphate, it is found from Figure 4/9 that at a stress level of 3.125 tons/sq.in. the specimen life would be of the order of 33×10^6 cycles. From Table 8/II the frequency of cycling is 1.44/hour and thus the life in hours of a 0.25 in. diameter specimen is $\frac{33 \times 10^6}{1.44}$, that is 23×10^6 hours. From this it appears that the reduction in fatigue life in thick sections due to the presence of a notch and moist superphosphate is not sufficient to cause alarm. However, it must be remembered that the above value is largely speculative and is based on 'G' values near the wing root, that is in major structural members. For sheet material and for riveted joints such as occur in the Fletcher aircraft a very much shorter fatigue life could be expected than for a thick section and thus accelerated failures of this type of structure can be expected under the influence of moist superphosphate. A further factor to be considered is the cumulative effect of all stress loadings on the aircraft.

What does emerge from the above analysis is that a major structural failure of say a wing spar is unlikely unless a crack is already present. In such a case, then a very rapid failure could be expected. The major implication of practical importance is the need for continued and thorough checking of top dressing aircraft for cracking, signs of corrosion and damaged paintwork. Components showing any of these features must be regarded as being suspect and would require to be carefully checked before being returned to service.

8.4 Suggested Future Work.

In order to check fully the theory of corrosion accelerated fatigue advanced in Section 8.1, further work on the problem of initiation and propagation of fatigue cracks in the presence of wet corrosive media is required. These studies would have to be designed fully to elucidate whether crack initiation times under corrosive conditions are the same as those in air or vacuum or whether the corrodent is having some effect at low stress levels. A clue to this would be the presence of persistent slip bands and other fatigue damage and whether corrosion pits are formed before or concurrent with the fatigue cracks. This study would possibly best be done using single crystals. The work should also be extended to other alloy systems particularly the steels, especially the newer high strength low alloy structural steels.

There is also a need to check the effects of random loading on corrosion accelerated fatigue both for notched and un-notched specimens. Any study of this nature should include the 2024 aluminium alloy in moist superphosphate.

In order to gain information of practical value to the aerial top dressing industry the study of the fatigue properties of the 2024 alloy in superphosphate should be extended to actual components and riveted joints in sheet metal preferably under random loading. With information now available on the load spectra of agricultural aircraft it would be possible to design suitable random loading tests which would simulate the actual aircraft loadings and thus be able to produce information of practical value to the industry.

If New Zealand is to continue selling the Fletcher agricultural aircraft to overseas buyers it is possible that at some stage a full-scale fatigue test on the aircraft will be required. While this would be a costly and time consuming research project it would be possible to incorporate into the test the effects of a superphosphate environment and thus answer the question originally posed as to the effect of this corrodent on the aircraft fatigue life. Such information would be of considerable value when deciding on a safe working life for the Fletcher aircraft.

CHAPTER NINE.

9. CONCLUSIONS.

These conclusions are based on the experimental conditions of the present research work and apply to the 2024 aluminium alloy. It is felt that the conclusions on fractography can be applied to other high strength aluminium alloys, but may not necessarily apply to other alloy systems such as the steels. The ideas postulated for the mechanism of corrosion accelerated fatigue are possibly applicable to all metals and alloys.

(1) Superphosphate in the presence of moisture causes accelerated fatigue failures in the 2024 - T4 aluminium alloy.

(2) Pre-corrosion of the specimens in the absence of stress also results in a reduction in fatigue life.

(3) Two fracture modes operate in air fatigue tests, the crack starting in the tensile mode at right angles to the applied tensile stress and then changing to the shear mode at 35^{o} to the tensile stress. In corrosion accelerated fatigue failures only the shear mode is operative.

(4) The presence of a suitable stress concentrator in high stress level tests in air can eliminate the tensile mode of cracking and produce pure shear mode fractures. The cycle frequency of the test has a considerable effect on this, the higher the frequency the greater the likelihood of shear mode fractures.

(5) Multiple cracking is a feature of corrosion accelerated fatigue failures especially at low stress levels.

(6) In metal fatigue, whether in air, vacuum or under highly corrosive conditions, essentially the same mechanisms of crack initiation and crack propagation operate.

(7) The corrodent has little, if any, effect on crack initiation.

(8) The effect of the corrodent is to accelerate crack propagation rates, therefore giving a greatly reduced fatigue life.

(9) The effect of the corrodent on crack propagation rates is most marked up to about 40% of the corrosion fatigue life, after this period crack propagation rates are the same regardless as to whether the test is continued in the corrodent or in air.

(10) The corrodent accelerates crack propagation rates by attacking the plastically deformed metal at the crack root thus weakening the metal bonds and permitting easy crack propagation under the applied stress.

(11) The effect of protective coatings whether anodic, painted or of any other form is simply to prevent the corrodent attacking the crack tip thus preventing any acceleration of crack propagation rates.

(12) The effect of cycle frequency on un-notched specimens in a corrosive environment is to stifle corrosive attack at the crack tip thereby prolonging the fatigue life under the corrosive conditions.

R E F E R E N C E S.

1. E. T. LABETT — 5th I.C.A.F. Symposium, Melbourne, May 1967.
2. P.J. FODEN — Ibid
3. J. STEPHENSON AND K.C. LEE — School of Engineering, Auckland University. Private communication.
4. T. MARSHALL AND L.G. NEUBAUER — Corrosion 11 (2) (1955) 84t
5. K.R.A. O'BRIEN AND M.R. RICE — Agric.Aviation 5 (4) (1963) 107
6. J.Y. MANN — ARL/SM 305, Aeronautical Research Laboratories, Australia.
7. F. ERDOGAN — NASA CR - 901 (1967)
8. A.K. HEAD — Phil. Mag. 44 (1953) 925
9. N.E. FROST AND D.S. DUGDALE — J. Mech. Phys. Solids 6 (1958) 92
10. H.W. LIU — J. Basic.Eng.Trans. ASME 83 (1961) 23
11. H.W. LIU — Ibid 85 (1963) 116
12. W. ILLG AND A.J. McEVILY — NASA Tech.Note D 52 (1959)
13. A.J. McEVILY AND R.C. BOETTNER — Acta Met. 11 (1963) 725
14. P.C. PARIS AND F. ERDOGAN — J.Basic Eng.Trans.ASME 85(1963)528
15. American Society for Testing and Materials, S.T.P. 415 (1967)

16.	J. WEERTMAN	Int. J. Frac. Mech. 2 (2)(1966)460
17.	S. PEARSON	Nature 211 (5053) (1966) 1077
18.	G.A. MILLER, D.H. AVERY AND W.A. BACKOFEN	Trans.Met.Soc. AIME 236(1966) 1667
19.	P.J.E. FORSYTH	Acta Met. 11 (1963) 703
20.	W.A. WOOD AND H.M. BENDLER	Trans. Met. Soc. AIME 224(1962)181
21.	W.A. WOOD AND H.M. BENDLER	Ibid p.18
22.	W.A. WOOD, S.McK. COUSLAND AND K.R. SARGANT	Acta Met 11 (1963) 643
23.	P.J.E. FORSYTH AND D.A. RYDER	Metallurgia 63 (1961) 117
24.	P.J.E. FORSYTH AND C.A. STUBBINGTON	RAE Tech.Note Met-Phys.394 (1962)
25.	P.J.E. FORSYTH, C.A. STUBBINGTON AND D. CLARK	J. Inst.Metals 90(1961-62) 238
26.	C.A. STUBBINGTON AND P.J.E. FORSYTH	Metallurgia 74 (1966) 15
27.	M.A. WILKOV AND R. SHIELD	AFOSR Final Scientific Report 66-0856 (Available from U.S. Department of Commerce, Springfield, Va).
28.	R.K. HAM	Canadian Met.Quarterly 5 (3) (1966) 161
29.	J. SCHIJVE	Am.Soc.Test.Mats. STP 415(1967)415

30.	G.Y. CHIN AND W.A. BACKOFEN	J.Inst.Metals 90 (1961) 13
31.	J. HOLDEN	Phil.Mag. 6 (1961) 547
32.	H.D. WILLIAMS AND G.C. SMITH	Ibid 13 (1966) 835
33.	J.C. GROSSKREUTZ AND P.W. WALDOW	Acta Met. 11 (1963) 717
34.	C. LAIRD	Am.Soc.Test.Mats. STP 415(1967)131
35.	B.P. HAIGH	J.Inst.Metals 18 (1917) 55
36.	H.J. GOUGH	Ibid 49 (1932) 17
37.	P.T. GILBERT	Metallurgical Reviews 1(3) (1956) 379
38.	A.J. GOULD	Int.Conf. on Fatigue. Instn.Mech. Engrs. (1956) 341
39.	U.R. EVANS	"The Corrosion and Oxidation of Metals" Edward Arnold Ltd.,London, 1960. 701
40.	N.J. WADSWORTH	"Internal Stresses and Fatigue in Metals" Eds. G.M.Rassweiler and W.L. Grube. Elsevier, New York, (1959)
41.	C.M. HUDSON	NASA Tech.Note D - 2563 (1965)
42.	M.R. ACHTER	Am.Soc.Test.Mats. STP 415(1967)181
43.	D.J. McADAM	Proc. A.S.T.M. 27(11) (1927) 102
44.	D.J. McADAM	Ibid 28(11) (1928) 117
45.	D.J. McADAM	Ibid 29 (1929) 250
46.	D.J. McADAM	Ibid 30(11) (1930) 411
47.	D.J. McADAM	Trans. AIME Inst.Metals Div.99 1932) 282

48. H.J. GOUGH AND D.G. SOPWITH — J. Inst. Metals 49 (1932) 93

49. H.J. GOUGH AND D.G. SOPWITH — Proc. Roy. Soc. (A) 135 (1932) 392

50. H.J. GOUGH AND D.G. SOPWITH — J. Inst. Metals 52 (1933) 57

51. H.J. GOUGH AND D.G. SOPWITH — J. Iron & Steel Inst. 127 (1933) 30

52. D.G. SOPWITH AND H.J. GOUGH — Ibid 135 (1937) 315

53. H.J. GOUGH AND D.G. SOPWITH — Ibid 135 (1937) 293

54. A.J. GOULD AND U.R. EVANS — Iron & Steel Inst., Special Report 24 (1939) 325

55. N. STUART AND U.R. EVANS — J. Iron & Steel Inst. 147 (1943) 131

56. U.R. EVANS AND M.T. SIMNAD — Proc. Roy. Soc. (A) 188 (1946-47) 372

57. D. WHITWHAM AND U.R. EVANS — J. Iron & Steel Inst. 165 (2) (1950) 72

58. S.G. VEDENKIN AND V.G. SINYAVSKIY — Russian J. Phys. Chem. 36 (10) (1962) 1189

59. H. KITAGAWA — Expt. Mech. 7 (1) (1967) 28

60. I. CORNET AND G. BEHRSING — Proc. 2nd Int. Congress on Met. Corrosion, (1963) 54

61. C.A. STUBBINGTON AND P.J.E. FORSYTH — J. Inst. Metals 90 (1962) 347

62. C.A. STUBBINGTON — Metallurgia. 68 (407) (1963) 109

63. W.M. LORKOVIC, D. VARALLYAY AND R.D. DANIELS — Mater.Protect. 3(11) (1964) 16

64. W.M. LORKOVIC — Ph.D. Thesis, University of Oklahoma, (1966)

65. C. PANSERI, L.MARI AND P. DETTIN — Brit.Corrosion J.1(7) (1966) 270

66. K. ENDO AND Y.MIYAO — Proc. 1st Japan Congress Test.Mats. (1957) 17

67. A.J. GOULD — Engineering 141 (1936) 495

68. I. CORNET AND S. GOLAN — Corrosion 15 (1959) 262t

69. I. CORNET AND G. BEHRSING — Proc. 2nd Int.Congress on Metallic Corrosion (1963) 62.

70. I.J. GERARD AND H. SUTTON — J.Inst.Metals 56 (1935) 29

71. E.G. SAVAGE, E.G.F. SAMPSON AND J.K. CURRAN — RAE Tech.Note Met.200 (1954)

72. E.G. SAVAGE AND E.G.F. SAMPSON — RAE Tech.Note Met.216 (1955)

73. N.P. INGLIS AND E.C. LAKE — J.Inst.Metals 83 (1954-55) 117

74. R.A.F. HAMMOND AND C. WILLIAMS — Metallurgical Reviews 5(18) (1960) 165

75. H.G. COLE AND R.J.M. PAYNE — Metallurgia 66 (1962) 11

76. A.C. LAW — NEL Report No.102 (1963)

77.	E.A.G. LIDDIARD, J.A. WHITTAKER AND H. KING	Proc. 1st Int. Congress on Metallic Corrosion, London (1961)
78.	J.A. WHITTAKER	J. Inst.Metals 91(1962-63) 346
79.	J.A. WHITTAKER, H. KING AND E.A.G. LIDDIARD	S & T Memo 6/63 British Ministry of Aviation (1963)
80.	J.A. WHITTAKER, H. KING AND E.A.G. LIDDIARD	Proc. 2nd Int.Congress on Metallic Corrosion (1963) 229
81.	E.G. EELES	J. Inst.Metals 95 (1967) 156
82.	W.L. HOLSHOUSER AND H.P. UTECH	Proc. A.S.T.M.61 (1961) 749
83.	H.E. FRANKEL, J.A. BENNET AND W.L. HOLHOUSER	J.Res.Nat.Bur.Stand.64(2)(1960)147
84.	F.J. RADD, L.H.CRAWDER AND L.H. WOLFE	Nature 184 Suppl.26 (1959) 2008
85.	F.J. RADD, L.H.CRAWDER AND L.H. WOLFE	Corrosion 16 (1960) 415t
86.	R.A. BURMEISTER AND R.A. DODD	Proc. A.S.T.M.62 (1962) 675
87.	K.U. SNOWDEN	Ibid 62 (1962) 681
88.	K.R.L. THOMPSON AND T.O. MULHEARN	J.Aust.Inst.Metals 10(3)(1965) 303
89.	H.J. GOUGH AND D.G. SOPWITH	J. Inst.Metals 56 (1935) 55
90.	H.J. GOUGH AND D.G. SOPWITH	Ibid 72 (1946) 415

91.	N.J. WADSWORTH AND J. HUTCHINGS	Phil.Mag.3(34) (1958) (viii) 1154
92.	N. THOMPSON, N.J. WADSWORTH AND N. LOUAT	Ibid 1 (1956) 113
93.	N.J. WADSWORTH	Ibid 6 (1961) 397
94.	K.U. SNOWDEN AND J.N. GREENWOOD	Trans.Met.Soc. AIME 212(1958) 626
95.	K.U. SNOWDEN	Acta Met. 12(3) (1964) 295
96.	K.U. SNOWDEN	Nature 189 (4758) (1961) 53
97.	M.R. ACHTER, G.J. DANEK AND H.H. SMITH	Trans.Met.Soc.AIME 227(6)(1963)1296
98.	M.J. HORDON	Acta Met. 14(10) (1966) 1173
99.	M.A. WRIGHT AND M.J. HORDON	Ibid 15(2) (1967) 430
100.	T. BROOM AND A. NICHOLSON	J. Inst.Metals 89(6)(1960-61) 183
101.	W.L. HOLSHOUSER AND J.A. BENNET	Proc. A.S.T.M. 62 (1962) 683
102.	H.A. LEYBOLD, H.F. HARDRATH AND R.L. MOORE	NACA Tech.Note 4331 (1958)
103.	J.A. DUNSBY AND W. WIEBE	NRC MS - 111 (1964) (National Research Council of Canada)
104.	F.J. BRADSHAW AND C.W. WHEELER	App.Mats.Research 5(2) (1966) 112
105.	A. HARTMAN	Int.J.Frac.Mech. 1(3)(1965) 167

106.	E.G. EELES AND R.C.A. THURSTON	J. Inst. Metals 95 (1967) 111
107.	D.G. DRUMMOND AND D.J. HOGAN	Report No. C.D.2076 (1965) 59 Chemistry Division, D.S.I.R.
108.	W.D. ROBERTSON	Trans. AIME 166 (1946) 216
109.	T.M. DOWELL	Engineering 185 (1958) 693
110.	J.M. FINNEY AND J.Y. MANN	Nature 182 (1958) 1366
111.	J.M. FINNEY	J. Inst. Metals 92 (1963) 30
112.	D. BROEK AND J. SCHIJVE	Aircraft Eng. 39(3) (1967) 10
113.	J.M. FINNEY	J. Inst. Metals 92 (1964) 380
114.	J.M. FINNEY	A.R.L./S.M. 283 (1963)
115.	H.W. LIU	Applied Mats. Res. 3(4)(1964) 229
116.	A.H. COTTRELL	"An Introduction to Metallurgy" Edward Arnold, London, (1967)

APPENDIX A:

Typical results of rotating beam fatigue tests in air, superphosphate/water and superphosphate/moist air.

Stress Level	Cycles to Failure		
Tons/sq.in.	Air	Super/H_2O	Super/Air
19.2	6.8×10^5	2.5×10^4	3.75×10^4
16.25	5×10^6	7.5×10^4	1×10^5
13.3	87×10^6	2.15×10^5	2×10^5
10.35	10^{8*}	3.75×10^5	9×10^5
7.4	10^{8*}	2.9×10^6	2.3×10^6
4.4	10^{8*}	24.1×10^6	39.8×10^6

* Specimen unbroken

APPENDIX B:

Typical results of rotating beam fatigue tests in potassic superphosphate, tap water and 3% NaCl.

Stress Level	Cycles to Failure		
Tons/sq.in.	Potassic	Tap Water	3% NaCl
19.2	2×10^4	6.25×10^4	3×10^4
16.25	5×10^4	1.5×10^5	7.5×10^4
13.3	2×10^5	2.8×10^5	1.35×10^5
10.35	6×10^5	8.5×10^5	3.25×10^5
7.4	8×10^5	4.9×10^6	9×10^5
4.4	3.1×10^6	58×10^6	7.5×10^6

APPENDIX C:

Typical results of notched rotating beam tests in air and superphosphate/moist air.

Stress Level Tons/sq.in.	Cycles to Failure	
	Air.	Super/Air.
12.2	3×10^5	1.5×10^4
10.6	4×10^5	-
9.2	5×10^5	1×10^5
		2×10^4
7.8	8×10^5	5.5×10^5
6.36	1.6×10^6	7.5×10^5
4.95	11.5×10^6	1.8×10^6
3.54	10^{8*}	37.6×10^6

* Specimen unbroken

APPENDIX D:

Typical results for painted specimens (un-notched) in air and superphosphate/moist air.

Stress Level Tons/sq.in.	Cycles to Failure	
	Air.	Super/Air.
19.2	1×10^5	1×10^5
17.2	2×10^5	-
16.25	7.5×10^5	3×10^5
14.3	4×10^6	1.2×10^6
13.35	9.1×10^6	2.3×10^6
13.3	86.5×10^6	2.8×10^6
10.35	10^{8*}	5.7×10^6

* Specimen unbroken

APPENDIX E:

Typical results of direct stress fatigue tests in air and in superphosphate/moist air for both notched and un-notched specimens.

Stress Level Tons/sq.in.	Cycles to Failure		
	Notched		Un-Notched
	Air.	Super/Air.	Super/Air.
20.2	-	-	1.25×10^5
17.2	4.3×10^5	-	1.8×10^5
16.2	6.19×10^5	4.48×10^4	3.15×10^5
14.18	1.43×10^6	2.14×10^5	6.34×10^5
12.15	$6 \times 10^{6*}$	4.37×10^5	1.56×10^6
10.13	-	1.04×10^6	$2.57 \times 10^{6*}$
6.08	-	$6.68 \times 10^{6*}$	-

* Specimen unbroken